Mutagenic and transgenic approaches to manipulate mineral phosphate solubilization with special reference to glucose dehydrogenase

Thesis submitted for the degree of

DOCTOR OF PHILOSOPHY

by

BURLA SASHIDHAR

Department of Plant Sciences
School of Life Sciences
University of Hyderabad
Hyderabad-500 046
INDIA

August 2008
Enrollment No. 02LPPH12

University of Hyderabad
(A Central University established in 1974 by the act of parliament)
HYDERABAD -500 046, INDIA

CERTIFICATE

This is to certify that Mr. Burla Sashidhar has carried out the research work embodied in the present thesis under supervision and guidance of Prof. Appa Rao Podile for a full period prescribed under the Ph. D. ordinance of this University. We recommend his thesis "**Mutagenic and transgenic approaches to manipulate mineral phosphate solubilization with special reference to glucose dehydrogenase**" for submission for the degree of Doctor of Philosophy of the University.

Prof. Appa Rao Podile
(Research Supervisor & Head,
Department of Plant Sciences)

Dean,
School of Life Sciences

University of Hyderabad
(A Central University established in 1974 by the act of parliament)
HYDERABAD -500 046, INDIA

DECLARATION

I hereby declare that the work embodied in this thesis entitled "**Mutagenic and transgenic approaches to manipulate mineral phosphate solubilization with special reference to glucose dehydrogenase"** has been carried out by Mr. Burla Sashidhar under the supervision of **Prof. Appa Rao Podile** and this has not been submitted for any degree or diploma in any other University earlier.

Burla Sashidhar

Prof. Appa Rao Podile
(Research Supervisor)

ACKNOWLEDGEMENTS

I am immensely grateful to all those individuals who have helped me in making this endeavour possible.

I take this opportunity to extend my sincere gratitude to my research supervisor **Prof. Appa Rao Podile** for his constant encouragement, support and for his meticulous guidance throughout my doctoral research, without whom this endeavor would not have been possible.

I thank the former Heads of the Department of Plant Sciences, Prof. M. N. V. Prasad, and Prof. P. B. Kirti & the present and former Deans, School of Life Sciences, Prof. A. S. Raghavendra and Prof. T. Suryanarayana for allowing me to use the facilities of the department and the school.

My heartfelt thanks to Dr. Lalitha Guruprasad (School of Chemistry) for the structure model of GDH and identifying mutation targets & Dr. K. Gopinath for his valuable suggestions in generation of SDMs and extending his lab facility to write my thesis.

I thank Dr. Ch. Venkata Ramana, Prof. S. Dayananda, Dr. G. Padmaja, Dr. K. Seshagirirao, and Prof. Aparna Datta Gupta and all the faculty members of the School of Life Sciences.

I thank Dr. Ch. Sasikala, Dr. Archana and Dr. Srinivas (JNTU Hyderabad) for allowing me to use Gas Chromatography and analyzing the data, Dr. Naresh Kumar, University of Baroda for *E. asburiae*.

I thank Prof. C. Kennedy, University of Arizona for *A. vinelandii* AvOP, Dr. Nora Goosen, University of Netherlands, The Netherlands for *E. coli* PP2418; Prof. M. Yamada, Yamaguchi University, Japan for *E. coli* YU423.

I thank all the research scholars of the School of Life Sciences for their cooperation. The help and cooperation of the non-teaching staff, School of Life Sciences is also acknowledged.

I thank DBT & CSIR for the award of junior and senior research fellowship for pursuing my research. I would like to acknowledge the infrastructural support provided by UGC-SAP and DST-FIST to the Department of Plant Sciences.

I wish to thank my seniors Dr. ShreeRam, Dr. Kishore, Dr. Tripura, Dr. Madhuri and Dr. Harish for their suggestions and help. I thank all my labmates Anil, Vasu, Neeraja, Debashish, Purushotham, Suma, Sippy, Uma, Swaroopa, Sharma, Nandu, Das & Suprava for their cooperation.

I also thank our lab assistants, Satyanarayana, Madhu, Gopal, Narasihma and Malla Reddy for their co-operation.

I wish to thank all my friends Dr. Malla Reddy, Bhuvan, Narahari, D.K. Srinivas, Jagadeesh from Chemistry, Dr. Vikram, Dr. Phani, Balaraju, Srinivas, Laxminarayana, Shankaraiah, form Physics and Harish from History for their cooperation and friendly atmosphere in the campus.

Many thanks to my friends Narander, Hari Krishna, Hari, Chinni, Srinivas from Nizam college and my friends at home Ruman, Ravinder, Bajaj, RPRPR, Jagadeesh, Purna, Mahesh, Shekar, Praveen, Ravi, Ramu Aravind, etc.

Special thanks to my dear friends Vijay and Kishore for their support and help at a short note even in their busy schedule. Many thanks to my friends Raja, Laxman, Rajkumar, Dina, Srinivas, Damu, Chandra mohan, Gopi, Nagi, Praveen, Ramgopal, Eros, Abjith, Shankar, Prasanna etc., for their help and cooperation.

My heartfelt thanks to my maternal uncle Gunda Shankar and paternal uncle Burla Rajaeshwar Rao and all my cousins for being there for me.

My special thanks to my dearest friend form my childhood, Pavan Khandelwal for being there form me all the time.

I am at a loss to find words to fully express my gratitude to my parents, brothers and my little heart (Sister) for their unwavering love, affection and patience. Without their blessings and best wishes I would not have been successful in completing this research work.

Sashidhar

Dedicated to my beloved
parents, esteemed teachers
and maternal uncle G. Shanker

CONTENTS

ABBREVIATIONS

AG medium	:	*Azotobacter* growth medium
ADH	:	alcohol dehydrogenase
ALP	:	alkaline phosphatase
ARA	:	acetylene reductase assay
AT medium	:	*Azotobacter* transformation medium
BCIP	:	5-bromo-4-chloro-3-indolyl phosphate
^{o}C	:	degree centigrade/degree Celsius
cm	:	chloramphenicol acetyl transferase gene
CMC	:	carboxy methyl cellulose
CFU	:	colony forming units
C-terminal	:	carboxy terminal
DNA	:	deoxy ribonucleic acid
dNTPs	:	deoxy nucleotide triphosphates
dATP	:	deoxy adenosine triphosphate
dCTP	:	deoxy cytidine triphosphate
dGTP	:	deoxy guanosine triphosphate
dTTP	:	deoxy thymidine triphosphate
2,5DKGA	:	2,5 di-keto gluconic acid
EDTA	:	ethylene diamine tetra acetic acid
EMS	:	ethyl methanesulfonate
g	:	gram
GA	:	gluconic acid
GADH	:	gluconate dehydrogenase
gcd	:	glucose dehydrogenase gene
GDH	:	glucose dehydrogenase
*gln*A	:	glutamine synthetase gene
*gln*A-p	:	glutamine synthetase gene promoter
h	:	hour (s)
HCR	:	highly conserved region

IPTG	:	isopropyl β-D-thiogalactoside
2KGA	:	2-keto gluconic acid
2KGADH	:	2-keto gluconate dehydrogenase
kb	:	kilobase pair
kDa	:	kilodalton
LB	:	Luria-Bertani
lit	:	litre
M	:	molar
MDH	:	methanol dehydrogenase
mg	:	milligram
min	:	minute
ml	:	milliliter
mM	:	millimolar
mm	:	millimeter
MPS	:	mineral phosphate solubilization
mGDH	:	membrane glucose dehydrogenase
NAD	:	nicotinamide adenine dinucleotide
NBRIP	:	national botanical research institute's phosphate
NBT	:	nitroblue tetrozolium
ng	:	nanogram
nm	:	nanometer
nM	:	nanomolar
N-terminal	:	amino terminal
OD	:	optical density
ORF	:	open reading frame
PAGE	:	polyacrylamide gel electrophoresis
PCR	:	polymerase chain reaction
PGPR	:	plant growth promoting rhizobacteria
pi	:	inorganic phosphate
PMF	:	proton motive force

PSB	:	phosphate solubilizing bacteria
PSM	:	phosphate solubilizing microorganisms
pts	:	phosphonate transport system gene
pts-p	:	phosphonate transport system gene promoter
PQQ	:	pyrrolo quinoline quinone
rpm	:	revolutions per minute
sGDH	:	soluble glucose dehydrogenase
SDM	:	site directed mutagenesis
SDS	:	sodium dodecyl sulphate
TBST	:	tris buffered saline tween
TCP	:	tricalcium phosphate
TE	:	tris-EDTA
Tris	:	tris-(Hydroxymethyl) aminoethane
U	:	unit
μg	:	microgram
μl	:	microlitre
μmol	:	micromole
X-gal	:	5-bromo 4-chloro 3-indiolyl β-D-galactoside

LIST OF FIGURES

LIST OF TABLES

Introduction

1.1 Importance, availability and acquisition of inorganic phosphate for plant nutrition:

Phosphorus is the second most important macro-nutrient, next to nitrogen, required by any organism. In plants, phosphorus plays an important role in transfer of high energy, cell division, photosynthesis, biological oxidation and many more vital functions. It plays a major role in plant metabolism for growth, reproduction and nutrient uptake. In nature, phosphorus occurs in fully oxidized state as phosphate. The total content of phosphorus in natural environment is normal, but invariably forms a large number of insoluble chemical complexes with many ions present in the soil, which indeed makes this nutrient a paradox. The availability of phosphorus in many soils is in the range of 10^{-6} M, but plants require ~ 0.03 mM to reach their maximum productivity. A major chunk of total phosphates in soil are bound to ions of calcium, iron and aluminum, forming insoluble phosphate salts and are not directly available as phosphorus to the crops. Most of the applied phosphatic fertilizers are also reprecipitated into insoluble mineral complexes and are not efficiently taken up by the plants. Certain group of higher plants evolved highly efficient mechanisms for absorbing phosphate even from very dilute solutions, and achieve maximum growth rates even with soil solution phosphate levels of 2 μM or less (Epstein, 1972). Some other plants have adapted to phosphate limiting conditions by secreting organic acids that facilitate the release of phosphates from inorganic ion complexes (Raghothama, 2000). However, this impressive capability shown only by a limited group of plants is not enough to allow maximizing agronomic productivity. Application of phosphatic fertilizers, therefore, has been considered essential for agronomic levels of crop production in most agro ecosystems.

The applied phosphatic fertilizers are either reprecipitated in the form of organic complexes by microbes, or form insoluble salts such as calcium orthophosphate ($Ca_3 (PO_4)_2$), hydroxyapatite [$Ca_5 (PO_4)_3 (OH)$] and fluoroapatite [$Ca_{10} (PO_4)_6 F_2$] in the alkaline soils or crystalline ferric phosphates [$FePO_4.2H_2O$ (Cr) or strengite] and crystalline aluminum phosphate [$AlPO_4.2H_2O$ (Cr) or Variscite] in acidic soils (Lindsay *et al*., 1962; Sample *et al*., 1980), by interacting with ions of calcium, iron and

magnesium. Plants are unable to utilize phosphate in these bound forms. Farmers are, therefore, advised to apply four times the phosphate requirement of a particular crop (Goldstein, 1986). This over fertilization often leads to an imbalance of nutrients in the soil and is one of the major environmental concerns. Certain activities in the soil made this phosphate biologically immobile and chemical precipitation would soon deplete the available phosphate supply, leaving very little physically available for the crops. The schematic over view of the phosphate status and important role played by the rhizobacteria in phosphate acquisition by plants is given in figure 1.

There has been a continuous search for viable alternatives to standard chemical phosphate fertilizers. A great deal of this effort was targeted on the intensive regulation of phosphate availability within the rhizosphere, and the well known ability of some bacterial species to dissolve rock phosphate ore (insoluble complexes of phosphate) has been the main area of focus.

1.2 Need and use of the phosphate solubilizing microorganisms (PSMs) for effective plant growth and yield:

Plants do have mechanisms to break open the insoluble phosphorous complexes in soil into soluble inorganic phosphate ions and make use of it. But, they have to spend more than 50 % of stored carbon either in the form of organic acids by acidifying the external environment or by secreting metal chelators for chelating the metal ions. Numerous soil microflora were reported to solubilize insoluble phosphorous complexes into solution and make it possible for its use by the plant (Tripura *et al*., 2005). Several groups of fungi and bacteria, popularly called as phosphate solubilizing microorganisms (PSMs) assist the plants in mobilization of insoluble forms of phosphate. Soil inoculation with PSMs improve solubilization of fixed soil phosphate and applied phosphates resulting in higher crop yields and are effectively used as biofertilizers in enhancing crop yields in phosphate deficient soils. A significant increase in the grain yield was observed for rice, chickpea, lentil, soybean, cowpea and also an increase in the phosphate uptake in

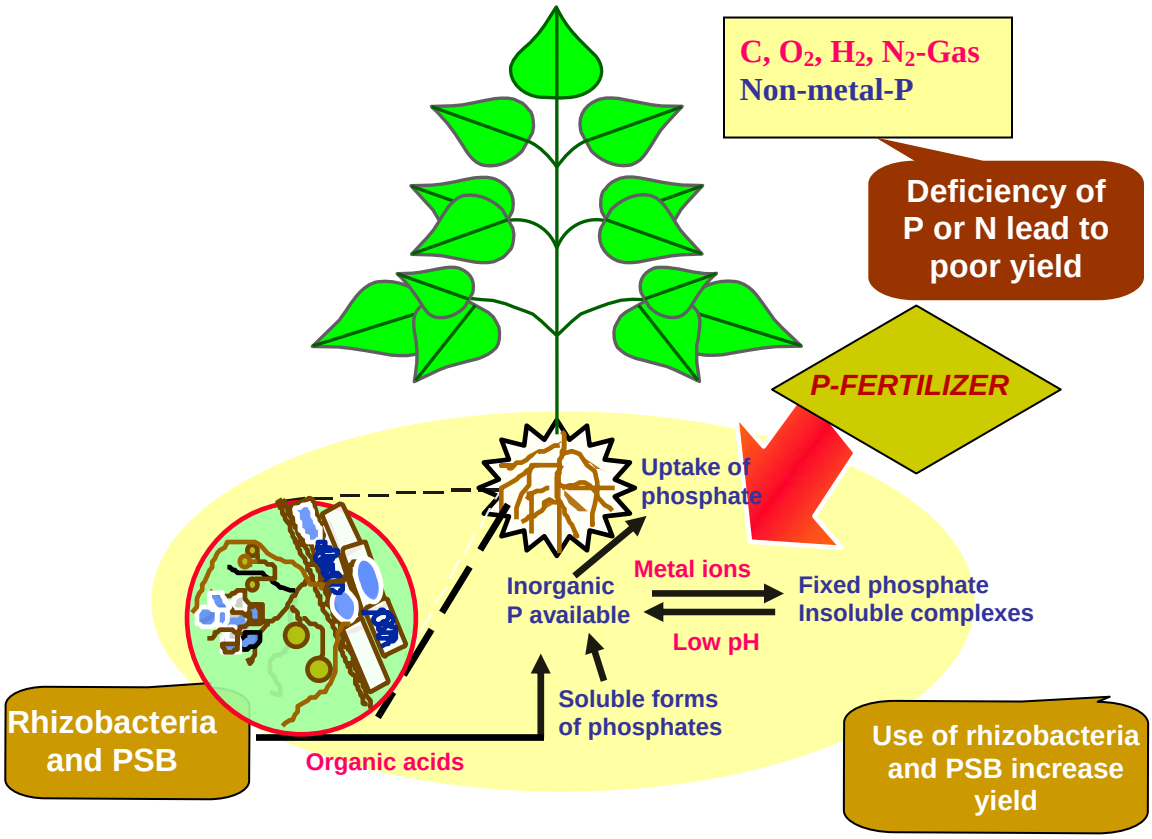

Figure 1: Phosphorus acquisition by plants and the role of rhizobacteria

Phosphorus is one of the major essential macronutrients required by plants for their optimal growth and production. Phosphorus reserves, although abundant in the soil, occur largely in an insoluble form unavailable to the plants. The available forms of phosphrous are supplied in the form of phosphatic fertilizers, but they are immediately fixed by metal ion (Ca^{+2}, Mg^{+2} and Fe^{+3}) present in the soil. The groups of bacteria present at or near the rhizosphere lower the pH of the soil either by H^{+} extrusion or by secretion of organic acids and chelating metabolites, releases phosphates from insoluble phosphatic compounds.

the potato tubers was observed when *Pseudomonas striata*, *Aspergillus awamori* and *Bacillus polymyxa* were used either alone or in combination (Gaur and Ostwal, 1972). Microbial solubilization of inorganic phosphate compounds is of great economic importance in plant nutrition (Gaur, 2002). Bacteria from genera such as *Achromobactrer, Agrobacterium, Bacillus, Enterobacter, Erwinia, Escherichia, Flavobacterium, Mycobacterium, Pseudomonas* and *Serratia* are highly efficient in solubilizing unavailable complexed phosphate into available inorganic phosphate ion (Goldstein, 2001). Phosphate solubilizing bacteria use different mechanism(s) to bring about the insoluble forms of the phosphate into soluble forms. The different mechanism(s) involve the possibility of the organic acids in mineral phosphate solubilization (MPS). Organic acids released by the microorganisms act as good chelators of divalent cations of Ca^{+2} accompanying release of phosphates from insoluble phosphatic compounds. Organic acids may also form soluble complexes with metal ions associated with insoluble 'P', thus releasing phosphate (Kepert *et al.*, 1979). A fall in the pH during the growth of a PSM in liquid medium, containing insoluble phosphate, brings about the solubilization of insoluble phosphates. Many of the PSMs lower the pH of the medium either by H^+ extrusion (Illmer and Schinner, 1995), or by secretion of organic acids such as acetic, lactic, malic, succinic, tartaric, gluconic, 2-ketogluconic, oxalic and citric acids (Kucey *et al*., 1989; Bolan *et al*., 1994). The proton released from the cytoplasm to the outer surface may happen in exchange for a cation (especially ammonium) uptake or with the help of translocating ATPase, which is located in the plasma lemma and uses the energy of ATP hydrolysis. Rock phosphate which is solubilized directly on the cell surface either as H_2PO_4 of HPO_4^{-2}, depending on the pH, could be rapidly absorbed (Beever and Burns, 1980).

1.3 Mineral phosphate solubilization by the products of direct oxidation of glucose:

MPS phenotype has been linked to the production of low molecular weight organic acids (Goldstein, 1986). 2-keto gluconic acid produced by bacteria plays an important role in weathering and solubilization of phosphate in soil (Duff *et al*., 1963) and as a major phosphate solubilizing compound released by rhizobacteria growing in

wheat roots (Moghimi *et al*., 1978) giving an evidence to support the role of the direct oxidation pathway in the MPS phenotype. High efficiency solubilization of rock phosphate ore by *Erwinia herbicola* and *Pseudomonas cepacia* is the result of gluconic and 2-keto gluconic acids produced by the direct oxidation (DO) pathway (described below) in the periplasmic space (Liu *et al*., 1992; Goldstein *et al*., 1993). Some bacteria express the DO pathway to such high levels that extra cellular glucose is rapidly and stoichiometrically converted to gluconic acid at concentrations of 1 mol/l or more (Goldstein *et al*., 1993). Gram-negative bacteria are more efficient at dissolving mineral phosphates compared to Gram-positive bacteria because of the secretion of a large number of organic acids into the extra cellular medium by the metabolism of sugars, predominantly glucose.

Glucose metabolism in Gram-negative bacteria can proceed *via* phosphorylation of glucose to glucose-6-phosphate mediated by the phospho transferase system (PTS) or by the direct oxidation of glucose to gluconate followed by induction of the Entner-Doudoroff pathway (Dawes, 1981; Fliege *et al*., 1992). The non- phosphorylating oxidation pathway that is otherwise known as the DO pathway is one of the four known principal pathways for aldose sugar metabolism in bacteria (Lessie and Phibbs, 1984; Anderson *et al*., 1985; Gottschalk, 1986). The DO pathway forms the metabolic basis for the strong MPS phenotype. The first evidence for the involvement of the DO pathway in MPS was provided by Katznelson *et al*., (1962), where bacteria from the rhizoplane of wheat were more active in glucose oxidation than either rhizosphere or soil bacteria. The phosphate solubilization is the result of acidification of the periplasmic space by the acids produced by the DO of glucose and other aldose sugars by the quinoprotein glucose dehydrogenase (PQQGDH). The DO pathway involves the enzymatic conversion of glucose to gluconic acid ($pK_a \sim 3.4$) by the quinoprotein GDH (Duine *et al*., 1979; Anthony, 1988; Duine, 1991). Gluconic acid often undergoes additional periplasmic oxidations to 2-ketogluconic acid ($pK_a \sim 2.4$) catalyzed by gluconate dehydrogenase (GADH) (Anderson *et al*., 1985). Gluconic and 2-keto gluconic acids are strongest naturally occurring acids secreted into the extracellular medium by bacteria (Duine, 1991), and are capable of acting as Ca^{+2} chelators under appropriate physico-chemical conditions and provide the acidification of the external environment, necessary to

dissolve the poorly soluble calcium phosphates such as tri calcium phosphate (TCP) or hydroxyapatite (HAP) (Krishnaraj and Goldstein, 2001). The levels of gluconic and 2-keto gluconic acids are more in the soils adjacent to the plant roots where the availability of glucose would be higher than in the bulk soils (Goldstein, 1986).

The enzymes of the DO pathway are anchored in the inner membrane but the catalytic domain is oriented in the outer face of the cytoplasmic membranes (Matsushita *et al*., 1980, 1986; Midgley and Dawes, 1973) as in figure 2. Glucose is oxidized in the periplasmic space for the production of the acids at the cell surface. Hence, oxidized products are directly released into the extra cellular space leading to the acidification of the surrounding medium. Each step in the DO of glucose is a two-electron, two-proton-mediated process and the electrons are transferred directly to ubiquinone in the cytoplasmic membrane (Goldstein, 1994). It is assumed that some of these protons freely diffuse out of the periplasmic space and are exchanged for the Ca^{2+} in the rock phosphate releasing either H_2PO_4 of HPO_4^{-2} from the crystal surface of the rock phosphate ore (Goldstein *et al*., 1993), which could be rapidly absorbed.

1.4 Glucose dehydrogenase is the first and key enzyme in phosphate solubilization:

Glucose dehydrogenase (GDH) is a member of the largest group of quinoproteins, that use the redox cofactor 2,7,9,-tricarboxyl-1H-pyrrolo[2,3-f] quinoline-4,5-dione (PQQ) (Duine *et al*., 1979). GDH requires PQQ and has binding sites for Mg^{2+} (*in vitro*), Ca^{2+} (i*n vivo*), ubiquinone, and as well as for substrate glucose (Hommes *et al*., 1984; Matsushita *et al*., 1997) for its activity. Based on the localization within the cell, two types of GDH enzymes have been identified, GDH A and GDH B. GDH B is soluble (s-GDH) and is reported only from *A. calcoaceticus* (Cleton-Jansen *et al*., 1988). GDH A is more widespread and is a membrane bound enzyme (m-GDH) reported from *A. calcoaceticus, P. aeruginosa, G. suboxydans, K. aerogenes A. lwoffi and E. coli.* The GDH of the DO pathway is anchored in the inner membrane but the catalytic domain is oriented in the outer face of the cytoplasmic membranes (Matsushita *et al*., 1980, 1986, Midgley and Dawes 1973), and the substrates are oxidized in the periplasmic space so that the production of the acids occurs at the cell surface. Hence, the products of

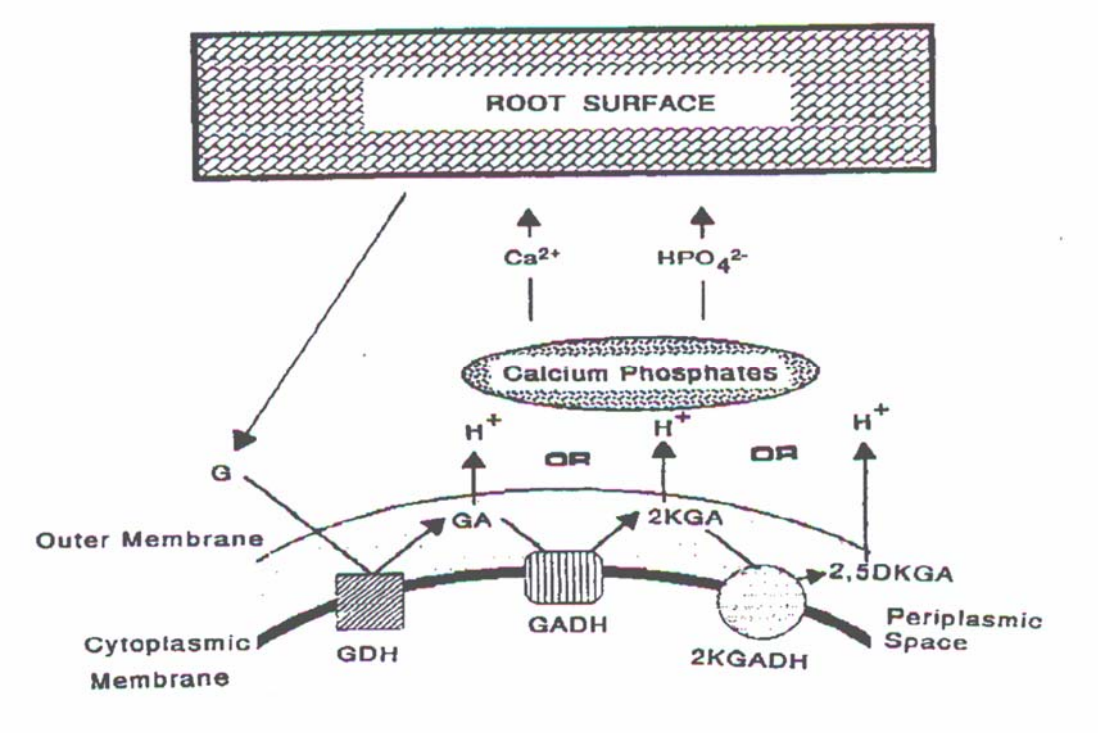

Figure 2: A possible ecophysiological role played by the direct oxidation (DO) pathway in mineral phosphate solubilization at or near the rhizosphere

Glucose provided by the plant either as a secretion product or produced as the result of biodegradation of a carbohydrate polymer becomes a substrate for DO pathway involved glucose dehydrogenase (GDH) in the periplasmic space to produce gluconic acid (GA). Gluconate dehydrogenase (GADH) oxidizes GA to 2-ketogluconic acid (2KGA), which is further oxidized to 2,5-diketogluconic acid (2,5DKGA) by 2-ketogluconate dehydrogenase (2KGADH). Each oxidation step is a two electron/two-proton process and the redox protons are constrained to the bioenergetic or membrane transport processes. However, one acidic proton may be released into extracellular space form any one of the three acidic species produced by the oxidation pathway for every glucose molecule catabolized. This proton is substituted for Ca^{2+} in the mineral phosphates and thus inorganic phosphate 'pi' is released (Source: Goldstein, 1995).

oxidation are directly released into the extra cellular space leading to the acidification of the surrounding medium. In addition to providing carbon for intra cellular metabolism, GDH plays a key regulatory and bioenergetic role in these bacteria. The protons generated in the oxidation contribute directly to the trans-membrane proton motive force (PMF), which results in the uptake of exogenous amino acids and other compounds (Duine, 1991). The acidic protons dissolve the calcium phosphate complexes. Proton substitution for calcium results in release of phosphoric acid from the crystal surface of the mineral phosphate (Goldstein, 1995).

m-GDHs from various bacteria are about 88 kDa monomeric proteins that are similar in primary structure to each other though they differ slightly in some of the properties such as substrate specificities (Yamada *et al*., 2003). Analysis of the protein fusions of m-GDH and the reporter proteins alkaline phosphatase and β-galactosidase, revealed the topological structure of *E. coli* GDH (Figure 3) (Yamada *et al*., 2003). m-GDH has an N-terminal hydrophobic domain (residues 1-150) consisting of five transmembrane segments that ensures a strong anchorage of the protein to the membrane, and a large conserved PQQ-binding C-terminal domain which has the catalytic function (Yamada *et al*., 1993). The location of a ubiquinone binding site and also a membrane-binding site (amphiphathic 80-amino acid residues) was demonstrated in the large C-terminal domain (c-GDH) of *E. coli* m-GDH (Elias *et al*., 2001). The N-terminal domain, interacts with C-terminal domain *via* domain-domain interaction and stabilizes the m-GDH and also as a potential signal sequence for the C-terminal domain (Yamada *et al*., 2003).

PQQ-dependent GDH is present in a wide variety of bacterial species, some of which such as *Acinetobacter calcoaceticus* (Hauge, 1966), *Gluconobacter suboxydans* (Ameyama *et al*., 1981), *Klebsiella aerogenes* (Neijssel *et al*., 1983), and *Pseudomonas aeruginosa* (Midgley and Dawes, 1973), produce the cofactor PQQ themselves. Organisms such as *Escherichia coli* (Hommes *et al*., 1984), *Klebsiella pneumoniae* (Neijssel *et al*., 1983) and *Acinetobacter lwoffi* (van Schie *et al*., 1984), produce PQQ-dependent GDH but are unable to produce PQQ themselves, and so require external supply of PQQ for GDH activity. The location of the GDH apoenzyme on the periplasmic side facilitates the binding of PQQ to form the holoenzyme.

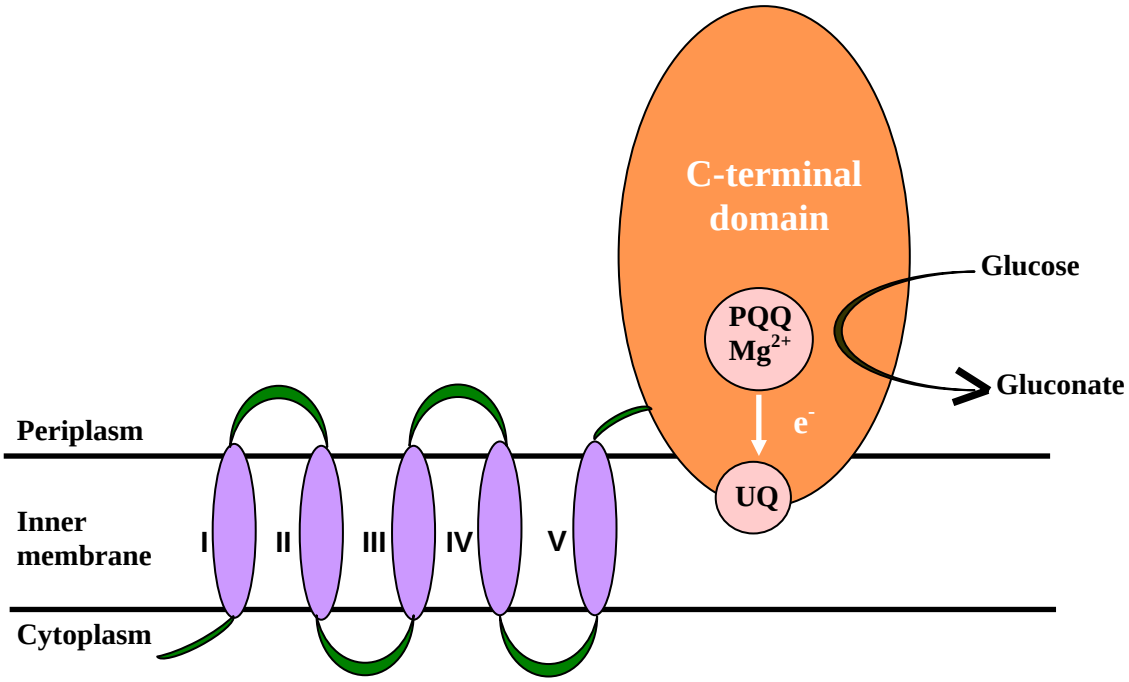

Figure 3: Topological model structure of the m-GDH of *E. coli* and other Gram-negative bacteria

m-GDH has an N-terminal hydrophobic region (residues 1-150) consisting of five transmembrane domains which ensure a strong anchorage of the protein to the membrane. The large C-terminal region (residues 151-786) present towards periplasmic space has the conserved PQQ-binding domain and also the catalytic site. The electrons which are generated during the oxidation of glucose to gluconic acid are directly transferred to the ubiquinone in the respiratory chain (Yamada *et al*., 2003).

Membrane-bound gluconate dehydrogenases (GADHs) which are involved in the further oxidation of gluconic acid to 2-ketogluconic acid have been purified and characterized from *Pseudomonas aeruginosa* (Matsushita *et al*., 1979), *P. fluorescens*, *Klebsiella pneumoniae*, *Serratia marcescens* (Matsushita *et al*., 1982), and *Gluconobacter dioxyacetonicus* (Shinagawa *et al*., 1984). Along with PQQ-dependent GDH, a soluble NADP-dependent GDH, was identified from *Gluconobacter oxydans* (Buchert and Viikari, 1988). GDH catalyzes the oxidation of β-D-glucose to gluconic acid using NAD^+ or $NADP^+$ as the coenzyme in *Bacillus* spp. (Heilmann *et al*., 1988).

1.5 Regulation of genes involved in DO pathway and MPS:

The information regarding the regulation of the genes encoding quinoproteins or the quinoprotein-mediated oxidative metabolism is limited. The gluconic acid phenotype is widely distributed among Gram-negative bacteria, but a major bioenergetic or ecological advantage for this trait could not be identified (Goldstein, 2001). The MPS trait is induced or repressed by low or high levels of inorganic phosphate (Goldstein and Liu, 1987). A cosmid library of *Erwinia herbicola* in *E. coli* screened for MPS phenotype resulted in isolation of a recombinant clone that showed either induced or repressed in presence of soluble or insoluble form of phosphate levels comparable with *E. herbicola* suggested that these genes play a role in bacterial phosphate starvation metabolism and governed by catabolite repression like behavior (Goldstein and Liu, 1987). It was proposed that the oxidative glucose pathway might be important for the survival of enteric bacteria in aerobic, low-phosphate, aquatic environments (Fliege *et al*., 1992).

MPS phenotype is regulated by low molecular weight compounds and expressed when these molecules are present in the medium. MPS genes from *Serratia marcesens* were cloned into *E. coli* DH5α. The clone pKG3791 was capable of inducing holo GDH (PQQGDH) activity and TCP solubilization in the presence of stationary phase *S. marcescens*, suggests the possibility of existence of quorum sensing for induction of the GDH (Krishnaraj and Goldstein, 2001). *Enterobacter cloacae*, isolated from phosphate-limited desert environment, showed no MPS activity and gluconic acid

production. However, high levels of gluconic acid could be induced by the addition of concentrated root wash solutions. The bioactive compound in the root wash was not PQQ suggesting the compound to function either as a regulator or inducer of the PQQ biosynthesis (Goldstein *et al*., 1999).

The biochemical or genetic mechanisms regulating the synthesis or assembly of the GDH/PQQ holoenzyme, and also the mechanisms by which a given species switches between the direct phosphorylative and periplasmic oxidative modes remain unknown (Goldstein, 2001). GDH of *E. asburiae* showed a five-fold increase in activity upon phosphate starvation though the activity was not completely repressed by the presence of available phosphate in the medium (Gyaneshwar *et al*., 1999). *Pseudomonas aeruginosa* expresses the DO pathway in the presence of glucose, but oxidizes less than 1 % of the glucose (Goldstein, 1995). GDH in *P. aeruginosa* is inducible by glucose, gluconate, mannitol and glycerol. Conversely, in *Acinetobacter calcoaceticus* the enzyme is constitutive and glucose is stoichiometrically converted into gluconic acid, but the organism is incapable of utilizing either glucose or gluconic acid for energy metabolism (Goldstein, 1994). The term "dissimilatory bypass" has been used to describe the apparent inefficient utilization of the DO pathway, and the metabolically undefined role of the DO pathway in a particular species (van Schie *et al*., 1985). MPS^- mutants of *E. asburiae* deficient in the GDH activity failed to release phosphate from alkaline soils indicating that GDH activity is required to solubilize phosphate (Gyaneshwar *et al*., 1999).

1.6 Genes involved in DO pathway and MPS:

Genes involved in the DO pathway and MPS, mainly related to *gcd*, *gadh* and *pqq* biosynthesis, were cloned from a number of bacteria. Gene encoding glucose dehydrogenase (*gcd*) involved in the DO pathway was cloned and characterized from *A. calcoaceticus* and *E. coli* (Cleton-Jansen *et al*., 1988, 1990) and *Enteobacter asburiae* (Tripura *et al*., 2007). In addition to the membrane bound *gcd*, a soluble form of *gcd* has also been cloned from *A. calcoaceticus* and *G. oxydans* (Cleton-Jansen *et al*., 1989, 1991).

Five genes involved in the biosynthetic pathway for PQQ production (*pqq* I, II, III, IV, V) have also been cloned from *A. calcoaceticus* (Goosen *et al*., 1987, 1989, 1992). *K. pneumoniae pqq* genes showed homology to the five-*pqq* genes from *A. calcoaceticus* and contain an additional *pqq* F essential for the PQQ biosynthesis, which apparently belongs to the family of proteases *(*Meulenberg *et al*., 1992). *pqq* genes from *G. oxydans* (*pqq* A-E) also share homology to *pqq* I-V of *A. calcoaceticus* (Felder *et al*., 2000). Genes other than *gcd* and involved in MPS were cloned from *E. herbicola*. A 1.8 kb region from the clone pMCG898 having a 4.5 kb insert from *E. herbicola* was found to encode a protein with a M_r of 42,160. The protein shares high homology to *pqq* III of *A. calcoaceticus* and *pqq* E of *K. pneumoniae* and is identified as PQQ synthase involved in PQQ biosynthesis (Liu *et al*., 1992). Expression of this gene conferred gluconic acid producing ability to *E. coli* HB101 and thus MPS^+ phenotype. The gene isolated from *Pseudomonas cepacia* designated as *gabY* confers gluconic acid production and MPS^+ phenotype to *E. coli* JM109. *gabY* shared no homology to the *pqq* sequences, and based on the homology to other proteins it was proposed to play some role in the expression and/or regulation of the DO pathway in *P. cepacia* and therefore may act as a functional MPS gene *in vivo* (Babu-Khan *et al*., 1995). pKIM10 carrying a 7.0 kb *Eco* R I fragment of *Rahnella aquatilis* produced high levels of gluconic acid in *E. coli* DH5α as compared to native *R. aquatilis*. Analysis of the fragment revealed two complete ORFs, and the deduced amino acid sequence was sharing homology with *pqq* D or *pqq* E of *E. herbicola, K. pneumoniae* and *A. calcoaceticus* (Kim *et al*., 1998).

The cosmid library of *Enterobacter agglomerans* in *E. coli* DH5α, when screened for MPS on medium containing HAP, showed that the clone pKKY exhibits phosphate solubilization. However, the solubilization by pKKY was lesser than native *E. agglomerans*. This lesser solubilization could be due to the partial transformation of the genetic information or the presence of multiple genes for phosphate solubilization in *E. agglomerans* (Kim *et al*., 1997b). In *Enterobacter cloacae* a gene with homology to the highly conserved region of the *gcd* of *E. coli* identified through DNA hybridization experiments indicating the existence of the DO pathway (Goldstein *et al*., 1999). A gene cluster encoding three subunits of membrane bound GADH from *Erwinia cypripedii* ATCC 29267 has been cloned and expressed (Yum *et al*., 1997).

1.7 Site directed mutagenesis of GDH to improve/alter the properties:

Many site directed mutations were done on GDH (Table 1) to understand the importance of the given amino acids at specific position and also to understand the structure-function relationship. Many studies on the improvement of enzyme properties suggested that the site specific closer mutations (mutations at or near the active site) to be more efficient rather than random mutagenesis methods which target the entire enzyme making large number of distant mutations (which are less effective) (Morley and Kazlauskas, 2005). However, mutations just outside the active site that alter the substrate binding site could be more effective than mutations directly in the active site which make large changes that can disrupt the catalysis or drastically alter the shape of the binding pocket. GDH from various bacteria differ considerably in enzymatic properties such as EDTA tolerance, substrate specificity, thermal tolerance, cofactor binding site and bivalent metal ion requirement. In *E. coli* GDH substitution at S771M increased in the thermal stability (Sode *et al*., 1995a) and mutation of glutamate 742 to lysine enhanced the EDTA tolerance of *E. coli* PQQGDH (Sode and Sano, 1994).

Yamada *et al*., (1998) demonstrated that mutation of H775R and H775A reduced the affinity of GDH for the prosthetic group PQQ indicting that His-775 contributes to interaction of GDH with PQQ. Where as, D730N and D730A mutations reduced glucose oxidase activity with out influence on affinity of PQQ or Mg^{2+} indicated that this Asp-730 plays specific role for GDH in intermolecular electron transfer to PQQ. D466A and K493A showed very low glucose oxidase activity suggested that Asp-466 is responsible to interact directly and initiates glucose oxidation by abstraction of a proton from glucose and Lys-493 is involved in electron transfer form $PQQH_2$ (Elias *et al.,* 2000). Mutation of His-262 to tyrosine on *E. coli* PQQGDH (Cozier *et al*., 1999) resulted in a major effect on the substrate binding. A protein engineering approach was also used to elucidate the regions responsible for EDTA tolerance, thermal stability and substrate specificity and an ideal chimeric protein, possessing high cofactor stability, was constructed (Yoshida *et al*., 1999). Glodstein *et al*., (2003) demonstrated with a series of mutations at P757X that

Table 1: Details of the known SDMs in glucose dehydrogenase

S. No	Organism	Targeted amino acids	Altered properties	Reference
1	*E. coli*	Arg93 to Ala/Asn	No corresponding amino acid interacts with UQ and electron transfer	Yamada *et al*., 2003
2	*E. coli*	Asp95 to Ala/Asn	No corresponding amino acid interacts with UQ and electron transfer	"
3	*E. coli*	His262 to Tyr	Increased substrate specificity	Cozier *et al*., 1999
4	*E. coli*	His262 to Ala	8-10 fold decrease in affinity for glucose and PQQ	Elias *et al*., 1999
5	*E. coli*	The353 to Leu	Increased *Km* for PQQ	James & Anthony, 2003
6	*E. coli*	Asp354 to Asn	Only 9 % activity compared to wild type	"
7	*E. coli*	Asn355 to Asp	Thermal tolerant & Only 25 % activity compared to wild type	"
8	*E. coli*	Ser357 to Leu	Increased Km for PQQ	Yamada *et al*., 1998
9	*E. coli*	Trp404 to Ala	Reduced affinity for PQQ, PMS reductase, glucose oxidase and only 40 % targeted to membrane	Elias *et al*., 1999
10	*E. coli*	Trp404 to Phe	Relatively high activity and 90 % targeted to membrane	"
11	*E. coli*	Asp466 to Asn/Glu/Ala	Very low glucose oxidase and Q-2 reductase activity	"
12	*E. coli*	Lys493 to Ala/Arg	Very low glucose oxidase and Q-2 reductase activity	"
13	*E. coli*	Lys685 to Ala	Only 75 % targeted to the membrane	Yamada *et al*., 1998
14	*E. coli*	Arg687 to Asp/Ala	Only 2 % targeted to the membrane	"
15	*E. coli*	Gly689 to Asp/Ala	Increased *Km* for PQQ	"
16	*E. coli*	Asp693 to Ala	Only 18 % targeted to the membrane	"
17	*E. coli*	Asp730 to Ala/Asn	Very low glucose oxidase activity with out influencing on PQQ	"
18	*E. coli*	Asp730 to Arg	Very low glucose oxidase activity and reduced affinity for PQQ	"
19	*E. coli*	Gly741 to Ser	Less than 10 % targeted to membrane	"
20	*E. coli*	Glu742 to Gly	Higher *Km* for metal ion	"
21	*E. coli*	Glu742 to Lys	EDTA tolerance	Sode and Sano, 1994
22	*E. coli*	Leu744 to Ala	Only 58 % activity compared to wild type	Goldstein *et al*., 2003
23	*E. coli*	Pro757 to X (Any other amino acid)	0 to 70 % activity & no corresponding amino acid interacts with PQQ and metal ion	"
24	*E. coli*	Gly764 to Ala	Only 52 % activity compared to wild-type	"
25	*E. coli*	Tyr767 to Ala	No activity	"
26	*E. coli*	Se771 to Met	Increased thermal tolerance	Sode & Kojima, 1997
27	*E. coli*	His775 to Ala/ Arg	Decreased affinity for PQQ	Yamada *et al*., 1998
28	*E. coli*	His775 to Asn/Asp	Increased substrate affinity with out affecting affinity for PQQ	Sode & Kojima, 1997
29	*E. coli*	His782 to Asp	EDTA tolerance	Yoshida *et al*., 2000
30	*E. coli*	Stop797 to Lys	Reduced Q1 oxidase activity	Yamada *et al*., 1998
31	*G. suboxydans*	His787 to Asn/Asp	Increased substrate specificity	Cleton-Jansen *et al*., 1991
32	ES chimera	Glu742 to Lys	EDTA tolerance	Tripura & Podile, 2007
33	ES chimera	Tyr771 to Met	Low activity and EDTA tolerance	"
34	ES chimera	His775 to Ala	Substrate affinity marginally affected and EDTA tolerance	"

provide a range of activity form 77 % of wild type (P757) to knockouts (P757F and P757Y) indicated that the highly conserved region (HCR) of PQQDHs may regulate the funnel diameter of the super barrel. This Pro-757 in GDH was compared to Pro-520 of PQQMDH α subunit of *Methylobacterium extorquens.*

Apart from SDMs there were also many chimeric GDH constructions which improved the properties of the enzyme. Using protein engineering approach, constructed an ideal chimeric protein possessing EDTA tolerance, thermal stability, substrate specificity and high cofactor stability. The construction and characterization of chimeric proteins is a versatile and powerful method to elucidate the region(s) responsible for enzymatic activity (Ogawa *et al*., 1992). PQQGDH from *E. coli* and *A. calcoaceticus* has been extensively studied. A chimeric PQQGDH with 97 % of N-terminal region of *E. coli* PQQGDH and 3 % of *A. calcoaceticus* PQQGDH was constructed for increased thermal stability. Different multi-chimeric constructs with varying N-terminal and C-terminal regions of *E. coli* and *A. calcoaceticus* identified the region responsible for EDTA tolerance to be located between 45 and 56 % of the distance from the N-terminal region of *A. calcoaceticus* PQQGDH, corresponding to about 90 amino acid residues (Sode *et al*., 1995b).

1.8 Transgenic bacterial inoculants for agriculture benefits:

The problems associated with the availability of phosphate in soluble form, and also the associated problems with phosphate fertilizers, necessitate use of bioinoculants, which bring about MPS as a source of biofertilizers. In the early 1960s cultures of *Bacillus megaterium*, in the name "Phosphobacterin", were used as phosphatic fertilizer in the Soviet Union and several eastern European countries (Tisdale and Nelson, 1975). Only a small increase in the yield was observed and the effect was not consistent with other crops. A major problem therefore with the microbial inoculants was their inconsistency in field performance. This could be due to inefficient colonization of rhizosphere, difference in soil, nature, plant, type, competition with the native microflora etc. This problem may be circumvent by introducing the genes responsible for MPS trait into microbes, which are well adapted in the rhizosphere.

Genetic manipulation is considered as the most promising way to create more effective PGPR. Using transgenic approaches the agronomic efficiency of these strains has to be enhanced above their natural plateau by introducing the MPS genes. It is also essential to develop strains with multiple agronomic beneficial traits. Many rhizospheric bacteria show plant growth enhancement due to mechanisms involving plant growth promoting substances and nitrogen fixation both symbiotically and asymbiotically. These plant growth promoting rhizobacteria (PGPR), mostly represented by the fluorescent pseudomonads such as the *Pseudomonas fluorescens*, *P. aeruginosa*, *P. cepacia*, *P. putida* and the other species of *Azospirillum*, *Azotobatcer*, *Bacillus*, *Bradyrhizobium*, *Enterobacter*, *Erwinia*, and *Rhizobium* show a proficient colonization at the root zone. Most of the *Pseudomonas* species have an ability to utilize a wide variety of organic substrates found in root exudates and thus form a very versatile group of PGPR.

The genes involved in the DO pathway encoding GDH, GADH and PQQ could be introduced into any of these rhizobacteria imparting them additional properties of MPS in addition to their plant growth promotion and nitrogen fixation thus generating more effective bioinoculants. pMCG898 harboring the 1.8 kb gene in a 4.5 kb insert encoding PQQ synthase when transferred into two rhizobacteria, *Pseudomonas spp*. PSS and *Burkhordelia cepacia* IS-16, using a broad-host-range vector pKT230 was shown to enhance the MPS ability of these organisms *in vitro* (Rodriguez *et al*., 2000). Mineral phosphate solubilizing genes that are not involved in the DO pathway have also been cloned from *Synechocystis* PCC 6803 (Gyaneshwar *et al*., 1998b). Phosphoenolpyruvate carboxylase (*ppc*) gene of *Synechococcus* PCC 7942 when introduced into the rhizobacterium *Pseudomonas fluorescens*, imparted MPS trait to the latter organism (Tripura *et al*., 2005). Development of such strains can help harvest the fixed phosphate reserve that is present in the soils and help to reduce the dependence on the imported phosphatic fertilizers by utilizing the rock phosphate.

1.9 Overview of the present work:

The different bacteria isolated form our laboratory were screened for their ability to solubilize the insoluble complexes of phosphate supplements as tri calcium phosphate

in PVK and NBRIP medium, *Serratia marcescens* GPS5, a biocontrol agent isolated form groundnut phyllosphere emerged as best phosphate solubilizer. We made an attempt to improve the MPS ability of this organism. Random mutagenesis with mild doses of ethyl methanesulfonate (EMS) was selected.

Azotobacter, a free-living nitrogen fixer, is known to increase the fertility of the soil and in turn productivity of different crops. *Azotobacter* is a poor phosphate solubilizer. We made an attempt to enhance the biofertilizer potential of *Azotobacter* in terms of MPS with out affecting the nitrogen fixation ability. The *gcd* gene involved in the MPS trait, introduced into *Azotobacter* under regulation of *Azotobacter*-specific promoters, may confer dual benefit to the agriculture in terms of both nitrogen fixation and phosphate solubilization by a single strain is the main focus of this work.

To further understand the GDH structure we made an attempt to build the homology model 3D structure of this protein to identify the critical amino acid residues in the active site. Through site directed mutagenesis of critical amino acid residues we made attempts to study the role of these amino acid residues at specific position(s) and correlated to the structure-function relationship.

1.10 Objectives:

Three main objectives were designed for the present work.

- Isolation of MPS-related mutants of *Serratia marcescens* GPS 5 by chemical mutagenesis.
- Development of transgenic *Azotobacter* to confer MPS as an added trait to this nitrogenous biofertilizer.
- Homology modeling and site directed mutagenesis of *Escherichia coli* glucose dehydrogenase to understand structure-function relation.

Materials and Methods

2. 1. 1 Bacterial culture and plasmids

The details of the various bacterial isolates, *E. coli* strains and plasmids used in the work are listed in Tables 2 and 3.

2. 1. 2 Culture media

The various media used for culturing bacteria for different purposes were as follows:

a) National Botanical Research Institute's Phosphate (NBRIP**)** agar medium (Nautiyal, 1999) with a slight modification having Hydroxyapatite (HAP) in place of tri calcium phosphate (TCP), [per litre: glucose, 10.0 g; HAP 5.0 g; $MgCl_2.6H_2O$, 5.0 g; $MgSO_4.7H_2O$, 0.25 g; KCl, 0.2 g; and $(NH_4)_2\ SO_4$, 0.1 g] was used for screening of the bacterial isolates for their MPS ability. NBRIP liquid medium was used for the quantitation of the phosphate solubilization. NBRIP agar and liquid medium with ampicillin (for pUC18 and pQE30 based vectors) and chloramphenicol (for pMMB206 based vector), with and with out IPTG and PQQ were used to study the MPS ability of the different *gcd* clones.

b) Minimal medium [per litre glucose, 10.0 g, KH_2PO_4, 10.9 g; $(NH_4)_2\ SO_4$, 1.0 g; $MgSO_4.7H_2O$, 0.16 g; $FeSO_4.7H_2O$, 0.005 g; $CaCl_2.2H_2O$, 0.011 g; and $MnCl_2.4H_2O$, 0.002 g] to raise the inoculum used for the purpose of EMS mutagenesis of *S. marcescens* GPS 5.

c) LB medium (per lite: 1 % tryptone, 0.5 % yeast extract and 1 % sodium chloride) was used as general growth medium for the *E. coli* cultures and for the *gcd* clones with appropriate antibiotics.

d) LB medium with out NaCl (per lite: 1 % tryptone and 0.5 % yeast extract) was used for preparation of high efficient competent cell of *E. coli* XL1 Blue MRF'.

d) MacConkey glucose agar (per lite: 2 % peptone, 0.5 % sodium tauroglycocholate, 1 % glucose, 2 % neutral red) indicator plates, supplemented with ampicillin (for pUC18 and pQE30 based vectors) and chloramphenicol (for pMMB206 based vector), with and with

Table 2: List of the bacterial cultures used for isolation of *gcd*, cloning and expression

Bacterial cultures	Purpose	Source
Enterobacter asburiae	*gcd* isolation	Dr. Naresh Kumar
Serratia marcescens GPS5	*gcd* isolation & EMS mutagenesis	Dr. G. K. Kishore
Azotobacter vinelandii AVOP	Promoter isolation & expression host	Dr. C. Kennedy
Escherichia coli DH5α	*gcd* isolation & cloning host	Our collection
E. coli XL1 Blue MRF'	Transformation	Stratagene
E. coli PP2418 (*gcd*::*cm* & *pts*$^-$)	Expression host	Dr. N. Goosen
E. coli YU423 [del (*pts* HI crr) *gal*P::Tn10 *gcd*::*cm*]	Expression host	Dr. M. Yamada
E. coli AT15 (*gcd*::*cm*) (pREP4)	Expression host	Dr. C. B. Tripura

Table 3: List of plasmids used or generated in this work

Plasmid	Size (kb)	Purpose/ Description	Source
pUC18	2.6	Cloning vector	Our collection
pUCGS1	2.83	*Azotobacter*-specific *gln*A-*p*1 in pUC18	This work
pUCGS2	2.73	*Azotobacter*-specific *gln*A-*p*2 in pUC18	This work
pUCPS1	2.78	*Azotobacter*-specific *pts*-*p*1 in pUC18	This work
pUCPS2	2.72	*Azotobacter*-specific *pts*-*p*2 in pUC18	This work
pUCGDE	5.0	*E. coli gcd* in pUC18	This work
pGDEGS1	5.23	*E. coli gcd* under *gln*A-*p*1 in pUC18	This work
pGDEPS1	5.18	*E. coli gcd* under *pts*-*p*1 in pUC18	This work
pGDESGS1	5.23	*ES* chimeric *gcd* under *gln*A-*p*1 in pUC18	This work
pGDESPS1	5.18	*ES* chimeric *gcd* under *pts*-*p*1 in pUC18	This work
pGDNTGS1	5.23	*E. asburiae gcd* under *gln*A-*p*1 in pUC18	This work
pGDNTPS1	5.18	*E. asburiae gcd* under *pts*-*p*1 in pUC18	This work
pMMB206	9.31	broad-host range cloning vector	Prof. S. Dayananda
pMMBEGS1	11.9	*E. coli gcd* under *gln*A-*p*1 in pMMB206	This work
pMMBEPS1	11.8	*E. coli gcd* under *pts*-*p*1 in pMMB206	This work
pQE30	3.4	Expression vector	Qiagen
pATEE	5.8	*E. coli gcd* in pQE30	Dr. C. B. Tripura
pATESE	5.8	*ES* chimeric *gcd* in pQE30	Dr. C. B. Tripura
pATEE R201A	5.8	*gcd* mutant R201A (CGT-GCC) on pATEE	This work
pATEE D204A	5.8	*gcd* mutant D204A (GAT-GCC) on pATEE	This work
pATEE E217L	5.8	*gcd* mutant E217L (GAA-CTT) on pATEE	This work
pATEE E217Q	5.8	*gcd* mutant E217Q (GAA-CAG) on pATEE	This work
pATEE E217A	5.8	*gcd* mutant E217A (GAA-GCC) on pATEE	This work
pATEE R266E	5.8	*gcd* mutant R266E (CGT-GAA) on pATEE	This work
pATEE R266Q	5.8	*gcd* mutant R266Q (CGT-CAG) on pATEE	This work
pATEE E591L	5.8	*gcd* mutant E591L (GAA-CTT) on pATEE	This work
pATEE E591Q	5.8	*gcd* mutant E591Q (GAA-CAG) on pATEE	This work
pATEE E591K	5.8	*gcd* mutant E591K (GAA-AAA) on pATEE	This work
pATEE L712W	5.8	*gcd* mutant L712W (CTG-TGG) on pATEE	This work
pATEE L712R	5.8	*gcd* mutant L712R (CTG-CGT) on pATEE	This work
pATEE G776A	5.8	*gcd* mutant G776A (GGT-GGC) on pATEE	This work
pATEE G776L	5.8	*gcd* mutant G776L (GGT-CTT) on pATEE	This work
pATEE G776D	5.8	*gcd* mutant G776D (GGT-GAT) on pATEE	This work
pATEE G776K	5.8	*gcd* mutant G776K (GGT-AAA) on pATEE	This work

out IPTG and PQQ were used for the GDH complementation tests.

e) 2XYT medium (per lite: 1.6 % tryptone, 1 % yeast extract and 5 % sodium chloride) was used for the expression and purification of glucose dehydrogenase.

f) *Azotobacter* Growth (AG) medium (per liter: $MgSO_4$ $7H_2O$, 0.2 g; $CaSO_4$, 0.1 g; Yeast extract, 0.5 g; Sucrose, 20 g; K_2PO_4, 0.8 g; and KH_2PO_4, 0.2 g; with trace amount of $FeCl_3$ and Na_2MoO_4 and pH 7.2) was used for growing *Azotobacter* (Glick *et al*., 1985).

g) *Azotobacter* Transformation (AT) medium (per liter: $MgSO_4$ $.7H_2O$, 1.9718 g; $CaSO_4$, 0.0136 g; CH_3COONH_4, 1.1 g; Glucose, 10.0 g; KH_2PO_4, 0.25 g; K_2HPO_4, 0.55 g and pH 7.1) was used preparation of competent cells of *Azotobacter* and mobilization of high molecular weight plasmids into *Azotobacter* (Glick *et al*., 1985).

h) Burk's nitrogen free medium consisted of Salt I, Salt II, Salt III and 1 % Sucrose. (per liter: **Salt I** (100 X) K_2HPO_4, 64.0 g; KH_2PO_4, 16.0 g; Na_2SO_4, 14.2 g; **Salt II** (1000 X) $MgCl_2$ $.6H_2O$, 203.0 g; $CaCl_2$. $2H_2O$, 4.41 g; **Salt III** (1000 X) Na_2MoO_4, 2.0 g; Fe EDTA, 5.0 g; Conc. HCl 2.0 ml) was used for reviving the *Azotobacter* from glycerol stocks and for acetylene reduction assay (Newton *et al*., 1953).

2. 1. 3 Chemicals

Hydroxyapatite (HAP), Tri calcium phosphate, and Pyrroloquinoline quinone (PQQ) from Sigma-Aldrich (USA) and isopropyl-β-D-thiogalactoside (IPTG) and X-Gal from Eppendorf (Germany) were used. Ampicillin (75 µg/ml for cloning vectors and 100 µg/ml for expression vectors) was from Sigma-Aldrich while chloramphenicol (50 µg/ml) was from Himedia (India). All other chemicals and routine media components of analytical grade were from Himedia laboratories.

2. 1. 4 Enzymes

All restriction enzymes, T4 DNA ligase, used for molecular cloning were procured either from Pharmacia (USA), or MBI Fermentas (Germany), and used as per the manufacturers' instructions. Dynazyme II was from Finnzymes and *Pfu* DNA polymerase was from MBI Fermentas (Germany). $VENT^+$ DNA polymerase and *Dpn* I was form NEB (England).

.

2. 1. 5 Kits

Kits from Eppendorf (Germany), Qiagen (Germany) or Sigma-Aldrich (USA) were used for plasmid isolation, gel extraction, PCR product purification and genomic DNA isolation.

2. 2 SCREENING OF EFFICIENT PHOSPHATE SOLUBILIZING BACTERIA

2. 2. 1 Screening of phosphate solubilizing bacteria on solid media

The bacterial cultures were screened for their mineral phosphate solubilizing ability by spotting in triplicates on NBRIP media having HAP as the sole source of phosphate. After 1 week of incubation at 28 ^{o}C, PSB were detected based on the zone of clearance around the colony. The extent of phosphate solubilizing ability was determined by subtracting the diameter of the zone from the diameter of the colony.

2. 2. 2 Quantitative determination of phosphate solubilization in liquid media

Quantitative estimation of phosphate solubilization was carried out in 150 ml Erlenmeyer flasks containing 30 ml of buffered (100 mM Tris.Cl, pH 7.2) NBRIP medium inoculated (1 % inoculum) with the bacterial strains in triplicates and incubated at respective growth temperature conditions (For *E. coli* and *E. asburiae* at 37 ^{o}C and for *S. marcescens* GPS 5 at 28 ^{o}C) and 150 rpm. Uninoculated medium served as the control. One ml samples were withdrawn, after every 24 h, for 1 week and centrifuged at 6000 g for 5 min. The cell-free supernatant was used for inorganic phosphate ('pi') estimations (Ames, 1964). Known concentration of KH_2PO_4 served as standard. To 0.3 ml of the appropriately diluted cell free supernatant, 0.7 ml of the reaction mixture (1 part of 10 % ascorbic acid: 6 parts of 0.42 % ammonium molybdate in conc. sulphuric acid) was added. After incubation at 37 ^{o}C for 1 h the absorbance was measured at 820 nm.

2. 3 ETHYL METHANESULFONATE (EMS) MUTAGENESIS OF *S. MARCESCENS* GPS 5

Ethyl MethaneSulfonate (EMS) causes transitions by methylation of G residues but can yield a spectrum of mutations such as deletions in the DNA and acts as mild mutagen. EMS is not lethal but causes optimal mutations in the bacteria (Coulondre and Miller, 1977), therefore, was used as mutagen. The pH of the buffer A was 7.3 instead of pH 7.0, since it was known that EMS is highly active under alkaline pH than in neutral pH. *S. marcescens* GPS 5 cells grown in minimal medium, up to mid log phase, were incubated on ice for 30 min. The cell pellet obtained by centrifugation at 10,000 rpm for 10 min at 4 ^{o}C was washed twice in buffer A and resuspended in the same buffer having EMS at 1.4 %. Samples were withdrawn after every 15 min for 1 h, washed twice with buffer A and resuspended in half the volume of the same buffer. Serial dilutions were plated on LB medium. Eighty to ninety well-isolated colonies at 10^{-7} dilution were spotted in NBRIP agar. A total of 1700 individual colonies were randomly selected to test if there was alternation in the MPS phenotype of these mutants. After 7 days of incubation at 28 ^{o}C, the zone of solubilization was measured by subtracting the colony diameter from the diameter of the zone of solubilization. A few selected mutants were further inoculated in buffered NBRIP liquid medium and the cell free supernatant of the samples drawn, after every 24 h for one week were analyzed for the 'pi' estimations, as described in 2.2.2.

2. 4 PCR-BASED CLONING OF *AZOTOBACTER*-SPECIFIC PROMOTERS

The molecular biology methods, PCR, agarose gel electrophoresis, plasmid isolation, restriction digestion, cloning and transformation were according to the protocols described by Sambrook *et al*., (1989). The details of the primers and templates used in the PCR for cloning of *Azotobacter*-specific promoters and *gcd* are listed in Table 4. Oligonucleotide primers were synthesized either by Sigma-Aldrich (USA) or MWG Biotech (Germany).

2. 4. 1 Genomic DNA isolation: Genomic DNA from *Azotobacter vinelandii* AVOP, *E. coli* DH5α, *S. marcescens* GPS 5 and *E. asburiae* was isolated using DNeasy kit (Qiagen).

2. 4. 2 Amplification and cloning of *Azotobacter*-specific glutamine synthetase (*gln*A) gene promoter: Promoter specific primers were designed upstream to the glutamine synthetase (*gln*A) gene of *Azotobacter vinelandii* AvOP with two forward primers, Fp GS1and Fp GS2 starting at different positions and a common reverse primer, Rp GS. These promoters were designated as *gln*-p1 for large expected amplicon (228 bp) and *gln*-p2 for small expected amplicon (134 bp). The promoter sequences were amplified with an annealing temperature of 56 ^{o}C and *Pfu* DNA polymerase using the genomic DNA of *A. vinelandii* AvOP as the template. pUC18 and the purified PCR (Qiagen PCR purification kit) amplicons were double digested with *Hind* III and *Bam* HI, gel purified, and ligated using T4 DNA ligase at 16 ^{o}C for 16 h.

2. 4. 3 Amplification and cloning of *Azotobacter*-specific phosphonate transport system (*pts*) gene promoter: Primers were designed upstream to the phosphonate transport system (*pts*) gene of *Azotobacter vinelandii* AvOP with two forward primers, Fp PS1 and Fp PS2 starting at different positions and a common reverse primer, Rp PS. These promoters were designated as *pts*-p1 for large expected amplicon (182 bp) and *pts*-p2 for small expected amplicon (128 bp). The promoter sequence was amplified with an annealing temperature of 56 ^{o}C and *Pfu* DNA polymerase using the genomic DNA of *Azotobacter vinelandii* AvOP as the template. pUC18 and the purified PCR (Qiagen PCR purification kit) amplicons were double digested with *Hind* III and *Bam* HI, gel purified, and ligated using T_4 DNA ligase at 16 ^{o}C for 16 h.

2. 4. 4 Transformation: Competent cells of either *E. coli* DH5α or *E. coli* XL1 blue were transformed with the ligation mixture (described in section 2. 4. 2 and 2. 4. 3) and the recombinants were screened by α- complementation. Minipreps of a few randomly selected white colonies were checked for the presence of insert both by restriction

analysis and PCR. The sequence was verified by sequencing at Bioserve Biotechnologies (India) or at Sigma-Aldrich (USA).

2. 5 PCR-BASED CLONING OF GLUCOSE DEHYDROGENASE (*gcd*) GENE FORM SELECTED GRAM-NEGATIVE BACTERIA

2. 5. 1 Amplification of *gcd* from *E. asburiae*: *E. asburiae gcd* was amplified from the genomic DNA of *E. asburiae* with gene specific primers Fp EGD & Rp EGD (Table 4) using *Pfu* DNA polymerase at an annealing temperature of 58 ^{o}C and polymerization for 5 min.

2. 5. 2 Amplification of *E. coli*-*S. marcescens* GPS 5 (ES) chimeric *gcd*: *ES chimeric gcd* was amplified from the pATESE (*ES* chimeric *gcd* in pQE30) DNA as templates with gene specific primers Fp EGD & Rp SMGD (Table 4) using *Pfu* DNA polymerase at an annealing temperature of 58 ^{o}C and polymerization for 5 min.

2. 5. 3 Amplification and cloning of *gcd* from *E. coli*: *E. coli gcd* was amplified from the genomic DNA of *E. coli* DH5α with gene specific primers Fp EGD & Rp EGD (Table 4) using *Pfu* DNA polymerase at an annealing temperature of 58 ^{o}C and polymerization for 5 min. pUC18 and the purified PCR (Qiagen PCR purification kit) amplicon were double digested with *Bam* HI and *Eco* RI, gel purified, and ligated using T_4 DNA ligase at 16 ^{o}C for 16 h.

2. 5. 4 Cloning of *gcd* under *Azotobacter*-specific promoters: *gcd* of ES chimera and *E. asburiae* purified PCR (Qiagen PCR purification kit) amplicons were double digested with *Bam* HI and *Eco* RI, gel purified, and ligated to the *Bam* HI and *Eco* RI digestion of pUCGS1 (*Azotobacter*-specific *gln*A-*p*1 in pUC18) and pUCPS1 (*Azotobacter*-specific *pts*-*p*1 in pUC18) using T_4 DNA ligase at 16 ^{o}C for 16 h. where as *E. coli gcd* cloned in the cloning vector was released form the plasmid pUCGDE and ligated to the *Bam* HI

Table 4: List of primers used for amplification of *Azotobacter*-specific promoters and *gcd*

S. No.	Primer code	Primer sequence (5'→ 3')	Restriction site	Product amplified
1	Fp GS1	ATC**AAGCTT**CCCAGGCACATAAACAGAGC	*Hind* III	*gln*A-*p1* (228 bp) with Fp GS1 and Rp GS & *gln*A-*p2* (134 bp) with Fp GS2 and Rp GS
	Fp GS2	GCC**AAGCTT**GTGGCATGAAACTTGCTCC	*Hind* III	
	Rp GS	GCGACTTCG**GGATCC**TGTCCTCCAGGTGG	*Bam* HI	
2	Fp PS1	GC**AAGCTT**GAGGACCGATTATAGCGG	*Hind* III	*pts- p1* (182 bp) with Fp PS1 and Rp PS & *pts-p2* (128bp) with Fp PS2 and Rp PS.
	Fp PS2	CGA**AAGCTT**AATGTCAAGCGGCGGC	*Hind* III	
	Rp PS	CCGCGTGAC**GGATCC**ATGAATACAAGATG	*Bam* HI	
3	Fp EGD	AGC**GGATCC**ATGGCAATTAACAATACAGG	*Bam* HI	*E. coli gcd* (2.4 kbp) and *E. asburiae gcd* (2.4 kb)
	Rp EGD	CCC**GAATTC**TTACTTCACATCATCCGGCA	*Eco* RI	
4	Fp EGD	AGC**GGATCC**ATGGCAATTAACAATACAGG	*Bam* HI	*E. coli –S. marcescens* (ES) chimeric *gcd* (2.4 kb)
	Rp SMGD	ACG**GAATTC**TTTACTTCTGATCGGGCAGGG	*Eco* RI	

Fp: Forward primer; Rp: Reverse primer
The restriction site added in the primer is indicated in bold and underlined

and *Eco* RI digestion of pUCGS1 (*Azotobacter*-specific *gln*A-*p*1 in pUC18) and pUCPS1 (*Azotobacter*-specific *pts*-*p*1 in pUC18) using T_4 DNA ligase at 16 ^{o}C for 16 h. Minipreps of few randomly selected colonies were checked for the presence of insert both by restriction analysis and PCR.

2. 6 EXPRESSION OF GLUCOSE DEHYDROGENASE (*gcd*) UNDER REGULATION OF AZOTOBACTER-SPECIFIC PROMOTERS IN *E. COLI* PP2418

2. 6. 1 Complementation of *E. coli, E. asburiae* and ES chimeric GDH in *E. coli* PP2418: The expression of *gcd* was detected by the GDH complementation in MacConeky glucose agar medium and by the mineral phosphate solubilization in NBRIP medium.

2. 6. 1. 1 Complementation of the clones in MacConkey medium: For the complementation test on a solid medium *E. coli* PP2418 harboring pGDEGS1, pGDEPS1, pGDNTGS1, pGDNTPS1, pGDESGS1, and pGDESPS1 were spotted in triplicates on MacConkey glucose (1 %) agar supplemented with 100 µg/ml of ampicillin, with 200 nM PQQ and without PQQ. The growth pattern was compared after 24 h incubation at both 37 ^{o}C (for *E. coli* and *E. asburiae gcd* clones) and 28 ^{o}C (for ES chimeric *gcd* clones). *E. coli* PP2418 harboring pUCPS1 and pUCGDE served as the negative control where as *E. coli* DH5α harboring pUC18 served as positive control.

2. 6. 1. 2 Mineral phosphate solubilization by the *gcd* clones on NBRIP agar: To evaluate the mineral phosphate solubilizing ability, *E. coli* PP2418 harboring pGDEGS1, pGDEPS1, pGDNTGS1, pGDNTPS1, pGDESGS1, and pGDESPS1 were spotted in triplicates on NBRIP agar supplemented with 100 µg/ml ampicillin and with 200 nM PQQ. The zone of solubilization was measured after 1 week of incubation at 37 ^{o}C (for *E. coli* and *E. asburiae gcd* clones) and 28 ^{o}C (for ES chimeric *gcd* clones). *E. coli* PP2418 harboring pUCPS1 and pUCGDE served as the negative control where as *E. coli* DH5α harboring pUC18 served as positive control.

2. 6. 1. 3 Mineral phosphate solubilization by the *gcd* clones in NBRIP liquid medium: Quantitative estimation of phosphate solubilization was done in 150 ml Erlenmeyer flasks containing 30 ml of NBRIP medium supplemented with ampicillin (100 μg/ml) and 200 nM PQQ. The medium was inoculated (1 % inoculum of culture at an OD_{600} of approx. 1.0) with *E. coli* PP2418 harboring pUCPS1, pUCGDE, pGDEGS1, pGDEPS1, pGDNTGS1, pGDNTPS1, pGDESGS1, and pGDESPS1 in triplicates and incubated at 37 ^{o}C (for *E. coli* and *E. asburiae gcd* clones) and 28 ^{o}C (for ES chimeric *gcd* clones) and 150 rpm. Uninoculated medium served as the control. One ml samples were withdrawn, after every 24 h, for 1 week and centrifuged at 10,000 rpm for 10 min. The cell-free supernatant was used for 'pi' estimations were done as described in section 2. 2. 2.

2. 7 CLONING OF *E. COLI GCD* UNDER *AZOTOBACTER*-SPECIFIC PROMOTERS IN pMMB208 AND MOBILIZATION INTO *AZOTOBACTER*

The recombinant plasmids pGDEGS1 and pGDEPS1 was not maintained stable in *Azotobacter*, hence for a alternative *E. coli gcd* with promoter sequences were cloned in broad-host-range vector pMMB206 (Morales *et al*., 1991).

2. 7. 1 Cloning of *E. coli gcd* under *Azotobacter*-specific *gln*A and *pts* gene promoters: *E. coli gcd* along with *gln*A-p1 and *E. coli gcd* with *pts*-p1 promoter, cloned in the cloning vectors was released from the plasmids pGDEGS1 & pGDEPS1 respectively. Since the double digested bands from pGDEGS1 and pGDEPS1 were inseparable entire mixture was used to ligate the *Eco* RI and *Hind* III digested broad-host-range vector pMMB206. The recombinant clones were selected with blue white screening. From these the clones having the desired insert (*glnA*1+ *gcd* and *pts*1+ *gcd*) were selected by replica plating. Colonies that were spotted on LB containing chloramphenicol were replica plated on LB containing ampicillin plate. The colonies that were not growing on LB ampicillin plate were considered as the clones of interest. Colonies from chloramphenicol plate were inoculated into liquid medium containing

chloramphenicol as a selectable marker. Minipreps of few randomly selected colonies were checked for the presence of desired insert both by restriction analysis and PCR.

2. 7. 2 Mobilization of pMMBEGS1 and pMMBEPS1 clones into *Azotobacter* and verification: For standard transformation protocol (Glick *et al*., 1985), single isolated *Azotobacter* colony was picked form freshly streaked cells, inoculated in transformation (TF) medium and incubated at 30 ^{o}C and 150 rpm for 24 h. One % of inoculum was transferred in to 20 ml fresh TF medium and grown under same conditions. The cells were harvested at 10,000 rpm for 5 min and suspended in 1 ml of fresh TF medium. A 50 µl portion of cells was suspended in to 300 µl of fresh TF medium and 50 µl of plasmid DNA (25 ng/µl) and incubated for 30 min at 30 ^{o}C. The cells were centrifuged at 10,000 rpm for 5 min, the supernatant was discarded immediately and the pellet was suspended in 400 µl of TF medium, incubated for 1 h at 30 ^{o}C. Serial dilutions were made and plated on *Azotobacter* growth (AG) medium. The growth pattern was compared after incubation at 30 ^{o}C for 48 h. Minipreps of few randomly selected large colonies were checked for the presence of *gln*A and *pts* promoter and *E. coli gcd* was analyzed using specific primers in PCR.

2. 8 EXPRESSION OF *E. COLI GCD* UNDER REGULATION OF *AZOTOBACTER*-SPECIFIC PROMOTERS IN *AZOTOBACTER*

The expression of *E. coli gcd* under regulation of *Azotobacter*-specific *gln*A and *pts* promotes was detected in MacConeky glucose agar medium, by the mineral phosphate solubilization in NBRIP medium and by RT-PCR analysis.

2. 8. 1 Expression of the clones in MacConkey glucose medium: For the expression of *E. coli gcd* under regulation of *Azotobacter*-specific promoters in *Azotobacter* were test on a solid MacConkey medium. *Azotobacter* harboring pMMBEGS1 and pMMBEPS1 and *E. coli* PP2418 harboring pGDEGS1 and pGDEPS1 were spotted in triplicates on MacConkey glucose (1 %) agar supplemented with 30 µg/ml chloramphenicol and with out PQQ (for *Azotobacter* harboring clones) and 100 µg/ml of ampicillin, with 200 nM

PQQ (for *E. coli* PP2418 harboring clones). The growth pattern was compared after 24 h incubation at 30 ^{o}C (for *Azotobacter* harboring *gcd* clones) and 37 ^{o}C (for *E. coli* PP2418 harboring *gcd* clones). *Azotobacter* harboring pMMB206, *E. coli* PP2418 harboring pUC18 and pUCGDE served as the negative control where as *E. coli* DH5α harboring pUC18 served as positive control.

2. 8. 2 Mineral phosphate solubilization by the *gcd* clones in NBRIP agar: To evaluate the mineral phosphate solubilizing ability, *Azotobacter* harboring pMMBEGS1 and pMMBEPS1 and *E. coli* PP2418 harboring pGDEGS1 and pGDEPS1 were spotted in triplicates on NBRIP agar supplemented with 30 μg/ml chloramphenicol and with out PQQ (for *Azotobacter* harboring clones) and 100 μg/ml of ampicillin, with 200 nM PQQ (for *E. coli* PP2418 harboring clones). The growth pattern was compared after one week incubation at 30 ^{o}C (for *Azotobacter* harboring *gcd* clones) and 37 ^{o}C (for *E. coli* PP2418 harboring *gcd* clones). *Azotobacter* harboring pMMB206, *E. coli* PP2418 harboring pUC18 and pUCGDE served as the negative control where as *E. coli* DH5α harboring pUC18 served as positive control.

2. 8. 3 Mineral phosphate solubilization by the *gcd* clones in liquid NBRIP medium: Quantitative estimation of phosphate solubilization was done in 150 ml Erlenmeyer flasks containing 30 ml of NBRIP medium supplemented with chloramphenicol (30 μg/ml) and with out PQQ. The medium was inoculated (1 % inoculum of culture at an OD_{620} of approx. 0.6) with *Azotobacter* harboring pMMB206, pMMBEGS1 and pMMBEPS1 in triplicates and incubated at 30 ^{o}C and 150 rpm. Uninoculated medium served as the control. One ml samples were withdrawn, after every 24 h, for eight days and centrifuged at 10,000 rpm for 10 min. The cell-free supernatant was used for 'pi' estimations were done as described in section 2. 2. 2.

2. 8. 4 Expression of the clones by RT-PCR analysis: For semi-quantitative estimation of expression of *gcd* in transgenic *Azotobacter* and *E. coli* PP2418 RT-PCR was done. *E. coli* PP2418 harboring pGDEGS1 & pGDEPS1 and *Azotobacter* harboring pMMBEGS1 and pMMBEPS1 were grown in LB medium up to mid log phase. Total

RNA was isolated using Tri-reagent (Sigma), first strand cDNA was synthesized using *gcd* specific primers (Fp EGD & Rp EGD) and promega cDNA synthesis kit. The synthesized cDNA was then used as template for PCR using *gcd* specific primers

2. 9 NITROGENASE ACTIVITY OF WILD TYPE AND TRANSGENIC *AZOTOBACTER* STRAINS

To check whether or not the transgenic *Azotobacter*, expressing *gcd* gene of *E. coli*, was affected in terms its ability to fix nitrogen was analyzed by acetylene reduction assay (ARA). *Azotobacter* harboring pMMB206, pMMBEGS1 and pMMBEPS1 were grown in 20 ml of Burk's nitrogen free medium for 48 h, harvested the cells at 10,000 rpm for 5 min and cells were suspended in equal volume of fresh Burk's nitrogen free medium aseptically. Four ml of the culture was transferred to 15 ml test tube and the tubes were air tight with suba seal, inside gas was replaced by argon gas. One ml of the argon was removed from the tube and 1 ml of the acetylene gas was injected. Tubes were incubated in slanting position for 3, 12 and 24 h at room temperature. Every 3, 12 and 24 h 0.5 ml of the gas was removed and analyzed for the conversion of acetylene to ethylene by nitrogenase through gas chromatography (SasiKala *et al*., 1990).

2. 10 GREEN HOUSE EVALUATION OF TRANSGENIC *AZOTOBACTER* STRAINS

2. 10. 1 Seed sterilization: Sorghum seeds were surface sterilized using crude ethanol for few seconds later socked twice in 10 % sodium hypo chlorite with one drop of Tween100. Seeds were then repeatedly washed five times with sterile double distilled water to remove the detergent.

2. 10. 2 Seed bacterization: *Azotobacter* strains harboring pMMB206, pMMBEGS1 and pMMBEPS1 were grown in Burk's nitrogen free agar for 48 hours, culture was then scraped and suspended in 0.5 % carboxy methyl cellulose (CMC). The surface sterilized

seed were suspended in culture medium containing 0.5 % CMC and air-dried under laminar flow for 4 hours (Kishore *et al*., 2005).

2. 10. 3 Green house evaluation: Bacterized sorghum seeds were sowed in the green house experimental pots (diameter 18 cm and 15 cm deep) containing 2 kg of sterilized vermiculite for 2 h at 130 ^{o}C, 200 mg TCP per pot and raised in green house with about 12 h of light and 12 h of dark at 30 ^{o}C. Similarly controls were maintained with 500 mg/pot super phosphate, only vermiculate *Azotobacter* and different combinations. Every week after sprouting the seeds, plant wet weight and plant height was measured for 1 month. Experiment was repeated thrice with 10 replicas containing 5 plants in each pot. The mean comparison of the data was subjected to one way ANOVA using SigmaStat (Systat Software Inc., California, USA).

2. 11 HOMOLOGY MODELING AND SITE DIRECTED MUTAGENESIS OF *E. COLI* GDH TO UNDERSTAND STRUCTURE-FUNCTION RELATIONSHIP

2. 11. 1 Homology modeling of *E. coli* GDH: Three dimensional structure modeling of *E. coli* GDH was done using the crystal structure of the heavy chain α subunit of PQQ-dependent methanol dehydrogenase (MDH) of *Methylobacterium extorquens* (Zheng, *et al*., 2001), and *Methylophilus methylotrophus* W3A1 (Afolabi *et al*., 2001) and a PQQ-dependent ethanol dehydrogenase (ADH) of *Pseudomonas aeruginosa* (Keitel *et al*., 2000) as templates. Modeling was performed using InsightII suite of programs provided by Accelrys Inc, USA. For molecular modeling of GDH, the N-terminal 150 amino acids corresponding to five membrane spanning domains and irregularities (regions of insertions and deletions according to the multiple sequence alignments) were removed manually. The structure model of GDH was validated using Ramachandran plot (Ramachandran *et al*., 1963). The 5 Å region around the PQQ binding domain was analyzed on graphics. From this, we selected five amino acid residues in the PQQ binding region, and two amino acid residues on the surface of the model structure for site directed mutagenesis (SDM).

2. 11. 2 Site directed mutagenesis of *E. coli gcd* (pATEE): The mutagenesis was carried out using the high-fidelity long range $VENT_R$ DNA polymerase and *Dpn* I enzyme from NEB (England). The plasmid pATEE was purified from *E. coli* XL1-Blue using the Qiagen plasmid isolation kit and used for the mutations. The details of the mutagenic primers are listed in Table 5. The mutagenesis reaction mixtures contained: 125 ng of primers, 200 ng of pATEE, 1 µl of dNTP mixture (containing 25 mM dATP, 25 mM dCTP, 25 mM dGTP, 25 mM dTTP), 2 mM $MgSO_4$, 2.0 units of $VENT_R$ DNA polymerase and 3 µl of reaction buffer in a final volume of 30 µl. Twenty two rounds of PCR was performed, each consisting of a first denaturation step at 95 ^oC for 3 min, cycle denaturation step 95 ^oC for 45 sec, an annealing step at 45 ^oC for 1 min and an elongation step at 68 ^oC for 10 min. The PCR product was visualized on a 1 % agarose gel and the sample was digested with 10 units of *Dpn* I to eliminate the methylated parental DNA leaving behind the amplified mutated plasmid. The PCR product was then used to transform highly efficient competent cells of *E. coli* XL1-Blue MRF' prepared as described by Hanahan *et al*., (1991) with little modifications. Plasmid was isolated from 5 randomly selected colonies and sequenced to confirm the mutations. The mutations targeted were Arginine 201 to Alanine, Aspertate 204 to Alanine, Glutamate 217 to Leucine, Glutamine and Alanine, Arginine 266 to Glutamate and Glutamine, Glutamate 591 to Leucine, Glutamine and Lysine, Leucine 712 to Tryptophan and Arginine & Glycine 776 to Alanine, Lysine, Aspertate and Leucine using mutagenic forward and reverse primers that were listed in table 5.

2. 11. 3 Complementation of *E. coli* GDH mutants on pATEE in *E. coli* YU423: The GDH complementation studies in *E. coli* YU423 harboring pATEE and mutants of pATEE were spotted in triplicates on MacConkey glucose (1 %) agar supplemented with 100 µg/ml of ampicillin, with 200 nM PQQ and 1 mM IPTG. The growth pattern was compared after 24 h incubation at both 37 ^oC. *E. coli* YU423 harboring pQE30 served as the negative control.

Table 5: Details of the mutagenic primers used to generate mutations in *gcd* of *E. coli* using pATEE as template

S. No.	Primer code	Primer sequence (5' ⟶ 3')	Targeted amino acid
1	Fp R201A	AGA AGC CTG GGT GTT **GCT** TAC TGG CGA TGTGAA	Arg201 to Ala
	Rp R201A	TTC ACA TCG CCA GTG **AGC** AAC ACC CAG GCT TCT	
2	Fp D204A	CCT GGG **GCT** TCC GTA CTG GCG CCG TGA AGC AG	Asp204 to Ala
	Rp D204A	**G**GA TCG TTC GGC TGC **AGC** ACG GCG CCA GTA CG	
3	Fp E217L	ACC AAT **CTT** GTG ACG CCG ATT AAA GTG GGC	Glu217 to Leu
	Rp E217L	CGG CGT CAC **AAG** ATT GGT GAT TTC ACC CG	
4	Fp E217Q	ACC AAT **CAA** GTG ACG CCG ATT AAA GTG GGC	Glu217 to Gln
	Rp E217Q	CGG CGT CAC **TTG** ATT GGT GAT TTC ACC CG	
5	Fp E217A	ACC AAT **GCT** GTG ACG CCG ATT AAA GTG GGC	Glu217 to Ala
	Rp E217A	CGG CGT CAC **AGC** ATT GGT GAT TTC ACC CG	
6	Fp R266E	ACC TGC **GAG** GGT GTC TCT TAT CAT GAA GCC	Arg266 to Glu
	Rp R266E	GAT AAG AGA CAC C**CT C**GC AGG TTA CGT GCT G	
7	Fp R266Q	ACC TGC **CAG** GGT GTC TCT TAT CAT GAA GCC	Arg266 to Gln
	Rp R266Q	GAT AAG AGA CAC C**CT G**GC AGG TTA CGT GCT G	
8	Fp E591L	ATG TTC **CTG** TGG GGC GGG ATT TCC GTT G	Glu591 to Leu
	Rp E591L	CCC GCC CCA **CAG** GAA CAT CCC CAG GTT AC	
9	Fp E591Q	ATG TTC **CAG** TGG GGC GGG ATT TCC GTT G	Glu591 to Gln
	Rp E591Q	CCC GCC CCA **CTG** GAA CAT CCC CAG GTT AC	
10	Fp E591K	ATG TTC **AAG** TGG GGC GGG ATT TCC GTT G	Glu591 to Lys
	Rp E591K	CCC GCC CCA **CTT** GAA CAT CCC CAG GTT AC	
11	Fp L712W	CCG ATG **TGG** GGC GGG CCA ATC TCC ACG	Leu712 to Trp
	Rp L712W	GAT TGG CCC GCC **CCA** CAT CGG CAT ACC C	
12	Fp L712R	CCG ATG **CGC** GGC GGG CCA ATC TCC ACG	Leu712 to Arg
	Rp L712R	GAT TGG CCC GCC **GCG** CAT CGG CAT ACC C	
13	Fp G776A	GGC GGT CAC **GCT** TCA TTT GGT ACG AAG ATG G	Gly776 to Ala
	Rp G776A	CGT ACC AAA TGA **AGC** GTG ACC GCC TGC GGA G	
14	Fp G776L	GGC GGT CAC **CTG** TCA TTT GGT ACG AAG ATG G	Gly776 to Lue
	Rp G776L	CGT ACC AAA TGA **CAG** GTG ACC GCC TGC GGA G	
15	Fp G776D	GGC GGT CAC **GAC** TCA TTT GGT ACG AAG ATG G	Gly776 to Asp
	Rp G776D	CGT ACC AAA TGA **GTC** GTG ACC GCC TGC GGA G	
16	Fp G776K	GGC GGT CAC **AAG** TCA TTT GGT ACG AAG ATG G	Gly776 to Lys
	Rp G776K	CGT ACC AAA TGA **CTT** GTG ACC GCC TGC GGA G	

Fp: Forward primer; Rp: Reverse primer
The mutated sequence in the primer is indicated in bold and underlined

2. 11. 4 Expression and SDS-PAGE analysis of GDH mutants: Competent cells of *E. coli* AT15 were transformed with the mutated plasmids and used to study the expression of GDH mutants. The cells were harvested between 3 to 4 h after induction with 1 mM IPTG and the cells were sonicated. SDS-PAGE analysis of protein fractions was carried out on vertical slab gels according to the method of Laemmli (1970). The gels were stained in Coomassie blue stain (0.25 g of Coomassie Brilliant Blue R250 in 90 ml of methanol: H_20 (1:1 v/v) and 10 ml glacial acetic acid) for 1 h and washed repeatedly in the destaining solution (45 ml methanol and 10 ml glacial acetic acid and the final volume made up to 100 ml with water) till the protein bands were visible with a clear background.

2. 11. 5 Western blot analysis: The induced cell pellets obtained from the cultures of *E. coli* AT15 harboring pQE30, pATEE and pATEE mutants were resolved on a 10 % SDS poly acrylamide gel along with prestained protein molecular weight standards and then transferred onto nitrocellulose membranes (Millipore, USA). The membranes were blocked with 5 % BSA for 1 h, and then incubated with anti-His antibodies (Amersham, UK) in 10 ml of antibody-diluted TBST buffer (1x Tris buffered saline and 0.5 % Tween20) with gentle shaking at 4 ^oC for 8-12 h. The blot was washed with slow shaking with TBST buffer for 30 min and incubated with the anti-mouse IgG ALP conjugate for 1 h. The blot was again washed with TBST buffer for 25 min (5 min wash for five times) with slow shaking and the immunoblot was visualized by the alkaline phosphatase-catalysed colour reaction using BCIP-NBT, substrate for alkaline phosphatase (Burnette, 1981).

Results

3.1 SELECTION OF BACTERIAL STRAINS FOR MINERAL PHOSPHATE SOLUBILIZATION

We have screened 24 different bacterial isolates that are already known to solubilize mineral phosphate, on both solid and liquid media containing insoluble forms of inorganic phosphate (Tripura *et al*., 2006). Three Gram-negative bacterial isolates *Serratia marcescens* GPS 5, *Escherichia coli* DH5α and *Enterobacter asburiae* were selected for further studies based on their potential to release inorganic phosphate. *S. marcescens* GPS 5, isolated from the phylloplane of groundnut, was the best solubilizer of inorganic phosphate among the isolates screened in our lab. We have concentrated our efforts on the glucose dehydrogenase gene of these three organisms. We have also used a chemical mutagenesis approach to improve the MPS by *S. marcescens* GPS 5. Section 3.2 reports the EMS mutagenesis, selection and characterization of MPS altered mutants of *S. marcescens* GPS 5.

3.2 EMS MUTAGENESIS OF *S. MARCESCENS* GPS 5 AND ISOLATION OF MPS-RELATED MUTANTS

To isolate random mutants with altered MPS-phenotype *S. marcescens* GPS 5 cells exposed to EMS, for different time intervals, were plated on LB. The survivors were screened to test their MPS ability on NBRIP medium. The percentage of cells surviving after EMS mutagenesis decreased drastically with 60 min exposure (Figure 4). Therefore, colonies of *S. marcescens* GPS 5 resulted after 45 min exposure were selected and screened (Figure 5). All the mutants were similar in their morphology and growth pattern compared to the wild type, unless mentioned. A total of 1700 randomly selected colonies were screened to select mutants with altered MPS trait in buffered NBRIP liquid medium. Seven mutants showed enhanced MPS (Figure 6), while six mutants showed a reduced MPS (Figure 7) compared to the wild type *S. marcescens* GPS 5. Mutants designated as EMS VII *Sm* 12 and EMS VIII *Sm* 27 among the MPS enhanced mutants showed a solubilization zone of 21 mm and EMS XVIII *Sm* 35 had a zone of 16.5 mm, compared to 14 mm zone of *S. marcescens* GPS 5 (Figure 6 C).

The mutants released a maximum amount of phosphate in liquid medium at the end of 5th day, after which there was a decrease in the amount of soluble phosphate in the medium. There was a clear increase in the amount of phosphate released by the seven MPS enhanced mutants compared to *S. marcescens* GPS 5 (Figure 6 B). EMS XVIII *Sm* 35 released 40 % more phosphate, followed by EMS VII *Sm* 12, EMS III *Sm* 7 and EMS VIII *Sm* 27 compared to the wild type at the end of day five (Figure 6 B). Though the solubilization zone by mutant EMS III *Sm* 7 (13 mm) was smaller (Figure 6 C), the amount of phosphate released in liquid medium was much more compared to the wild type *S. marcescens* GPS 5 (Figure 6 B). EMS XVIII *Sm* 35 among the MPS enhanced mutants released maximum phosphate although the zone of solubilization was smaller than either EMS VII *Sm* 12 or EMS VIII *Sm* 27. Mutant EMS VIII *Sm* 27 had the largest solubilization zone among the MPS enhanced mutants, but the amount of phosphate released was less compared to EMS XVIII *Sm* 35.

Six mutants had reduced MPS ability compared to the wild type *S. marcescens* GPS 5 (Figure 7). EMS III *Sm* 3 released very less phosphate, while mutant EMS VII *Sm* 8 released 1674 µg/ml of phosphate compared to 1996 µg/ml released by the wild type (Figure 7 B). The zone of clearance was also small for EMS III *Sm* 3 (8 mm) compared to the wild-type 14 mm (Figure 7 C).

3. 3 CLONING OF *AZOTOBACTER*-SPECIFIC PROMOTERS

Azotobacters are abundantly available in the rhizosphere and are extensively used as bacterial inoculants to reduce the atmospheric nitrogen in free-living condition and enable variety of plants to use the reduced forms of atmospheric nitrogen. We made an attempt to augment the MPS ability of *A. vinelandii* AvOP using a transgenic approach. *Azotobacter*-specific promoters were first cloned (described in section 3.3) to construct and mobilize the *E. coli gcd* in to *Azotobacter* to enhance the MPS by *A. vinelandii* AvOP We have selected glutamine synthetase (*gln*A) and phosphonate transport system (*pts*) gene promoters form *Azotobacter* (partially annotated genome sequencing project available at http://www.azotobacter.org) to express the glucose dehydrogenase gene under regulation of *Azotobacter*-specific *gln*A and *pts* gene promoters, co-express

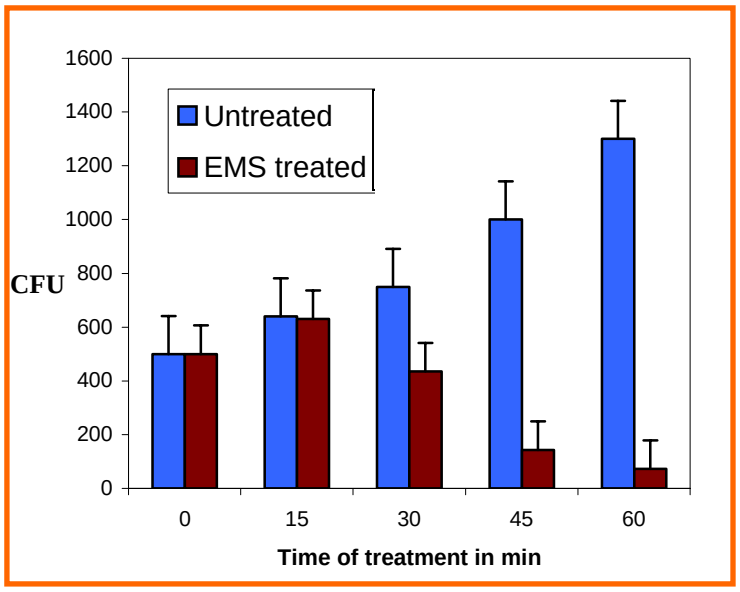

Figure 4: Survival of *Serratia marcescens* GPS 5 cells exposed to ethyl methane sulfonate

Samples were withdrawn at regular intervals of time from the concentrations of EMS-treated culture of *S. marcescens* GPS 5, and washed twice with buffer A and dissolved in same volume of buffer A. Serial dilutions were plated to record colony forming unit (CFU). The vertical bars indicate standard error.

`

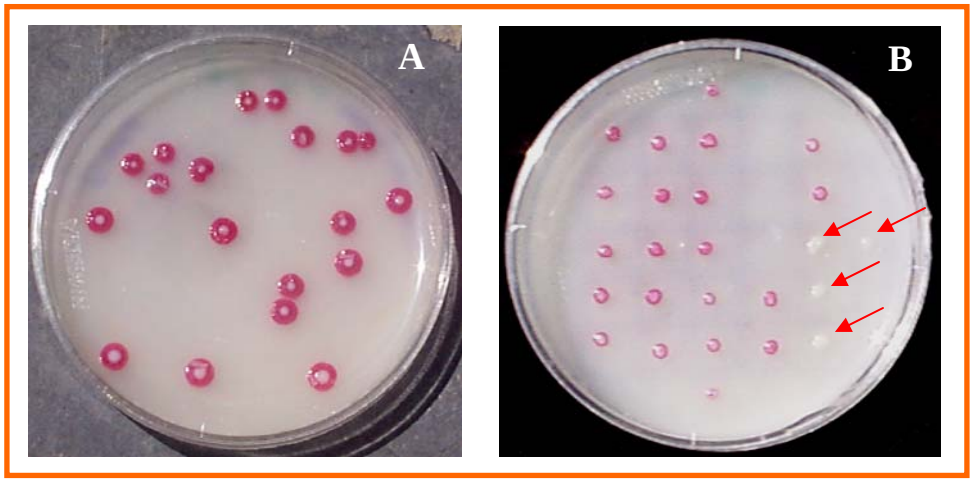

Figure 5: Isolation of MPS-regulated mutants of *S. marcescens* GPS 5

S. marcescens GPS 5 culture was exposed to EMS with different time interval was plated on buffered NBRIP medium. (A) Isolated colonies from 45 min sample and 10^{-7} dilution. (B) Randomly selected colonies spotted on buffered NBRIP agar and isolation of mutants that no more formed the pink pigment (shown with arrow).

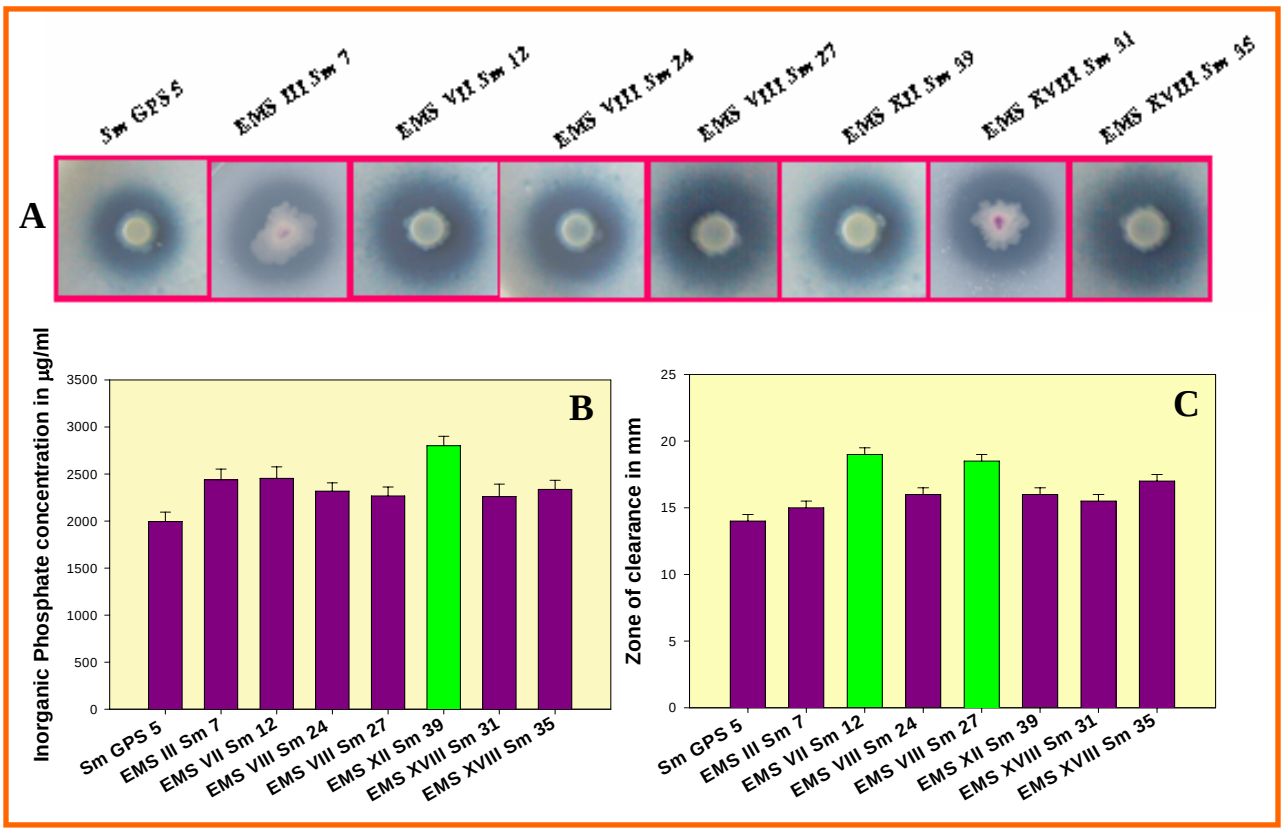

Figure 6: MPS up-regulated EMS mutants of *S. marcescens* GPS 5

EMS treated *S. marcescens* GPS 5 culture was screened for MPS-related mutants in buffered NBRIP medium. (A) Zone of solubilization on buffered NBRIP agar by MPS up-regulated mutants of *S. marcescens* GPS 5. (B) Histogram showing the comparison of inorganic phosphate released in liquid buffered NBRIP medium at the end of 5th day. (C) Histogram showing the comparison of zone of solubilization after incubated at 28 ^{o}C for 7 days by MPS up-regulated mutants on buffered NBRIP agar. The experiment was repeated thrice with three replications and the vertical bars in B and C indicate the standard error.

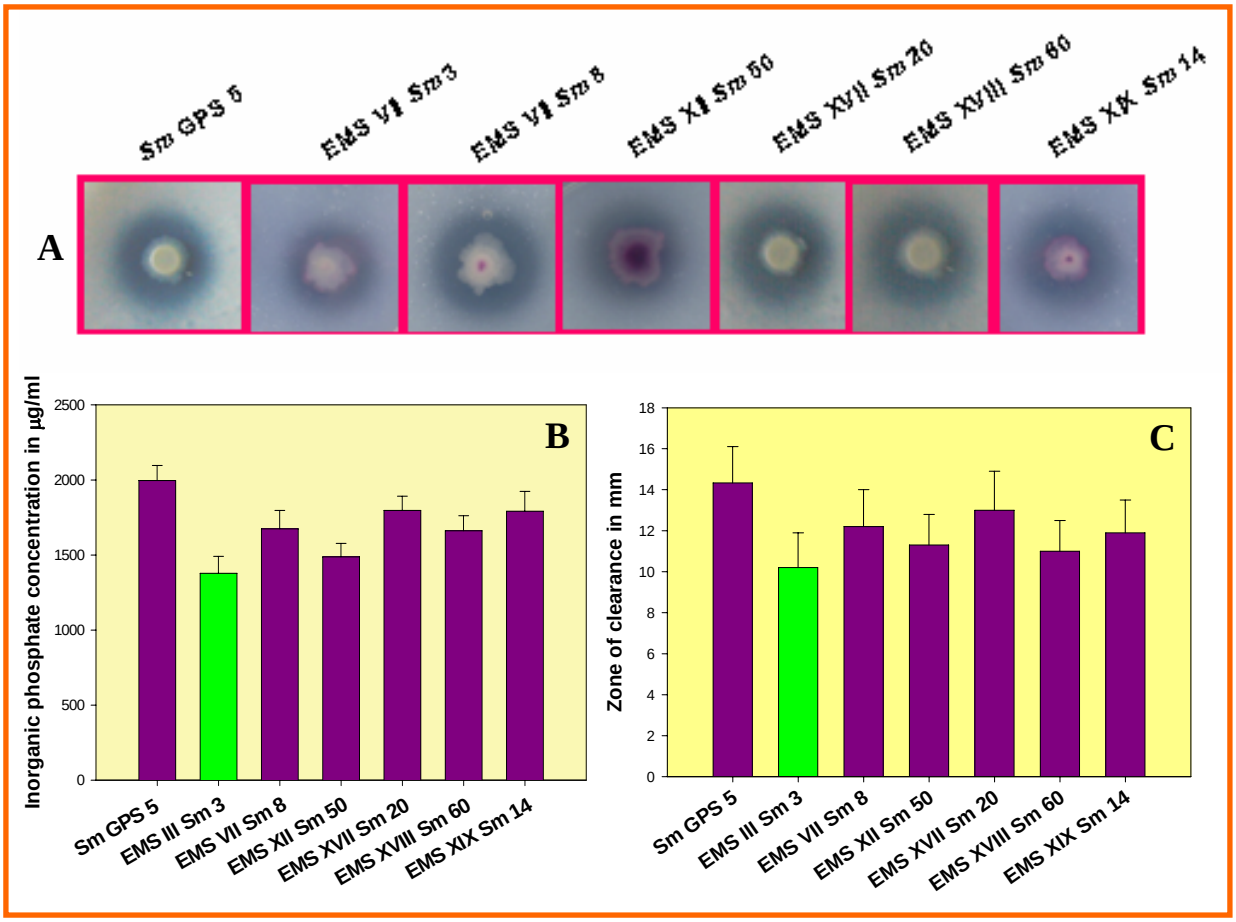

Figure 7: MPS down-regulated EMS mutants of *S. marcescens* GPS 5

EMS treated *S. marcescens* GPS 5 culture was screened for MPS-related mutants in buffered NBRIP medium. (A) Zone of solubilization on buffered NBRIP agar by MPS down-regulated mutants of *S. marcescens* GPS 5. (B) Histogram showing the comparison of inorganic phosphate released in liquid buffered NBRIP medium at the end of 5th day. (C) Histogram showing the comparison of zone of solubilization after incubated at 28 ^{o}C for 7 days by MPS down-regulated mutants on buffered NBRIP agar. The experiment was repeated thrice with three replications and the vertical bars in B and C indicate the standard error.

introduced MPS under nitrogen fixing conditions and to regulate the MPS phenotype under phosphate limiting conditions, respectively, in transgenic *A. vinelandii* AvOP.

3. 3. 1 PCR amplification and cloning of *Azotobacter*-specific *pts* gene promoter: PCR with the genomic DNA of *A. vinelandii* AVOP as template using Fp PS1 & Rp PS and Fp PS2 & Rp PS primers (Table 4) resulted in a 182 bp (*pts*-p1) and 128 bp (*pts*-p2) amplicons, respectively, corresponding to the expected size of the *pts* promoter of *A. vinelandii* AVOP (Figure 8). The amplicons were cloned in the *Bam* HI and *Hind* III sites of pUC18 and the resultant recombinant plasmids were designated as pUCPS1 and pUCPS2, respectively. *Hind* III digest of pUCPS1 (2.78 kb) and pUCPS2 (2.72 kb) revealed the difference in the size as compared with the *Hind* III digest of pUC18 (2.6 kb), confirmed the presence of the right insert (Figure 9). PCR amplification using vector specific M13 forward and reverse primers and pUC18, pUCPS1 & pUCPS2 as templates amplified 103 bp, 285 bp & 231 bp corresponding to multiple cloning sites (MCS) of the pUC18, MCS with *pts*-p1 gene promoter and MCS with *pts*-p2 gene promoter respectively, confirmed the cloning of *pts* promoters in pUC18 (Figure 9). Sequencing of the 182 bp and 128 bp insert of pUCPS1 and pUCPS2 further confirmed the faithfulness of *pts*-p1 and *pts*-p2 of *A. vinelandii* AVOP.

3. 3. 2 PCR amplification and cloning of *Azotobacter*-specific *gln*A gene promoter: PCR with the genomic DNA of *A. vinelandii* AVOP as template using Fp GS1 & Rp GS and Fp GS2 & Rp GS primers (Table 4) resulted in a 228 bp (*gln*A-p1) and 134 bp (*gln*A-p2) amplicons, respectively, corresponding to the expected size of the *gln*A promoter of *A. vinelandii* AVOP (Figure 8). The amplicons were cloned in the *Bam* HI and *Hind* III sites of pUC18 and the resultant recombinant plasmids were designated as pUCGS1 and pUCGS2, respectively. *Hind* III digest of pUCPS1 (2.83 kb) and pUCPS2 (2.73 kb) revealed the difference in the size as compared with the *Hind* III digest of pUC18 (2.6 kb), confirmed the presence of the right insert (Figure 10). PCR amplification using vector-specific M13 forward and reverse primers and pUC18, pUCPS1 & pUCPS2 as templates amplified 103 bp, 331 bp & 238 bp corresponding to multiple cloning sites (MCS) of the pUC18, MCS with *gln*A-p1 gene promoter and MCS with *gln*A-p2 gene

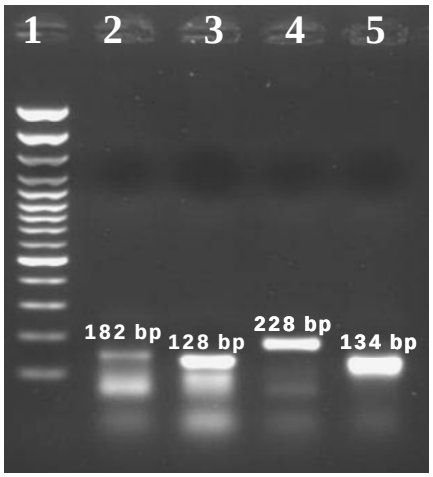

Figure 8: PCR amplification of *Azotobacter*-specific *gln*A and *pts* gene promoters

Azotobacter-specific *gln*A and *pts* gene promoters were amplified using promoter specific primers designed upstream of the respective genes with two forward primers starting form different positions and with a common reverse primer.

Lane 1: 100 bp plus DNA ladder mix, **Lane 2:** 182 bp *pts*-p1 promoter amplified using Fp PS 1 and Rp PS primers, **Lane 3:** 128 bp *pts*-p2 promoter amplified using Fp PS 2 and Rp PS primers, **Lane 4:** 228 bp *gln*A-p1 promoter amplified using Fp GS 1 and Rp GS primers, **Lane 5:** 134 bp *gln*A-p2 promoter amplified using Fp GS 2 and Rp GS primers. Promoter activity of the amplified sequences was confirmed using http://www.fruitfly.org /seq tools/promoter.html software.

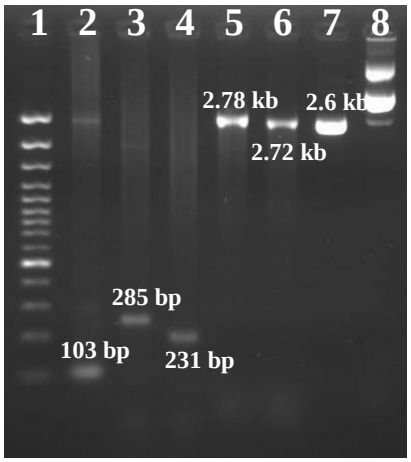

Figure 9: Cloning of *Azotobacter*-specific *pts* gene promoter in pUC18

Azotobacter-specific *pts*-p1 and *pts*-p2 gene promoters was PCR amplified and cloned in *Hind* III and *Bam* HI sites of pUC18 resulting in pUCPS1 and pUCPS2, respectively.

Lane 1: 100 bp plus DNA ladder mix, **Lane 2:** 103 bp MCS of pUC18 amplified using vector- specific M13 primers, **Lane 3:** 285 bp MCS with *pts*-p1 promoter amplified using vector- specific M13 primers, **Lane 4:** 231 bp MCS with *pts*-p2 promoter amplified using vector-specific M13 primers, **Lane 5:** *Hind* III digest of pUCPS1 (2.78 kb), **Lane 6**: *Hind* III digest of pUCPS2 (2.72 kb), **Lane 7**: *Hind* III digest of pUC18 (2.6 kb), **Lane 8**: Undigested pUCPS1.

promoter respectively, confirmed the cloning of *gln*A promoters in pUC18 (Figure 10). Sequencing of the 228 bp and 134 bp insert of pUCGS1 and pUCGS2 further confirmed the faithfulness of *gln*A-p1 and *gln*A-p2 of *A. vinelandii* AVOP

3. 4 AMPLIFICATION OF GLUCOSE DEHYDROGENASE (*GCD*) FORM SELECTED GRAM-NEGATIVE BACTERIA

This section describes the PCR-amplification of three sequences coding for *gcd* of Gram-negative bacteria. The *gcd* sequences of *E. coli*, *E. asburiae* and the chimera of *E. coli-S. marcescens* were amplified to study their suitability to enhance MPS ability of *A. vinelandii* AvOP under regulation of *pts* and *gln*A promoters.

3. 4. 1 PCR-amplification and cloning of *E. coli gcd*: To amplify *gcd* sequences the genomic DNA of *E. coli* was used as template using Fp EGD and Rp EGD primers (Table 4) resulted in a 2.4 kb amplicon, corresponding to the expected size of the *gcd* of *E. coli* (Figure 11). The amplicon was cloned in the *Bam* HI and *Eco* RI sites of pUC18 and the resultant plasmid was designated as pUCGDE. *Bam* HI digest of pUCGDE (5.0 kb) revealed the difference in size as compared to the *Bam* HI digest of pUC18 (2.6 kb), confirmed the presence of the right insert (Figure 13). *Bam* HI and *Eco* RI digest of pUCGDE released the 2.4 kb insert. PCR with pUCGDE using Fp EGD and Rp EGD resulted in 2.4 kb amplicon confirmed the cloning of *E. coli gcd* in pUC18 (Figure 13). Sequencing of the 2.4 kb amplicon provided the proof for the *gcd* of *E. coli*.

3. 4. 2 PCR-amplification of *E. asburiae gcd*: PCR with the genomic DNA of *E. asburiae* as template using Fp EGD and Rp EGD primers (Table 4) resulted in a 2.4 kb amplicon, corresponding to the expected size of the *gcd* of *E. asburiae* (Figure 12). Sequencing of the 2.4 kb amplicon confirmed the *gcd* of *E. asburiae*.

3. 4. 3 PCR-amplification of *E. coli-S. marcescens* (*ES*) chimeric *gcd*: PCR with the pATESE (*ES* chimeric *gcd* in pQE30) DNA as template using Fp EGD and Rp SMGD primers (Table 4) resulted in a 2.4 kb amplicon, corresponding to the expected size of the

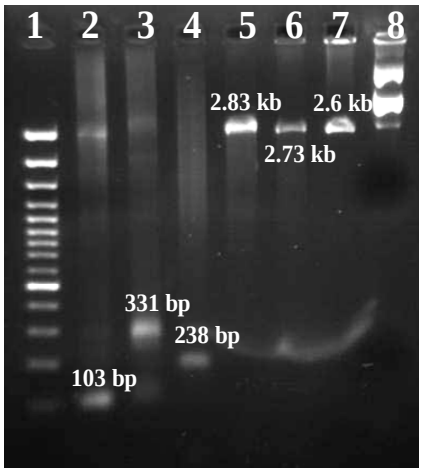

Figure 10: Cloning of *Azotobacter*-specific *gln*A gene promoter in pUC18

Azotobacter-specific *gln*A-p1 and *gln*A-p2 gene promoters was PCR amplified and cloned in *Hind* III and *Bam* HI sites of pUC18 resulting in pUCGS1 and pUCGS2, respectively.

Lane 1: 100 bp plus DNA ladder mix, **Lane 2:** 103 bp MCS of pUC18 amplified using vector- specific M13 primers, **Lane 3:** 331 bp MCS with *gln*A-p1 promoter amplified using vector- specific M13 primers, **Lane 4:** 238 bp MCS with *gln*A-p2 promoter amplified using vector-specific M13 primers, **Lane 5:** *Hind* III digest of pUCGS1 (2.83 kb), **Lane 6**: *Hind* III digest of pUCGS2 (2.73 kb), **Lane 7**: *Hind* III digest of pUC18 (2.6 kb), **Lane 8**: Undigested pUCGS1.

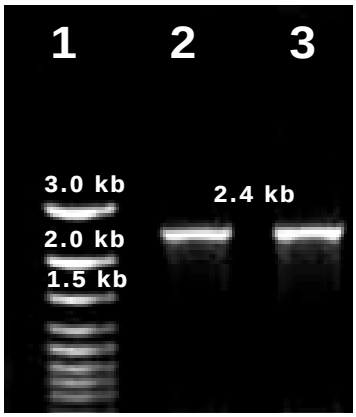

Figure 11: PCR amplification of *E. coli gcd* using gene specific primers

Full length *E. coli gcd* (2. 4 kb) was amplified using Fp EGD and Rp EGD primers

Lane 1: 100 bp DNA ladder mix, **Lane 2 & 3:** 2.4 kb *gcd* of *E. coli*

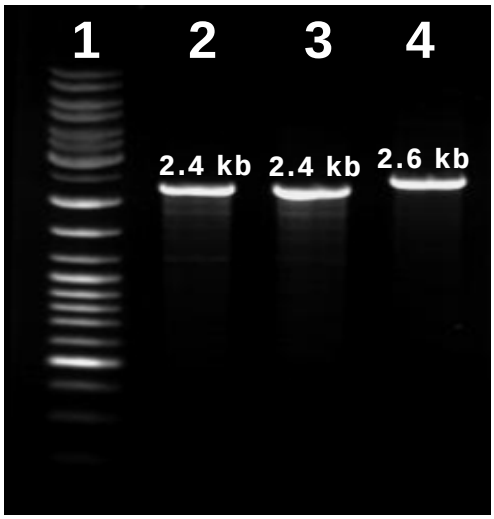

Figure 12: PCR amplification *Enterobacter asburiae* and ES chimeric *gcd* using gene specific primers

Full length *E. asburiae gcd* (2. 4 kb) was amplified using Fp EGD and Rp EGD primers and ES chimeric *gcd* was amplified using Fp EGD and Rp SMGD primers

Lane 1: 1 kb DNA ladder mix, **Lane 2:** 2.4 kb *E. coli-S. marcescens* GPS 5 chimeric *gcd*, **Lane 3:** 2.4 kb *E. asburiae gcd*, **Lane 4**: *Hind* III digest of pUC18 (2.6 kb)

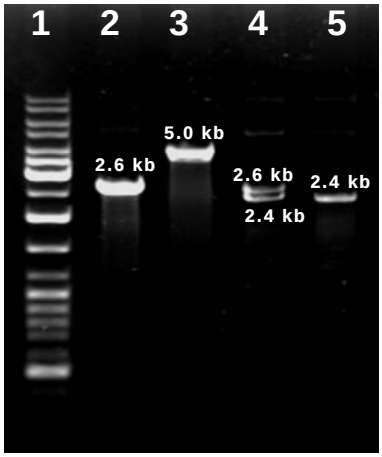

Figure 13: Cloning of *E. coli gcd* in pUC18

E. coli gcd was PCR amplified and cloned in *Bam* HI and *Eco* RI sites of pUC18 resulting in pUCGDE.

Lane 1: 1 kb DNA ladder mix, **Lane 2:** 2.6 kb *Bam* HI digest of pUC18, **Lane 3:** 5.0 kb *Bam* HI digest of pUCGDE, **Lane 4:** *Bam* HI and *Eco* RI digest of pUCGDE released the 2.4 kb insert, **Lane 5**: Amplification of the 2.4 kb *E. coli gcd* with pUCGDE as templates

gcd of *ES* chimera (Figure 12). Sequencing of the 2.4 kb amplicon confirmed the *gcd* of *ES* chimera.

3. 5 CLONING OF *GCD* UNDER *AZOTOBACTER*-SPECIFIC PROMOTERS

This section describes the PCR-based cloning of *gcd* sequences of *E. coli*, *E. asburiae* and the chimera of *E. coli*-*S. marcescens* under regulation of *Azotobacter*-specific *pts* and *gln*A gene promoters to study the expression pattern of these three *gcd* in *E. coli* PP2418 and in transgenic *A. vinelandii* AvOP.

3. 5. 1 Cloning of *E. coli gcd* under *Azotobacter*-specific *pts* and *gln*A promoters: *E. coli gcd* from pUCGDE was released and cloned in the *Bam* HI and *Eco* RI sites of pUCPS1 and pUCGS1 individually and the resulting plasmids were designated as pGDEPS1 (*E. coli gcd* under *pts*-p1) and pGDEGS1 (*E. coli gcd* under *gln*A-p1). *Bam* HI digest of pGDEPS1 (5.18 kb) revealed the difference in size as compared to the *Bam* HI digest of pUCPS1 (2.78 kb), confirmed the presence of the right insert (Figure 14). *Bam* HI and *Eco* RI digest of pGDEPS1 released the 2.4 kb insert. PCR with pGDEPS1 using Fp EGD and Rp EGD resulted in 2.4 kb amplicon, using Fp PS1 and Rp PS resulted in 182 bp amplicon & using M13 primers resulted in 2.88 kb amplicon confirmed the cloning of *E. coli gcd* in pUCPS1 (Figure 14). *Bam* HI digest of pGDEGS1 (5.22 kb) revealed the difference in size as compared to the *Bam* HI digest of pUCGS1 (2.82 kb), confirmed the presence of the right insert. *Bam* HI and *Eco* RI digest of pGDEGS1 released the 2.4 kb insert. PCR with pGDEGS1 using Fp EGD and Rp EGD resulted in 2.4 kb amplicon, using Fp GS1 and Rp GS resulted in 228 bp amplicon & using M13 primers resulted in 2.92 kb amplicon confirmed the cloning of *E. coli gcd* in pUCGS1 (Figure 15).

3. 5. 2 Cloning of *ES chimeric gcd* under *Azotobacter*-specific *pts* and *gln*A promoters: *S. marcescens* GPS 5 *gcd* was amplified and cloned in pQE30 vector (Tripura, 2006). The expression of the *S. marcescens* GPS 5 *gcd* was not confirmed because the GDH lacks the N-terminal membrane span domain. The N-terminal

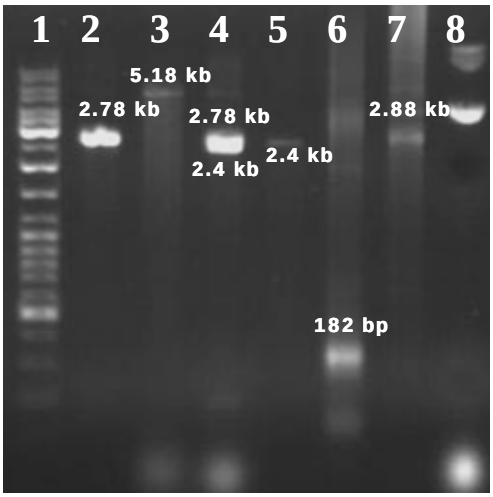

Figure 14: Cloning of *E. coli gcd* under *Azotobacter*-specific *pts*-p1 in pUCPS1

E. coli gcd was excised from pUCGDE using *Bam* HI and *Eco* RI and cloned in same sites of pUCPS1 resulting in pGDEPS1.

Lane 1: 1 kb DNA ladder mix, **Lane 2:** *Bam* HI digest of pUCPS1 (2.78 kb), **Lane 3:** *Bam* HI digest of pGDEPS1 (5.18 kb), **Lane 4:** *Bam* HI and *Eco* RI digest of pGDEPS1 released the 2.4 kb insert, **Lane 5:** Amplification of the 2.4 kb *E. coli gcd* with pGDEPS1 as templates, **Lane 6**: Amplification of the 182 bp *pts*-p1 gene promoter with pGDEPS1 as templates, **Lane 7**: Amplification of the 2.88 kb (182 bp *pts*-p1 gene promoter + 2.4 kb *gcd*) using M13 primers with pGDEPS1 as templates, **Lane 8**: Undigested pGDEPS1.

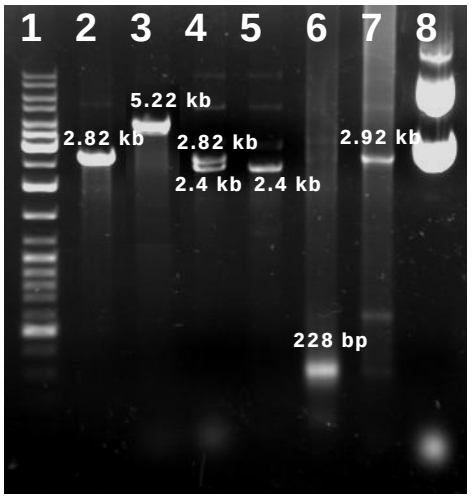

Figure 15: Cloning of *E. coli gcd* under *Azotobacter*-specific *gln*A-p1 in pUCGS1

E. coli gcd was excised from pUCGDE using *Bam* HI and *Eco* RI and cloned in same sites of pUCGS1 resulting in pGDEGS1.

Lane 1: 1 kb DNA ladder mix, **Lane 2:** *Bam* HI digest of pUCGS1 (2.82 kb), **Lane 3:** *Bam* HI digest of pGDEGS1 (5.22 kb), **Lane 4:** *Bam* HI and *Eco* RI digest of pGDEGS1 released the 2.4 kb insert, **Lane 5:** Amplification of the 2.4 kb *E. coli gcd* with pGDEGS1 as templates, **Lane 6**: Amplification of the 228 bp *gln*A-p1 gene promoter with pGDEGS1 as templates, **Lane 7**: Amplification of the 2.92 kb (228 bp *gln*A-p1 gene promoter + 2.4 kb *gcd*) using M13 primers with pGDEGS1 as templates, **Lane 8**: Undigested pGDEGS1.

transmembrane domain and a part of the periplasmic domain consisting of 228 amino acid residues (684 bp DNA fragment) of *E. coli* GDH was then fused to the C-terminal catalytic domain consisting of 1-567 amino acid residues (1-1704 bp DNA fragment) of *S. marcescens* GPS 5 GDH in a PCR-based approach. The resulted 2.4 kb amplicon, a chimera of *E. coli* and *S. marcescens* GPS 5, designated as ES chimera and successfully expressed in *E. coli* at 28 ^{o}C (Tripura, 2006).

The amplified ES chimeric *gcd* was cloned in the *Bam* HI and *Eco* RI sites of pUCGS1 and pUCPS1 individually, resulting in pGDESPS1 (chimeric ES *gcd* under *pts*-p1) and pGDESGS1 (chimeric ES *gcd* under *gln*A-p1). *Bam* HI digest of pGDESPS1 (5.18 kb) revealed the difference in size as compared to the *Bam* HI digest of pUCPS1 (2.78 kb), confirmed the presence of the right insert (Figure 16). *Bam* HI and *Eco* RI digest of pGDESPS1 released the 2.4 kb insert. PCR with pGDESPS1 using Fp EGD and Rp SMGD resulted in 2.4 kb amplicon, using Fp PS1 and Rp PS resulted in 182 bp amplicon confirmed the cloning of ES chimeric *gcd* in pUCPS1 (Figure 16). *Bam* HI digest of pGDESGS1 (5.22 kb) revealed the difference in size as compared to the *Bam* HI digest of pUCGS1 (2.82 kb), confirmed the presence of the right insert (Figure 17). *Bam* HI and *Eco* RI digest of pGDESGS1 released the 2.4 kb insert. PCR with pGDESGS1 using Fp EGD and Rp SMGD resulted in 2.4 kb amplicon, using Fp GS1 and Rp GS resulted in 228 bp amplicon confirmed the cloning of ES chimeric *gcd* in pUCGS1 (Figure 17).

3. 5. 3 Cloning of *E. asburiae gcd* under *Azotobacter*-specific *pts* and *gln*A promoters:
The amplified *E. asburiae gcd* was cloned in the *Bam* HI and *Eco* RI sites of pUCGS1 and pUCPS1 individually, resulting in pGDNTPS1 (*E. asburiae gcd* under *pts*-p1) and pGDESGS1 (*E. asburiae gcd* under *gln*A-p1). *Bam* HI digest of pGDNTPS1 (5.18 kb) revealed the difference in size as compared to the *Bam* HI digest of pUCPS1 (2.78 kb), confirmed the presence of the right insert (Figure 18). *Bam* HI and *Eco* RI digest of pGDNTPS1 released the 2.4 kb insert. PCR with pGDNTPS1 using Fp EGD and Rp EGD resulted in 2.4 kb amplicon, using Fp PS1 and Rp PS resulted in 182 bp amplicon confirmed the cloning of *E. asburiae gcd* in pUCPS1 (Figure 18). *Bam* HI digest of pGDNTGS1 (5.22 kb) revealed the difference in size as compared to the *Bam* HI digest

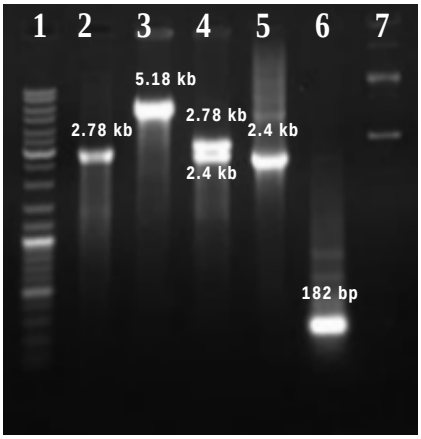

Figure 16: Cloning of *ES* chimeric *gcd* under *Azotobacter*-specific *pts*-p1 in pUCPS1

ES chimeric *gcd* was amplified using pATESE as templates with Fp EGD and Rp SMGD primers and cloned in *Bam* HI and *Eco* RI sites of pUCPS1 resulting in pGDESPS1.

Lane 1: 1 kb DNA ladder mix, **Lane 2:** *Bam* HI digest of pUCPS1 (2.78 kb), **Lane 3:** *Bam* HI digest of pGDESPS1 (5.18 kb), **Lane 4:** *Bam* HI and *Eco* RI digest of pGDESPS1 released the 2.4 kb insert, **Lane 5:** Amplification of the 2.4 kb *ES* chimeric *gcd* with pGDESPS1 as templates, **Lane 6**: Amplification of the 182 bp *pts*-p1 gene promoter with pGDESPS1 as templates, **Lane 7**: Undigested pGDESPS1.

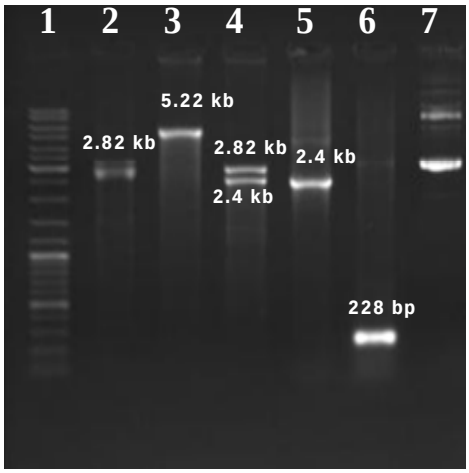

Figure 17: Cloning of *ES* chimeric *gcd* under *Azotobacter*-specific *gln*A-p1 in pUCGS1

ES chimeric *gcd* was amplified using pATESE as templates with Fp EGD and Rp SMGD primers and cloned in *Bam* HI and *Eco* RI sites of pUCPS1 resulting in pGDESGS1.

Lane 1: 1 kb DNA ladder mix, **Lane 2:** *Bam* HI digest of pUCGS1 (2.82 kb), **Lane 3:** *Bam* HI digest of pGDESGS1 (5.22 kb), **Lane 4:** *Bam* HI and *Eco* RI digest of pGDESGS1 released the 2.4 kb insert, **Lane 5:** Amplification of the 2.4 kb *ES* chimeric *gcd* with pGDESGS1 as templates, **Lane 6**: Amplification of the 228 bp *gln*A-p1 gene promoter with pGDESGS1 as templates, **Lane 7**: Undigested pGDESGS1.

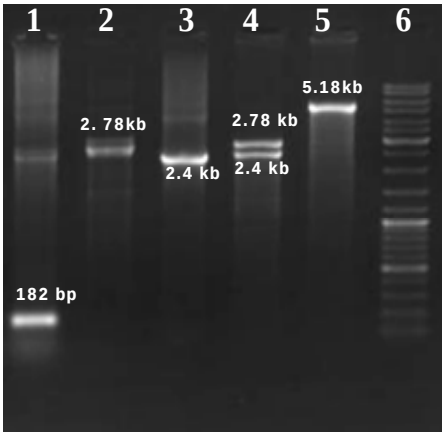

Figure 18: Cloning of *E. asburiae gcd* under *Azotobacter*-specific *pts*-p1 in pUCPS1

*E. asbu*RI*ae gcd* was amplified with Fp EGD and Rp EGD primers and cloned in *Bam* HI and *Eco* RI sites of pUCPS1 resulting in pGDNTPS1.

Lane 1: Amplification of the 182 bp *pts*-p1 gene promoter with pGDNTPS1 as templates, **Lane 2:** *Bam* HI digest of pUCPS1 (2.78 kb), **Lane 3:** Amplification of the 2.4 kb *E. asbu*RI*ae gcd* with pGDNTPS1 as templates, **Lane 4:** *Bam* HI and *Eco* RI digest of pGDNTPS1 released the 2.4 kb insert, **Lane 5:** *Bam* HI digest of pGDNTPS1 (5.18 kb), **Lane 6**: 1 kb DNA ladder mix.

of pUCGS1 (2.82 kb), confirmed the presence of the right insert (Figure 19). *Bam* HI and *Eco* RI digest of pGDESGS1 released the 2.4 kb insert. PCR with pGDNTGS1 using Fp EGD and Rp EGD resulted in 2.4 kb amplicon, using Fp GS1 and Rp GS resulted in 228 bp amplicon confirmed the cloning of *E. asburiae gcd* in pUCGS1 (Figure 19).

3. 6 EXPRESSION OF *GCD* UNDER *AZOTOBACTER*-SPECIFIC PROMOTERS

The expression of cloned *gcd* sequences of *E. coli*, *E. asburiae* and the chimera of *E. coli-S. marcescens* under regulation of *Azotobacter*-specific *pts* and *gln*A gene promoters in *E. coli* PP2418 on MacConkey glucose agar is described in this section. The complementation-confirmed *gcd* clones were then tested for solubilization of mineral phosphate in both semi-solid and liquid NBRIP medium. *E. coli* PP2418 harboring pUCPS1, pUCGDE, pGDEGS1, pGDEPS1, pGDNTGS1, pGDNTPS1, pGDESGS1, and pGDESPS1, spotted on MacConkey agar, with and with out PQQ were checked for the complementation after 24 h incubation at both 28 ^{o}C (for ES chimeric *gcd* clones) and 37 ^{o}C (for *E. coli* and *E. asburiae gcd* clones).

3. 6. 1 Complementation on MacConkey glucose agar: *E. coli* PP2418 harboring pUCPS1 and pUCGDE (negative control) showed no coloration at 37 ^{o}C temperatures with PQQ (Figure 20 B). *E. coli* PP2418 harboring pGDEGS1, pGDEPS1, pGDNTGS1, pGDNTPS1, pGDESGS1, and pGDESPS1 were pink with a purple halo around the colony at 28 ^{o}C (for ES chimeric *gcd* clones) and 37 ^{o}C (for *E. coli* and *E. asburiae gcd* clones) (Figure 20 B). The clones spotted in a similar fashion on MacConkey agar without PQQ and incubated at either 28 ^{o}C or 37 ^{o}C showed no colouration (Figure 20 A). *E. coli* DH5α harboring pUC18 served as positive control and showed pink with a purple halo around the colony with PQQ (Figure 20 B) and no colouration with out PQQ (Figure 20 A). The results suggested the expression of heterologous *gcd* in *E. coli* under *pts* and *gln*A promoters only in presence of PQQ

3. 6. 2 Mineral phosphate solubilization on NBRIP agar: Clear zones of phosphate solubilization were visible on NBRIP agar supplemented with PQQ spotted with *E. coli*

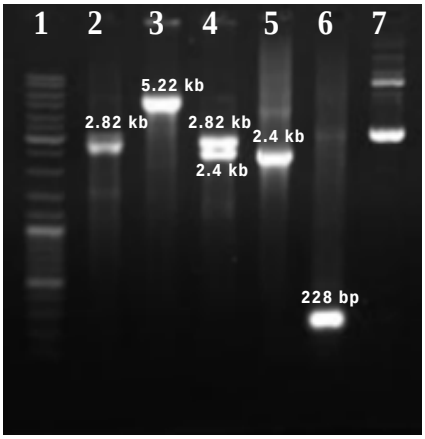

Figure 19: Cloning of *E. asburiae gcd* under *Azotobacter*-specific *gln*A-p1 in pUCGS1

E. asburiae gcd was amplified with Fp EGD and Rp EGD primers and cloned in *Bam* HI and *Eco* RI sites of pUCPS1 resulting in pGDNTGS1.

Lane 1: 1 kb DNA ladder mix, **Lane 2:** *Bam* HI digest of pUCGS1 (2.82 kb), **Lane 3:** *Bam* HI digest of pGDNTGS1 (5.22 kb), **Lane 4:** *Bam* HI and *Eco* RI digest of pGDNTGS1 released the 2.4 kb insert, **Lane 5:** Amplification of the 2.4 kb *E. asburiae gcd* with pGDNTGS1 as templates, **Lane 6**: Amplification of the 228 bp *gln*A-p1 gene promoter with pGDNTGS1 as templates, **Lane 7**: Undigested pGDNTGS1.

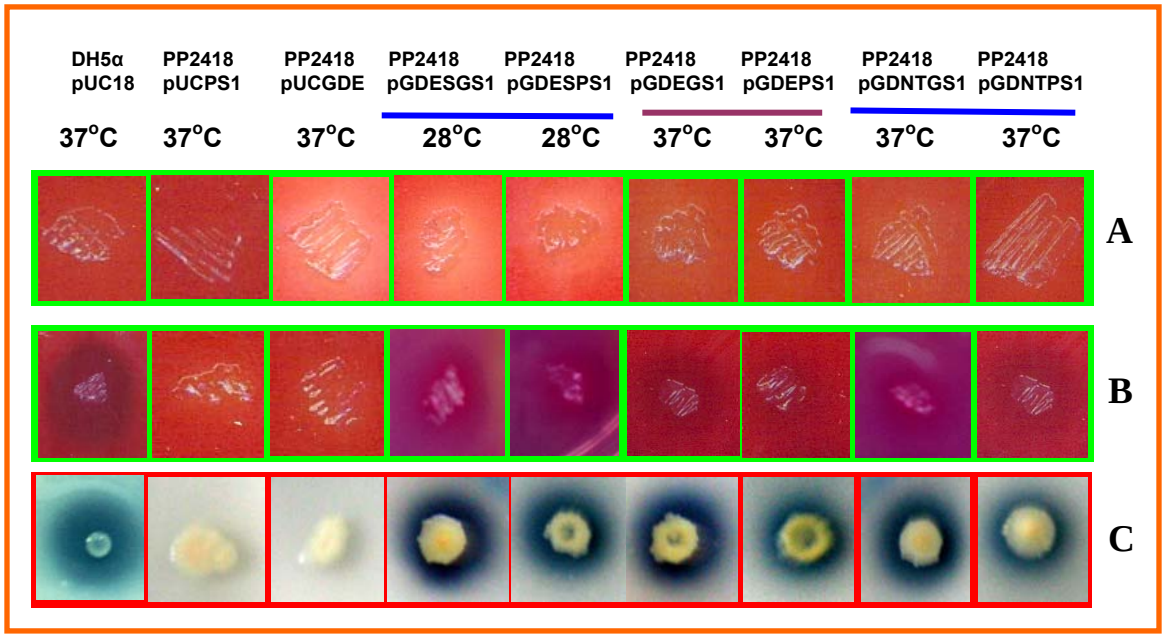

Figure 20: GDH complementation and mineral phosphate solubilization in *E. coli*

E. coli PP2418 harboring pUC18, pUCPS1, pUCGDE, pGDESGS1, pGDESPS1, pGDEGS1, pGDEPS1, pGDNTGS1and pGDNTPS1 were spotted on MacConkey glucose agar with out PQQ **(A)** and with PQQ **(B),** or buffered NBRIP agar with PQQ (**C**). The colour change around the colony on MacConkey agar at 37 ^{o}C (*E. coli* and *E. asburiae gcd* clones) and 28 ^{o}C (ES chimeric *gcd* clones) and zone of MPS after 7 days in buffered NBRIP agar.

PP2418 harboring pGDEGS1, pGDEPS1, pGDNTGS1, pGDNTPS1, pGDESGS1, & pGDESPS1 and no solubilization by *E. coli* PP2418 harboring pUCPS1 and pUCGDE after incubation at 28 ^{o}C (for ES chimeric *gcd* clones) and 37 ^{o}C (for *E. coli* and *E. asburiae gcd* clones) for 1 week (Figure 20 C). *E. coli* DH5α harboring pUC18 served as positive control and showed clear zone of solubilization on NBRIP medium (with PQQ) around the colony (Figure 20) after incubation at 37 ^{o}C for 1 week.

3. 6. 3 Mineral phosphate solubilization in liquid NBRIP medium: Quantitative estimation of phosphate solubilization by the recombinant clones was carried out in NBRIP liquid medium for 1 week. *E. coli* PP2418 harboring pGDEGS1, pGDEPS1, pGDNTGS1, pGDNTPS1, pGDESGS1, & pGDESPS1 showed maximum solubilization of 856 µg/ml, 655 µg/ml, 823 µg/ml, 580 µg/ml, 789 µg/ml and 583 µg/ml, respectively, at the end of 5th day, while it was 80 µg/ml, 93 µg/ml and 1238 µg/ml for *E. coli* PP2418 harboring pUC18, pUCPS1, and *E. coli* DH5α pUC18, respectively, at the end of 4th day (Figure 21). There was a gradual decrease in the amount of soluble phosphate in the medium from day 4.

3. 7 CLONING OF *E. COLI GCD* UNDER *AZOTOBACTER*-SPECIFIC PROMOTERS IN pMMB208 AND MOBILIZATION INTO *AZOTOBACTER*

Since the pUC18-based vectors are not stable for *Azotobacter* and also based on the codon bias studies (Figure 22) we have use a broad-host-range vector (pMMB206) for cloning and *E. coli gcd* for better expression in *Azotobacter*. This section describes the cloning of *E. coli gcd* under the regulation of *Azotobacter*-specific *gln*A and *pts* promoters.

3. 7. 1 Cloning of *E. coli gcd* under *Azotobacter*-specific *gln*A and *pts* gene promoters: *E. coli gcd* with *pts* promoter was released form pGDEPS1 and cloned in the *Bam* HI and *Hind* III sites of pMMB206 and the resulting plasmids were designated as pMMBEPS1 (*E. coli gcd* under *pts*-p1 in pMMB206). Similarly, *E. coli gcd* with *gln*A promoter was released form pGDEGS1 and cloned in the *Bam* HI and *Hind* III sites of

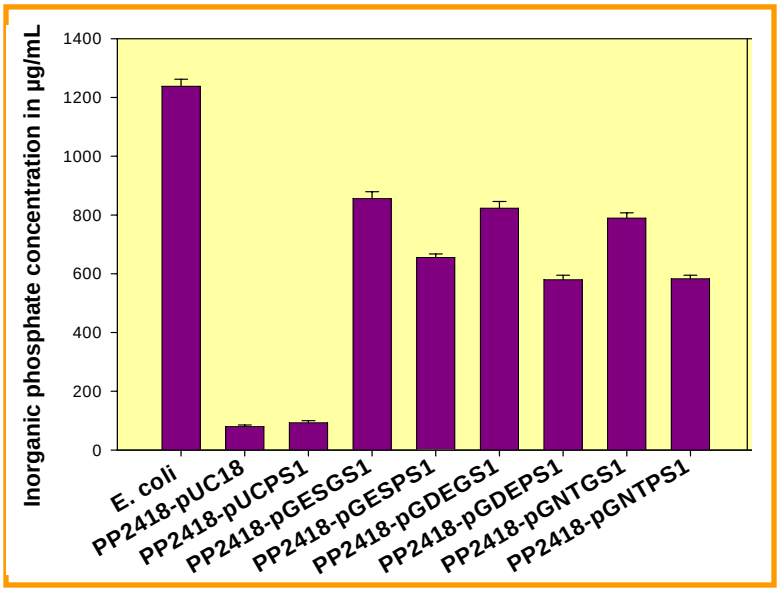

Figure 21: Mineral phosphate solubilization by pGDESGS1, pGDESPS1, pGDEGS1, pGDEPS1, pGDNTGS1and pGDNTPS1 in NBRIP liquid medium

Quantitative estimation of phosphate solubilization by *E. coli* PP2418 harboring pGDESGS1, pGDESPS1, pGDEGS1, pGDEPS1, pGDNTGS1and pGDNTPS1 was carried out in NBRIP liquid medium. The cell free supernatant of the samples withdrawn after 7 days of incubation at 37 ^{o}C (*E. coli* and *E. asburiae gcd* clones) and 28 ^{o}C (ES chimeric *gcd* clones) was used for the inorganic phosphate estimation. The values are averages of three independent experiments. Vertical bar represents standard deviations.

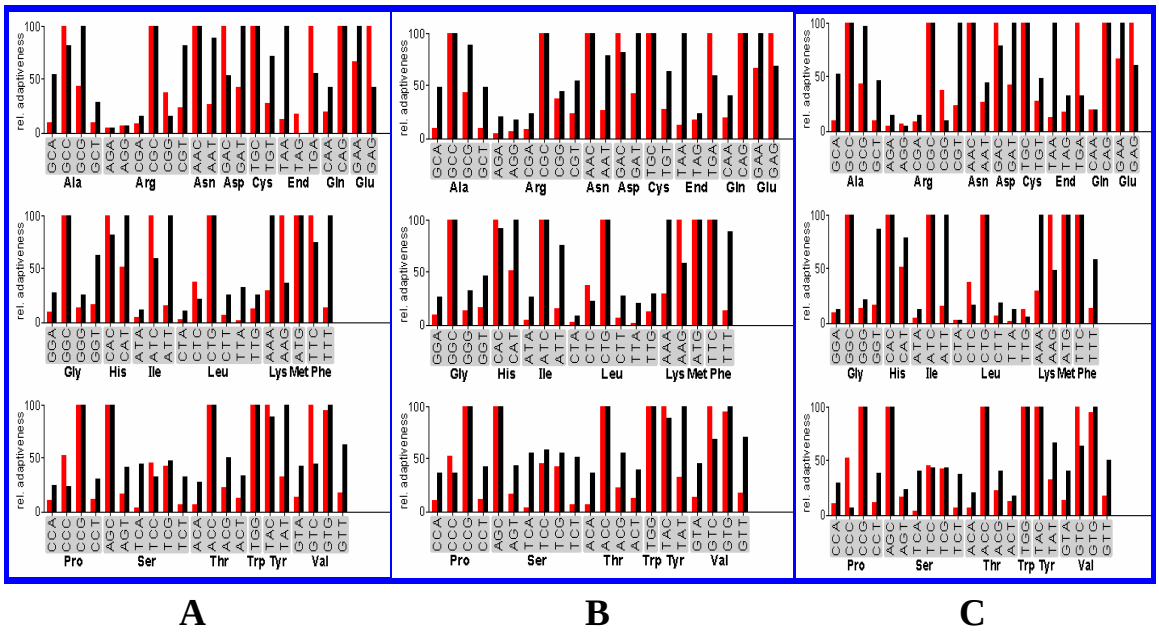

Figure 22: Comparison of codon usage between *Azotobacter*, *E. coli*, *S. marcescens* and *E. asburiae*

The codon preference between *Azotobacter*, *E. coli*, *S. marcescens* and *E. asburiae* was compared using Graphical Codon Usage Analyzer (GCUA). The codon preference between *Azotobacter* and *E. coli* with mean difference of 27.41 % (**A),** 24. 44 % between *Azotobacter* and *S. marcescens* **(B)** and 27.41 % between *Azotobacter* and *E. asburiae* **(C).**

pMMB206 and the resulting plasmids were designated as pMMBEGS1 (*E. coli gcd* under *gln*A-p1 in pMMB206). The details and generation of pMMBEPS1 (Figure 23) and pMMBEGS1 (Figure 24) clones were showed in schematic representation. *Hind* III and *Eco* RI digest of pMMBEGS1 released the 2.82 kb insert, confirmed the presence of the right insert. PCR with pMMBEGS1 using Fp EGD and Rp EGD resulted in 2.4 kb amplicon confirmed the cloning (Figure 25).

3. 7. 2 Mobilization of pMMBEGS1 and pMMBEPS1 clones into *Azotobacter* and verification: After incubation of *A. vinelandii* AVOP with pMMB296, pMMBEPS1 and pMMBEGS1 in fresh TF medium, the cells were plated in AG medium and incubated for 2 days at 30 ^{o}C. On this medium two distinct colony morphologies were observed after transformation. One type of colony was small and clear, where as the other was large and mucoid (Figure 26). Plasmids were isolated form the few selected ramdom large colonies. PCR with pMMBEPS1 as templates and using Fp EGD & Rp EGD and Fp PS1 & Rp PS primers resulted in a 2.4 kb and 182 bp amplicons, respectively (Figure 27). PCR with pMMBEGS1 as templates and using Fp EGD & Rp EGD and Fp GS1 & Rp GS primers resulted in a 2.4 kb and 228 bp amplicons, respectively (Figure 28), thus confirming the transfer of pMMBEPS1 and pMMBEGS1 into *A. vinelandii* AVOP.

3. 8 EXPRESSION OF *E. COLI GCD* UNDER REGULATION OF *AZOTOBACTER*-SPECIFIC PROMOTERS IN *AZOTOBACTER*

This section describes the expression of *E. coli gcd* under regulation of *Azotobacter*-specific *pts* and *gln*A gene promoters in transgenic *A. vinelandii* AvOP on MacConkey glucose agar. The expression of *gcd* was confirmed and then tested for solubilization of mineral phosphate in both semi-solid and liquid NBRIP medium and expression of *gcd* by semi-quantitative RT-PCR.

3. 8. 1 Expression of the clones in MacConkey glucose medium: *A. vinelandii* AVOP harboring pMMB206, pMMBEPS1 and pMMBEGS1 were spotted on MacConkey agar, with out PQQ were checked for the expression of *E. coli gcd* after 48 h incubation at

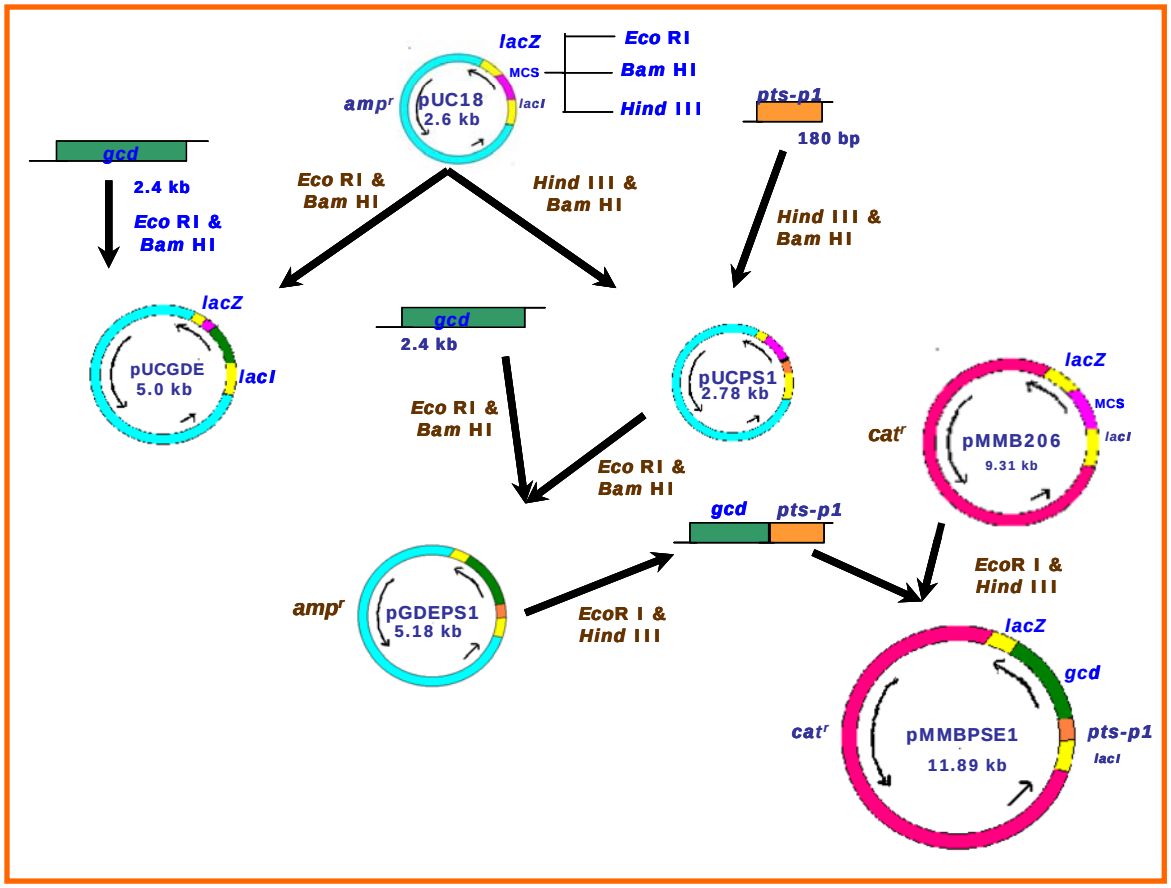

Figure 23: Schematic representation of cloning to generate pMMBEPS1

E. coli gcd (2. 4 kb) was amplified using gene specific primers Fp EGD and Rp EGD and cloned in *Bam* HI and *Eco* RI sites of pUC18 resulted in pUCGDE. *Azotobacter*-specific phosphonate transport system (*pts*-p1) gene promoter (182 bp) was amplified using promoter specific primers Fp PS1 and Rp PS and cloned in *Bam* HI and *Hind* III sites of pUC18 resulted in pUCPS1. *E. coli gcd* was excised from pUCGDE using *Bam* HI and *Eco* RI and cloned in same sites of pUCPS1 resulted in pGDEPS1. Promoter with *E. coli gcd* was excised using *Eco* RI and *Hind* III and cloned in same sites of broad-host range vector pMMB206 resulted in pMMBEPS1.

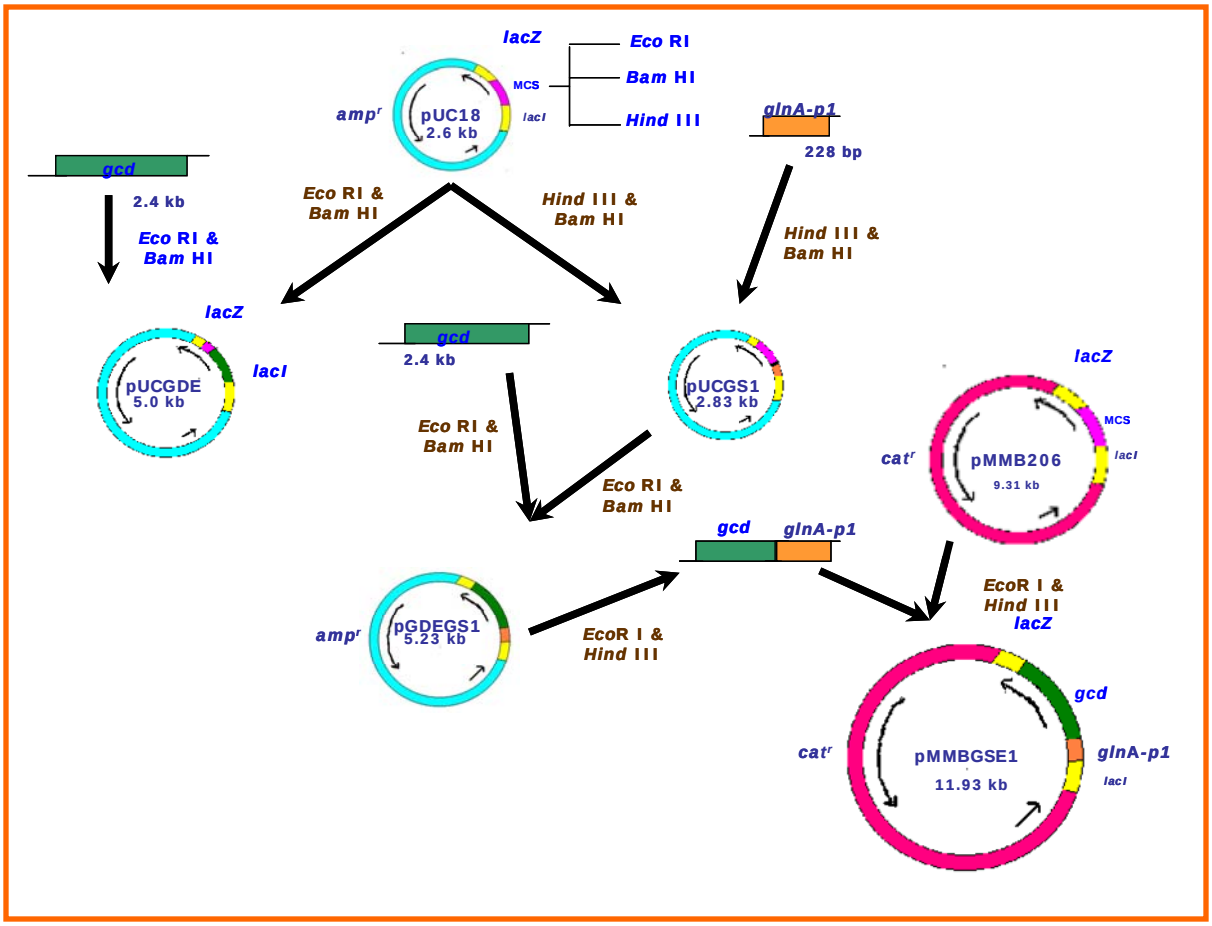

Figure 24: Schematic representation of cloning to generate pMMBEGS1

E. coli gcd (2. 4 kb) was amplified using gene specific primers Fp EGD and Rp EGD and cloned in *Bam* HI and *Eco* RI sites of pUC18 resulted in pUCGDE. *Azotobacter*-specific glutamine synthetase (*gln*A-p1) gene promoter (228 bp) was amplified using promoter specific primers Fp GS1 and Rp GS and cloned in *Bam* HI and *Hind* III sites of pUC18 resulted in pUCGS1. *E. coli gcd* was excised from pUCGDE using *Bam* HI and *Eco* RI and cloned in same sites of pUCGS1 resulted in pGDEGS1. Promoter with *E. coli gcd* was excised using *Eco* RI and *Hind* III and cloned in same sites of broad-host range vector pMMB206 resulted in pMMBEGS1.

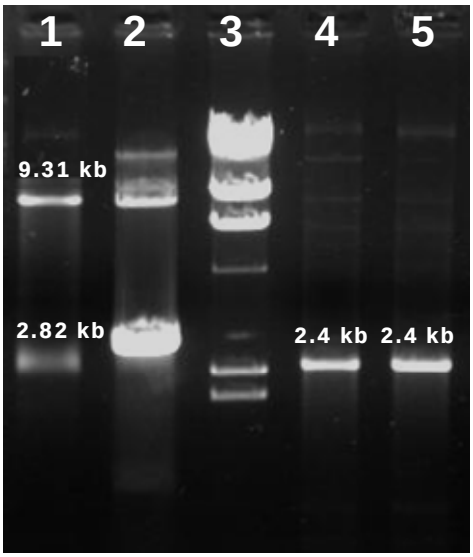

Figure 25: Cloning of *E. coli gcd* under *glnA-p1* promoter in pMMB206

E. coli gcd with *gln*A-p1 gene promoter was excised from pGDEGS1 using *Hind* III and *Eco* RI and cloned in same sites of pMMB206 resulting in pMMBEGS1.

Lane 1: *Hind* III and *Eco* RI digest of pMMBEGS1 released the 2.82 kb insert, **Lane 2:** undigested pMMBEGS1, **Lane 3:** λ DNA *Hind* III digest, and **Lane 4 & 5:** Amplification of the 2.4 kb *E. coli gcd* with pMMBEGS1 as templates

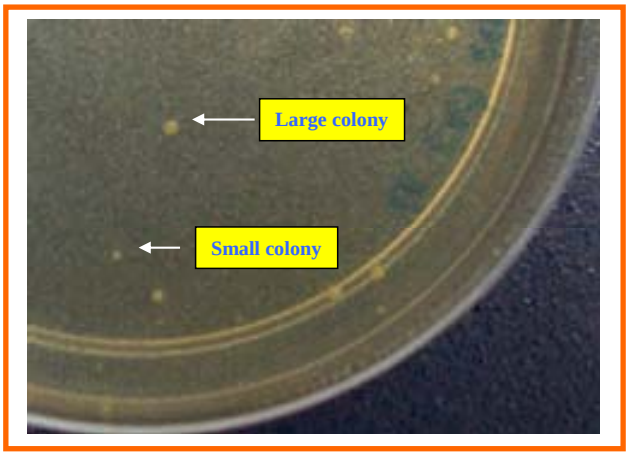

Figure 26: Transformation of *Azotobacter vinelandii*

E. coli gcd under *glnA-p1* promoter (pMMBEGS1) was mobilized into *A. vinelandii* AvOP (Glick *et al*., 1985). The transformed *Azotobacter* showed large and mucous colonies, the non-mucoid small colonies represented non-transformed *Azotobacter*.

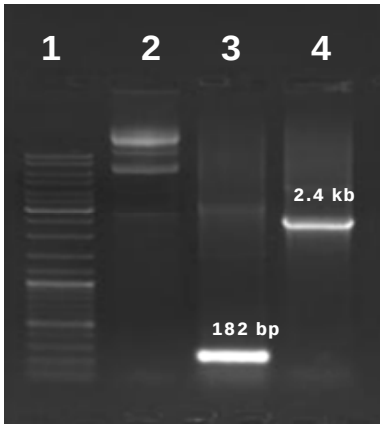

Figure 27: Confirmation of *Azotobacter vinelandii* transformed with pMMBPSE1

Plasmid miniprep of recombinant clone (pMMBPSE1) from transformed *Azotobacter*. *E. coli gcd* (2.4 kb) and *Azotobacter* specific phosphonate transport system gene promoter *pts-p1* (182 bp) were amplified using pMMBEPS1 as templates.

Lane 1: 1 kb DNA ladder mix, **Lane 2:** Native pMMBEPS1, **Lane 3:** Amplification of the 182 bp *pts*-p1 gene promoter with pMMBEPS1 as templates and **Lane 4:** Amplification of the 2.4 kb *E. coli gcd* with pMMBEPS1 as templates.

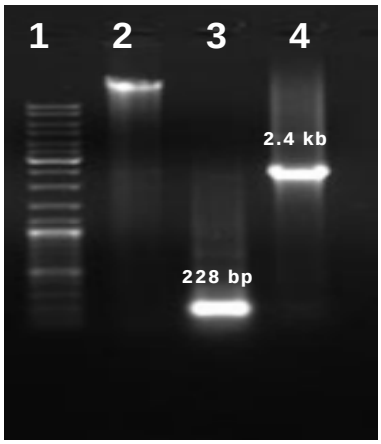

Figure 28: Confirmation of *Azotobacter vinelandii* transformed with pMMBGSE1

Plasmid miniprep of recombinant clone (pMMBGSE1) from transformed *Azotobacter. E. coli gcd* (2.4 kb) and *Azotobacter* specific glutamine synthase gene promoter *glnA-p1* (228 bp) were amplified using pMMBEGS1 as templates.

Lane 1: 1 kb DNA ladder mix, **Lane 2:** Native pMMBEGS1, **Lane 3:** Amplification of the 228 bp *gln*A-p1 gene promoter with pMMBEGS1 as templates and **Lane 4:** Amplification of the 2.4 kb *E. coli gcd* with pMMBEGS1 as templates.

30 ^{o}C. A. vinelandii AVOP harboring pMMB206 did not showed any colouration at 30 ^{o}C temperatures with out PQQ (Figure 29 A), where as *A. vinelandii* AVOP harboring pMMBEPS1 and pMMBEGS1 showed pink colour only on the colony (Figure 29 A) but not as in *E. coli* DH5α harboring pUC18 (positive control) and *E. coli* PP2418 harboring pGDEPS1 and pGDEGS1 (comparative controls) showed pink colouration on the colony with purple halo on MacConkey medium supplemented with PQQ (Figure 29 A).

3. 8. 2 Mineral phosphate solubilization by the *gcd* clones in NBRIP agar: *A. vinelandii* AVOP harboring pMMB206, pMMBEPS1 and pMMBEGS1 were spotted on buffered NBRIP medium. *A. vinelandii* AVOP harboring pMMB206 showed no zone of clearance where as *A. vinelandii* AVOP harboring pMMBEPS1 and pMMBEGS1 showed very small zone of clearance (Figure 29 C), while *E. coli* DH5α harboring pUC18 (positive control) and *E. coli* PP2418 harboring pGDEPS1 and pGDEGS1 (comparative controls) showed zone of clearance on buffered NBRIP medium supplemented with PQQ (Figure 29 C).

3. 8. 3 Mineral phosphate solubilization by the *gcd* clones in liquid NBRIP medium: Quantitative estimation of phosphate solubilization by the recombinant clones was carried out in NBRIP liquid medium for 8 days. *A. vinelandii* AVOP harboring pMMBEPS1 and pMMBEGS1 were spotted on semisolid buffered NBRIP medium resulted in very small zone of clearance (Figure 29 C) and in liquid buffered NBRIP medium there was no significant increase in solubilization when compared with the wild type *Azotobacter* strain (Data not shown). There was an increase in phosphate solubilization when liquid non-buffered medium was used, but *gcd* under *gln*A promoter (predicted to be a more active promoter) released less phosphate into the medium when compared to *gcd* under *pts* promoter. This observation could be due to presence of ammonium sulphate in the NBRIP medium. When ammonium sulphate was replaced with salt III of *Azotobacter* Burk's nitrogen free medium then phosphate release was even higher (Figure 30).

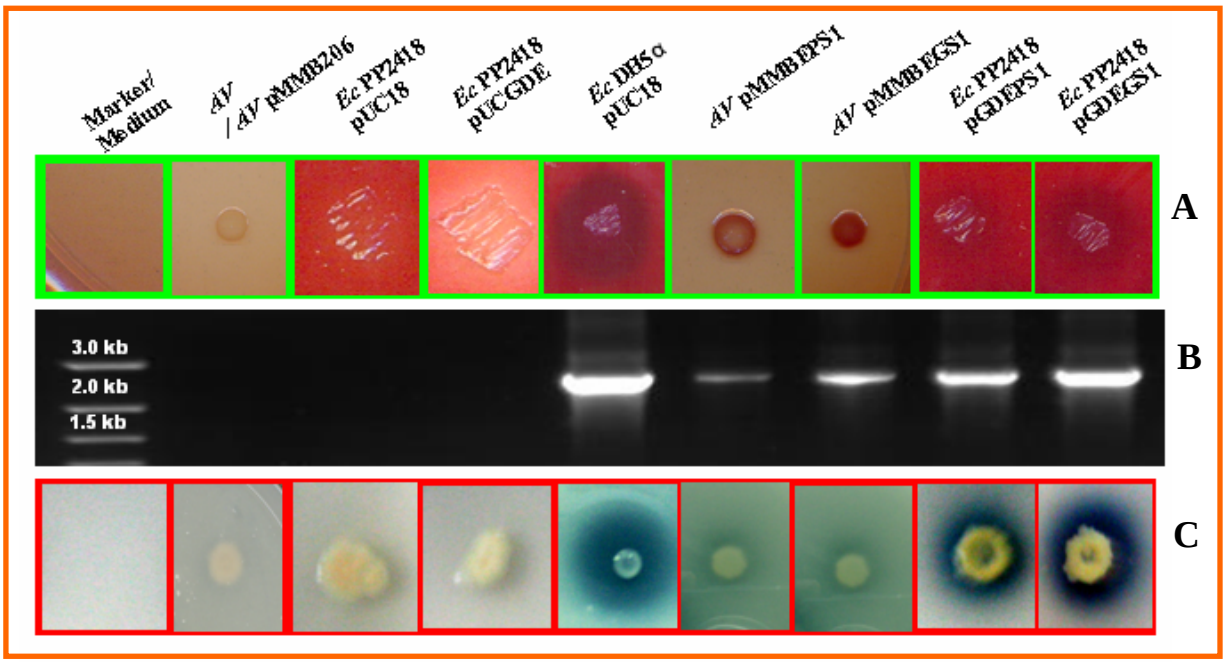

Figure 29: Heterologous expression of *E. coli gcd* and mineral phosphate solubilization by transgenic *Azotobacter*

Azotobacter harboring pMMB206, pMMBEPS1 and pMMBEGS1 & E. coli PP2418 harboring pUC18, pGDEPS1 and pGDEGS1 were checked for *gcd* expression by spotting on MacConkey glucose agar with out PQQ (*Azotobacter* strains) and with PQQ (*E. coli* strains) (**A**). The growth was compared after 24 h incubation at 37 ^{o}C (*E. coli* strains) and 28 ^{o}C (*Azotobacter* strains). The total RNA isolated from the log-phase cultures was used as template in an RT-PCR using *gcd*-specific primer and subjected to 1 % agarose gel electrophoresis with molecular size marker on the extreme left (**B**) and to check MPS ability by the clones were incubated for 7 days in buffered NBRIP agar (**C**).

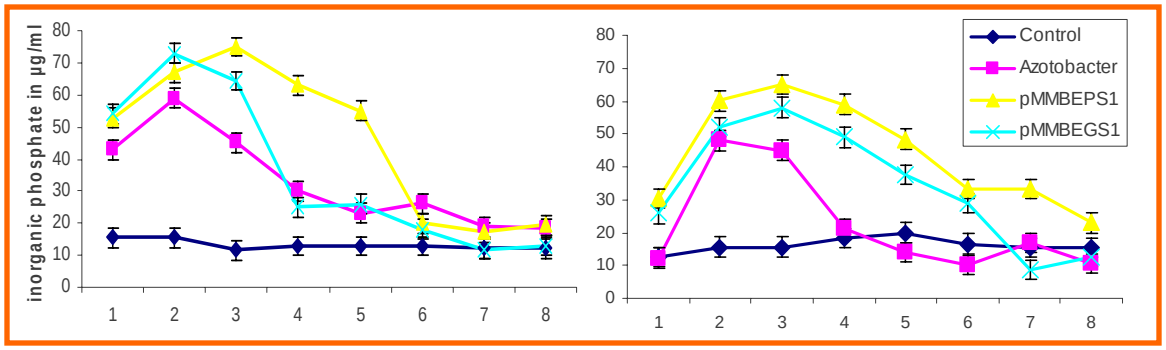

Figure 30: Inorganic phosphate release by azotobacters in non-buffered NBRIP liquid medium supplemented with/without ammonium sulphate

Transgenic and wild-type *Azotobacter* were separately inoculated in non-buffered NBRIP liquid media. Every day 1.5 ml of samples were with drawn, centrifuged at 13,000 rpm for 5 minutes, and the supernatant was used for estimation of inorganic phosphate over a period of 8 days. (**A**) Medium with ammonium sulphate and (**B**) Medium containing sodium molybdate and iron sulphate in place of ammonium sulpahte. The values represent the mean of the triplicates in three independent experiments. The vertical bars indicate standard error.

3. 8. 4 Expression of the clones by RT-PCR analysis: Semi-quantitative estimation of the *gcd* expression was done using RT-PCR analysis. Total RNA isolated form the *A. vinelandii* AVOP harboring pMMB206, pMMBEPS1 and pMMBEGS1, and *E. coli* DH5α harboring pUC18, *E. coli* PP2418 harboring pGDEPS1 and pGDEGS1 as templates in RT-PCR and using Fp EGD & Rp EGD primers resulted in a 2.4 kb amplicon. The level of expression was very low in *A. vinelandii* AVOP harboring pMMBEGS1 when compared to *A. vinelandii* AVOP harboring pMMBEPS1 (Figure 29 B). The level of expression in *E. coli* DH5α harboring pUC18 (positive control) was high when compared to the expression in *E. coli* PP2418 harboring pGDEPS1 and pGDEGS1 (Figure 29 B).

3. 9 NITROGENASE ACTIVITY OF WILD TYPE AND TRANSGENIC *AZOTOBACTER* STRAINS

Nitrogenase activity of transgenic *Azotobacter* expressing *gcd* gene of *E. coli* was not affected significantly in terms of acetylene reduction assay (Figure 31), except that the transgenic strains had slow growth rate when compared to the wild type. The transformants pMMBEPS1 and pMMBEGS1 reduced acetylene to ethylene at the rate 4833 and 4812 μmoles/OD of culture/24 h respectively, while the wild-type strain harboring pMMB206 reduced 5148 μmoles/OD of culture/24 h.

3. 10 GREEN HOUSE EVALUATION OF TRANSGENIC *AZOTOBACTER* STRAINS:

Green house studies of both transgenic and wild-type *A. vinelandii* AVOP showed better growth in terms of plant height and plant fresh weight in seed bacterization of sorghum. The fresh weight of sorghum seedlings was significantly higher in seedlings inoculated with transgenic *Azotobacter* as compared to that of non-transgenic *Azotobacter* treatment. At weekly intervals the plants fresh weight (Figure 32 A) and height (Figure 32 B) were measured for 4 weeks. Sorghum plants grown in TCP with *Azotobacter* and, superphosphate with *Azotobacter* served as controls. Seeds bacterised

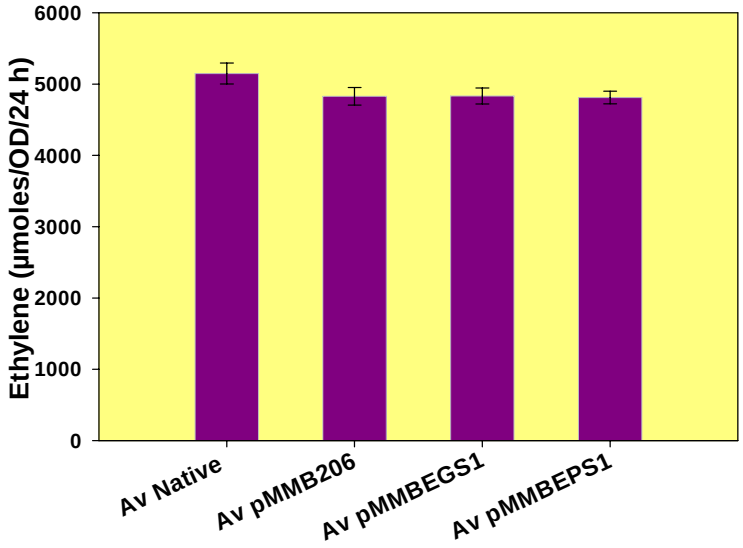

Figure 31: Nitrogenase activity of azotobacters

Nitrogenase activity of transgenic and wild-type azotobacters was evaluated by acetylene reduction assay. *Azotobacter* strains were grown in Bruk's nitrogen-free medium for 48 h. The cells were pelleted, transferred to fresh Bruk's nitrogen-free medium tubes with rubber stopper, flushed with argon and replaced with acetylene. Reduction of acetylene to ethylene was estimated after 24 h. The values represent the mean of the triplicates in three independent experiments. The vertical bars indicate standard error.

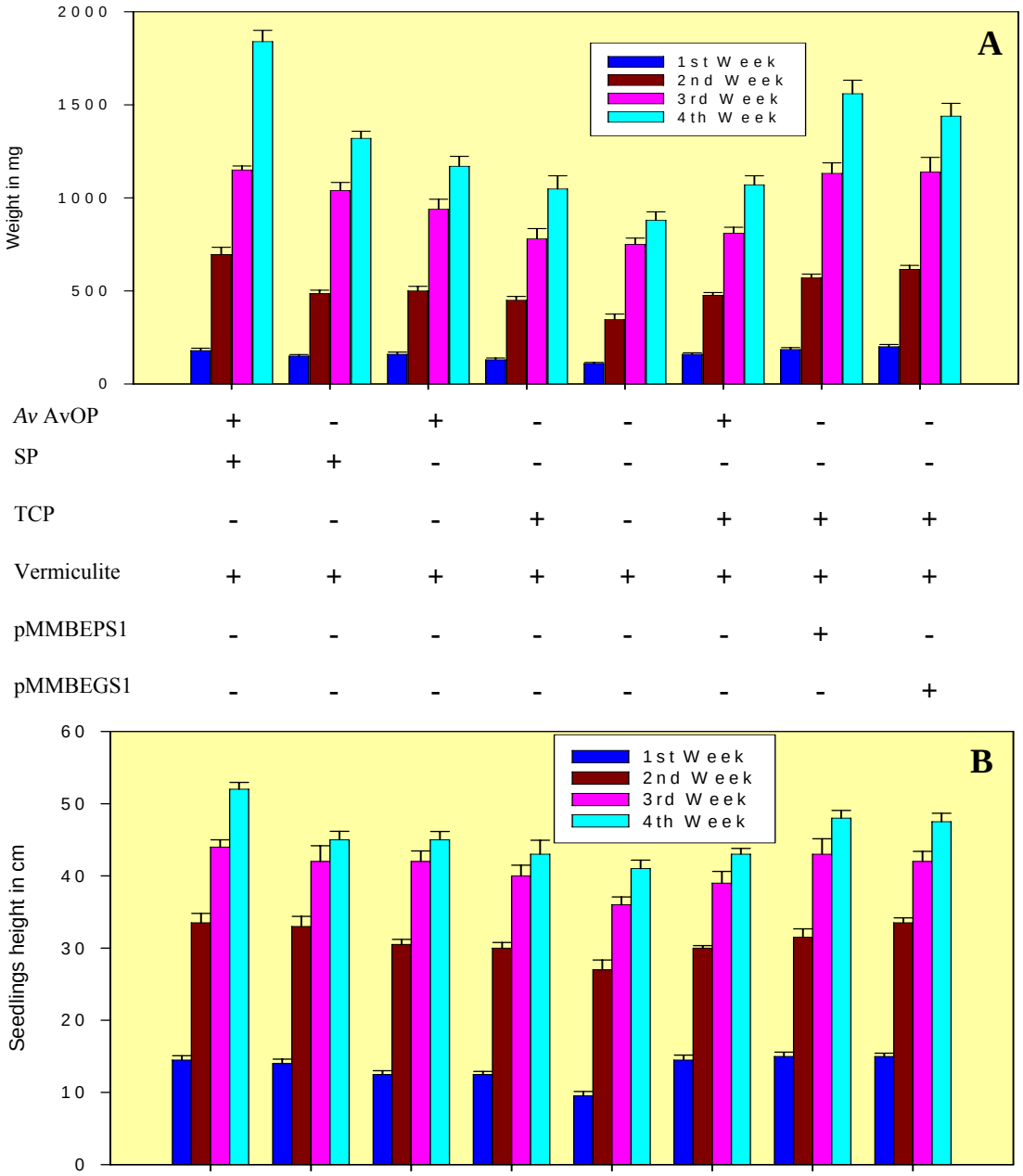

Figure 32: Plant growth promoting activity of transgenic *Azotobacter* in bacterized sorghum seedlings

Sorghum seeds bacterized with transgenic and wild-type azotobacters were raised in sterilized vermiculite-filled earthen pots in green house. Treatment consisted of duplicate pots containing five seedlings each and repeated three times. (**A**) The data on wet weight and (**B**) height of the seedlings was collected. The values represent the mean of three independent experiments and vertical bars represent standard error.

with transgenic *Azotobacter* strains showed a significant increase in height and fresh weight of the plants (Figure 33 A, B, C).

3. 11 HOMOLOGY MODELING AND SITE DIRECTED MUTAGENESIS OF *E. COLI* GDH TO UNDERSTAND STRUCTURE-FUNCTION RELATIONSHIP

We have built the 3D homology model structure of *E. coli* GDH using two methanol dehydrogenases (MDH) and alcohol dehydrogenase (ADH) models available at PDB and identified the amino acid residues in the active site for site directed mutagenesis. Further, mutagenesis was carried out to make substitutions of the identified amino acid residues to understand the importance of the target amino acid residue for the function of GDH. Expressivity of the mutants forms of *gcd* was confirmed by complementation tests and the physical presence of the protein by western blot analysis as described in the following sections 3.11.1 to 3.11.4

3. 11. 1 Homology modeling of *E. coli* GDH: The sequence homology of GDH with MDH is 37 % and with ADH of *P. aeruginosa* is 39 % (Figure 34). The model structure of GDH is a super barrel made up of eight topologically identical four stranded antiparallel β-sheets arranged with radial symmetry like blades of the propeller. The PQQ is buried in the interior of the super barrel in the active site. The Ca^{2+} ion maintains the PQQ in correct configuration by interacting directly with PQQ and amino acid residues present at that position (Figure 35 A). Structural overlay of the GDH with ADH showed the RMS deviation of the C-α back bone to be 0.68 Å (Figure 35 B). The Ramachandran plot analyzed for the structure model of *E. coli* GDH showed that more than 95.8 % amino acid residues were present in the allowed regions, whereas 2.2 % amino acid residues were present in the disallowed regions of Ramachandran plot (Figure 36). Mapping of these residues on the 3D structure indicated that the amino acid residues in the disallowed regions are located close to the anchoring regions of the deleted loops. These residues are far away form the PQQ binding site and hence will not hinder the structure-function correlation studies *in silico*. Five amino acids in the PQQ binding site

Figure 33: Green house evaluation of transgenic *Azotobacter*

Bacterial strains, both transgenic and wild type, were seed bacterized using 0.5% CMC. Bacterized sorghum seeds were sowed in pots containing autoclaved vermiculite, 200 mg/pot tricalcium phosphate, and 500mg/pot superphosphate. In different combinations of super phosphate, tricalcium phosphate, supplemented potting mixture, the growth and vigor of the sorghum seedlings was compared.

Figure 34: Multiple sequence alignment of *E. coli* GDH with MDH of *Methylobacterium extorquens* and *Methylophilus methylotrophus* and ADH of *Pseudomonas aeruginosa* obtained using FUGUE (http://tardis.nibio.go.jp/-fugue/prfsearch.html).

Multiple sequence alignment of *E. coli* GDH with known crystal structures of PQQ-dependent methanol dehydrogenase (MDH) from *Methylobacterium extorquens* (PDB_ID: 1H4J; 37 % homology), and *Methylophilus methylotrophus* (PDB_ID: 1G72; 38% homology) and PQQ-dependent ethanol dehydrogenase (ADH) from *Pseudomonas aeruginosa* (PDB_ID: 1FLG; 39 % homology). Long insertion loops in *E. coli* GDH excluded for protein structure modeling are indicated in red boxes. The code, a, b and 3 shown below the alignment indicate alpha helices, beta strands and 3_{10} helix, respectively. The key to the alignment is as follows: alpha helix (red), beta strand (blue), 3_{10} helix (maroon), solvent accessible lower case, solvent inaccessible (UPPER CASE), hydrogen bond to main-chain amide, **(bold),** hydrogen bond to main-chain carbonyl (underline), disulfide bond (cedilla), and positive phi torsion angle (*italic*).

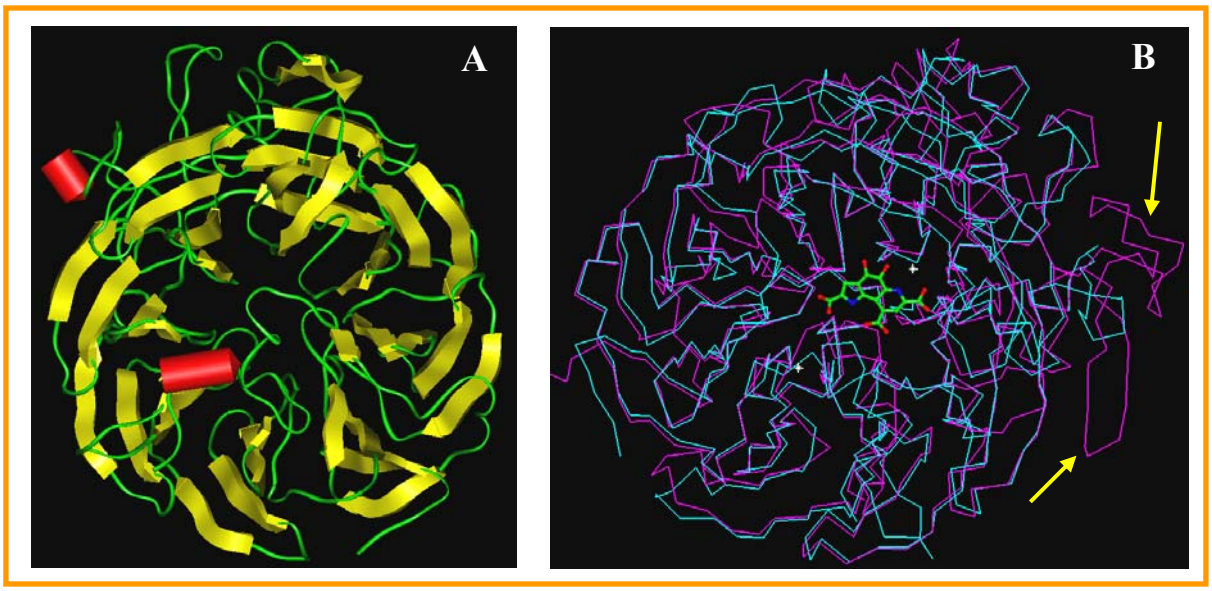

Figure 35: 3-D structure of the homology model of *E. coli* GDH and its C-α superimposition with PDB_ID: 1FLG

The homology model of *E. coli* GDH tertiary structure is shown to have super barrel fold made up of eight topologically equivalent antiparallel β-sheets arranged with radial symmetry like blades of a propeller (**A**). The C-α superimposition of *E. coli* GDH (cyan) with *P. aeruginosa* ADH (magenta) indicates high structural similarity with a root mean square deviation (RMSD) of 0.68Å. The non-homologous regions (insertions) that were looped out in structure building are as indicated by arrows. The PQQ cofactor is indicated in ball and stick (colouring according to atom type) (**B**).

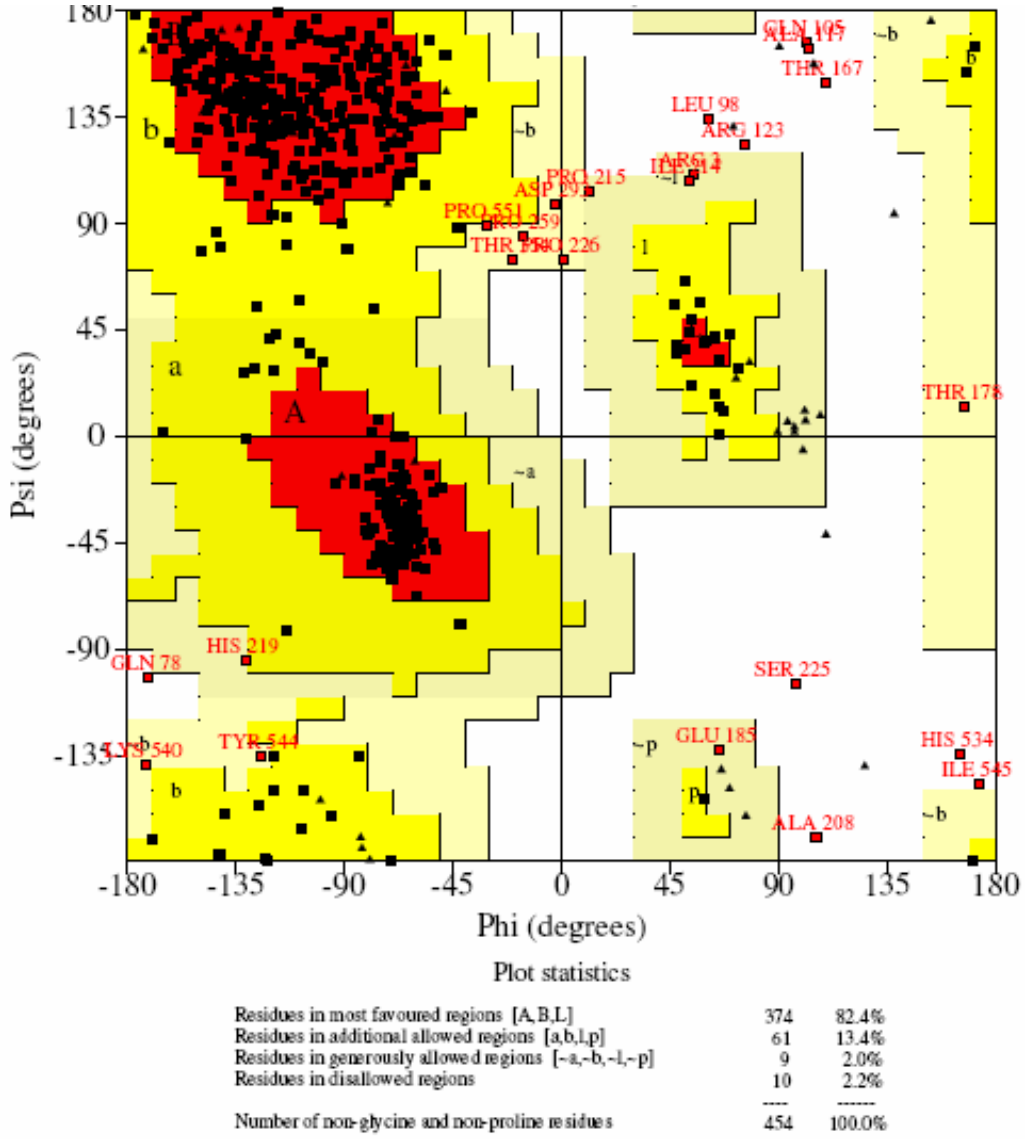

Figure 36: Ramachandran plot for *E. coli* GDH model structure

In order to check the correctness of the geometrical parameters of the homology model structure, Ramachandran plot (Ramachandran *et al*., 1963) was analyzed. The model has 95.8 % of residues in the allowed regions and 2.2 % of the residues in disallowed regions of the Ramachandran plot. The residues that were present in generously allowed and disallowed regions of the Ramachandran plot are close to the regions of insertions that were looped out during model building. These residues are away from the active site and hence do not affect the structure-function correlation studies of the protein.

(Figure 37 A & B) and two amino acids on the surface of model structure (Figure 37 A) were selected for site directed mutations.

3. 11. 2 Site directed mutagenesis of *E. coli gcd* (pATEE): pATEE (*E. coli gcd* in pQE30) was used as the template for the mutations using the $VENT_R$ DNA polymerase. Amplification of the entire plasmid, after 22 rounds of PCR, was confirmed by visualization of a single band on 1 % agarose gel. The methylated parental DNA was cleaved by *Dpn* I digestion and the amplified mutated plasmid was used to transform competent cells of *E. coli* XL1-Blue MRF'. Plasmid isolated from 5 randomly selected colonies was visualized on a 1 % agarose gel (Figure 38), sequenced to confirm the mutations. Mutation of the target codon CGT to GCT confirmed change in the amino acid Arg 201 Ala and the mutated plasmid designated as pATEE R201A. Similarly D204A (Asp 204 Ala), E217L (Glu 217 Leu), E217A (Glu 217 Ala), E217Q (Glu 217 Gln), R266Q (Arg 266 Gln), R266E (Arg 266 Glu), E591L (Glu 591 Leu), E591Q (Glu 591 Gln) E591K (Glu 591 Lys), L712W (Leu 712 Trp), L712R (Leu 712 Arg), G776A (Gly 776 Ala), G776K (Gly 776 Lys), G776D (Gly 776Asp) and G776L (Gly 776 Leu) and the mutated plasmids were designated as pATEE R201A, D204A, E217L, E217Q, E217A, R266Q, R266E, E591L, E591Q, E591K, L712W, L712R, G776A, G776K, G776D and G776L, respectively (Table 6), were generated and confirmed by sequencing.

3. 11. 3 Complementation of *E. coli* GDH mutants on pATEE in *E. coli* YU423: The GDH complementation studies were carried out on MacConkey glucose medium with PQQ. *E. coli* YU423 harboring pATEE and pATEE mutants E217Q and G776A were pink, with a purple halo around the colony, after 24 h incubation at 37 ^{o}C (Figure 39). The was no pink colour with no purple zone around the *E. coli* YU423 harboring pATEE mutants R201A, D204A, E217L, E217A, R266Q, R266E, E591L, E591Q, E591K, L712W, L712R, G776K, G776D and G776L indicated that these mutations affected the function of the GDH (Figure 39).

The amino acid residues substitutions and the altered properties in the *E. coli* GDH form our 3D model structure were explained in table 6. The mutants R201A and

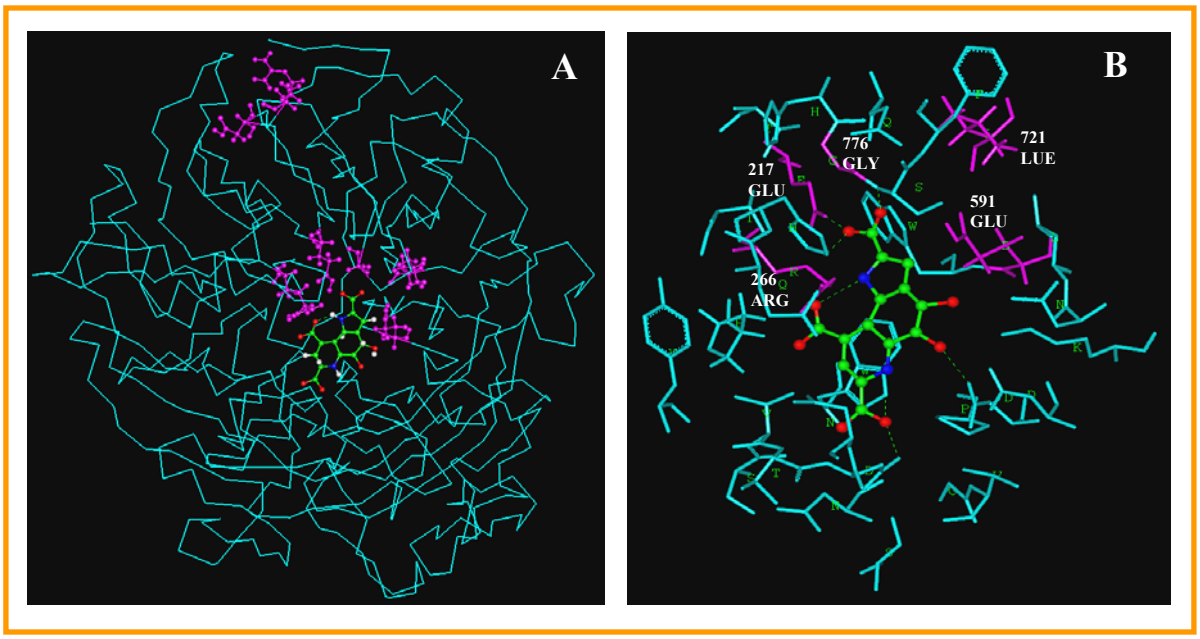

Figure 37: Amino acids targeted for site directed mutagenesis in *E. coli* GDH are indicated in the model structure

C-α trace of the *E. coli* GDH tertiary structure (cyan), side chains of the amino acid residues mutated (purple) and PQQ (colouring according to atom type) are indicated (**A**). The amino acid residues that lie within 5 Å region around the PQQ (indicated in ball and stick) are shown and the amino acid residues shown in purple have been selected for mutation (**B**).

Table 6: Site directed mutants of *E. coli* GDH and their properties

S. No.	Mutagenesis codon		Change in amino acid		Observation	Assumption
	Target	Altered	From	To		
1	CGT	GCT	Arginine	Alanine	No active GDH	Corresponding amino acid lost the interaction with UQ and electron transfer ability
2	GAT	GCT	Aspartic acid	Alanine	No active GDH	Corresponding amino acid lost the interaction with UQ and electron transfer ability
3	GAA	CTT	Glutamic acid	Leucine	No active GDH	Hydrogen bonding with PQQ lost
4	GAA	CAA	Glutamic acid	Glutamine	Active GDH	Glutamine can substantiate the hydrogen bonding with PQQ instead of Glutamate
5	GAA	GCT	Glutamic acid	Alanine	No active GDH	Hydrogen bonding with PQQ lost
6	CGT	GAA	Arginine	Glutamic acid	No active GDH	Hydrogen bonding with PQQ lost
7	CGT	CAA	Arginine	Glutamine	No active GDH	Hydrogen bonding with PQQ lost
8	GAA	CTG	Glutamic acid	Leucine	No active GDH	Hydrogen bonding with PQQ lost
9	GAA	CAG	Glutamic acid	Glutamine	No active GDH	Hydrogen bonding with PQQ lost
10	GAA	AAG	Glutamic acid	Lysine	No active GDH	Hydrogen bonding with PQQ lost
11	CTG	TGG	Leucine	Tryptophan	No active GDH	Bulky group hindrance of Phe-532 position
12	CTG	CGT	Leucine	Arginine	No active GDH	Bulky group hindrance of Phe-532 position
13	GGT	GCT	Glycine	Alanine	Active GDH	Amino acid alanine being small side chain can fit in the pocket
14	GGT	CTG	Glycine	Leucine	No active GDH	Only small side chain amino acids are allowed in the pocket
15	GGT	GAC	Glycine	Aspartic acid	No active GDH	Only small side chain amino acids are allowed in the pocket
16	GGT	AAG	Glycine	Lysine	No active GDH	Only small side chain amino acids are allowed in the pocket

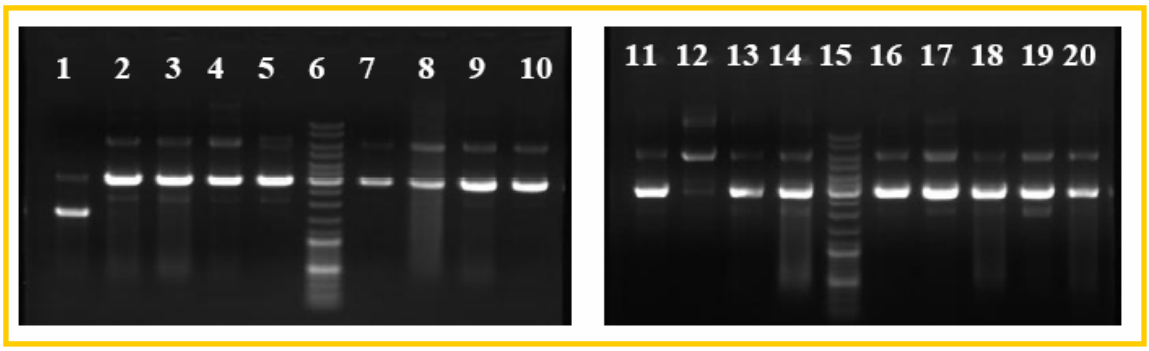

Figure 38: Mini prep of putative clones of pATEE mutants generated through site directed mutagenesis

The plasmid pATEE was used as template in a PCR with the mutagenic primers (Table 5). After 20 cycles of PCR the mutated plasmid, a nick circular form was transformed into *E. coli* XL1 blue MRF'. The putative plasmids were isolated from the transformed colonies were visualized on a 1 % agarose gel.

Lane 1: E217L, **Lane 2:** E217L, **Lane 3:** E217Q, **Lane 4:** E217A, **Lane 5:** E266Q, **Lane 6:** 1 kb DNA ladder mix, **Lane 7:** E266L, **Lane 8:** E591L, **Lane 9:** E591Q, **Lane 10:** E591K, **Lane 11:** R201A, **Lane 12:** D204A, **Lane 13:** L712W**, Lane 14:** L712W**, Lane 15:** 1 kb DNA ladder mix, **Lane 16:** L712R**, Lane 17:** G776L**, Lane 18:** G776Q**, Lane 19:** G776K**, Lane 20:** G776A

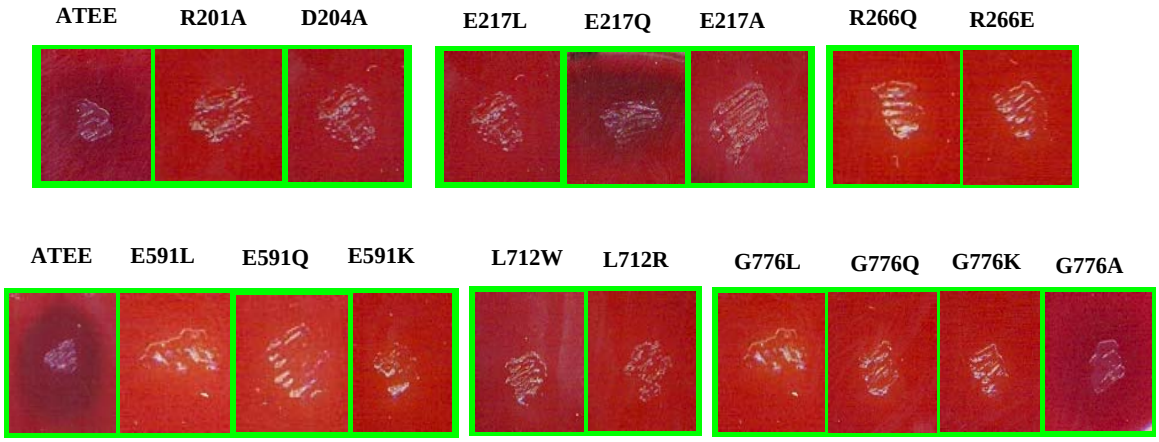

Figure 39: GDH complementation by the *E. coli* GDH mutants on MacConkey glucose agar

E. coli YU423 harboring pATEE, R201A, D204A, E217L, E217Q, E217A, E266Q, E266L, E591L, E591Q, E591K, L712W**,** L712R**,** G776L**,** G776Q**,** G776K and G776A were spotted on MacConkey glucose agar medium with PQQ. The growth pattern was compared after 24 h of incubation at 37 ^{o}C.

D204A have lost the GDH activity, mainly because of the loss of its interaction with ubiquinone and concomitant transfer of electron in the respiratory chain hence there was no complementation seen on MacConkey medium (Figure 39). Multiple sequence alignment among 17 different GDHs, observed that the basic nature of amino acid at position 201 is conserved and Asp-204 is highly conserved (Figure 40 A). The 5 Å region around these amino acid residues in the 3D model of *E. coli* GDH suggests that this domain region is in the neighbourhood of hydrophobic amino acids and that Arg-201 and Asp-204 are embedded in the hydrophobic core (Figure 40 B). These amino acid residues directly interact with the UQ and transfer electrons. The mutants E217L, E217A, R266Q, R266E, E591L, E591Q and E591K have lost the activity of the GDH mainly because of the loss of the hydrogen bonding interactions with the PQQ cofactor (Figure 41 and 42). These amino acids are directly involved in interaction with PQQ through hydrogen bonding, which is embedded in the active site of the GDH in the native protein.

The mutants L712W and L712R have lost the GDH activity. Multiple sequence alignment among MDH, ADH and GDH, Leu-712 position in *E. coli* GDH is occupied by tryptophan in MDH and ADH we observed that a phenylalanine at 532 position is spatially close to W712 (Figure 43). These close contacts of hydrophobic bulky group amino acid residues may disturb the confirmation of the protein at active site and thus leads to loss of the activity. Similarly the long side chain charged amino acid substitution at L712R leads to the confirmation change in the active site and GDH lost its activity (Figure 43). The mutants G776K, G776D and G776L have also lost the activity of GDH. The multiple sequence alignment of 17 different GDHs showed highly conserved nature of Gly-776 (Figure 44 A). From graphical examination, we observe that Gly-776 is close to the PQQ binding site and there is no room for a large side chain at this position. The mutants G776K, G776D and G776L, in order to accommodate large side chain, the main chain C-α of the protein may get deviated (Figure 44 B).

3. 11. 4 Expression, SDS-PAGE and Western blot analysis of GDH mutants: *E. coli* glucose dehydrogenase mutants pATEE R201A, D204A, E217L, E217A, E217Q, R266Q, R266E, E591L, E591Q, E591K, L712W, L712R, G776A, G776K, G776D, G776L and native pATEE were expressed in *E. coli* AT15 and the cells were sonicated.

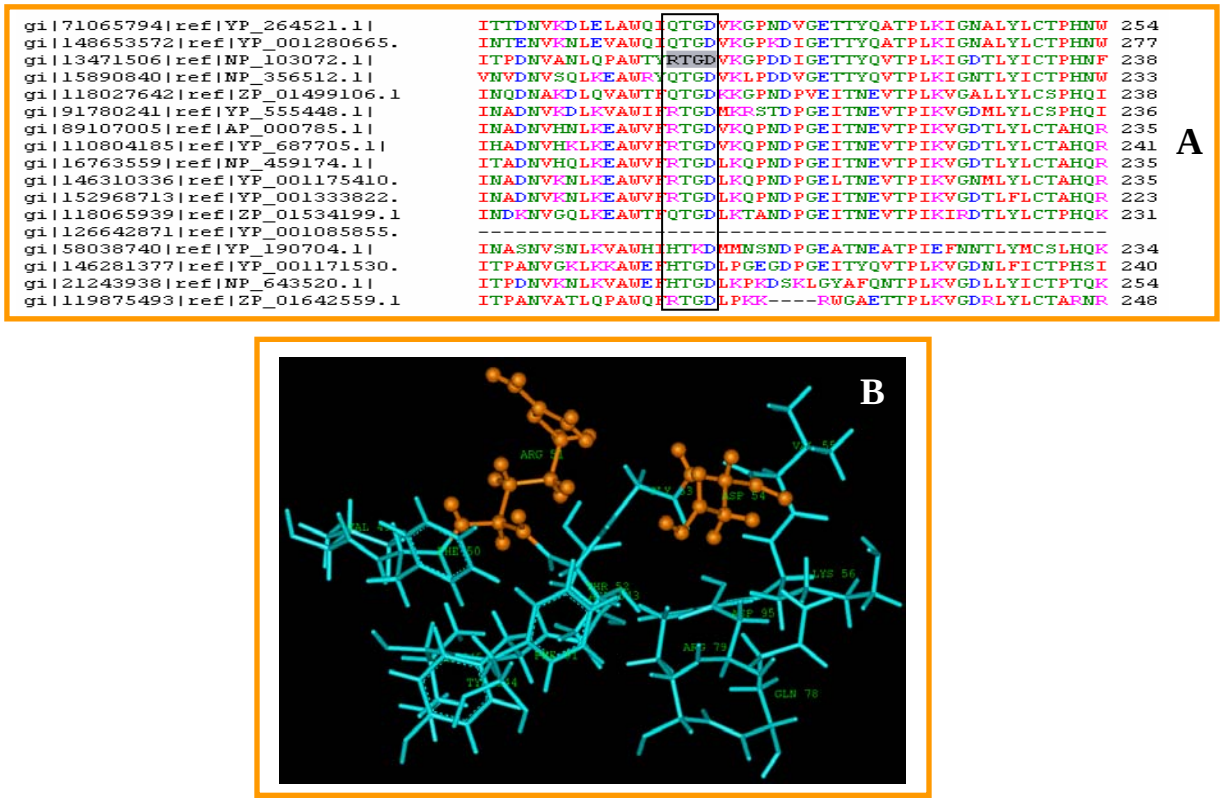

Figure 40: Site directed mutants of R201A and D204A

Multiple sequence alignment of mGDHs from seventeen different Gram-negative bacteria showed the presence of conserved basic amino acid at 201 position and conserved acidic amino acid at position 204 (**A**). The 5 Å region around Arg-201 and Asp-204 residues (indicated in ball and stick) showed the cluster of hydrophobic amino acids (**B**).

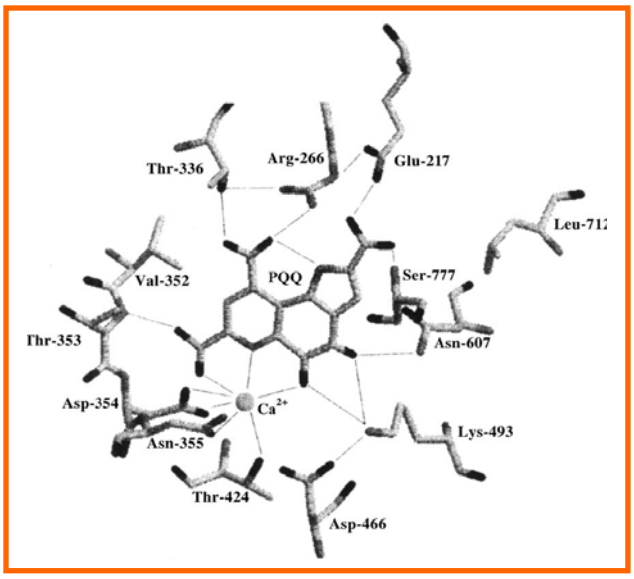

Figure 41: Site directed mutagenesis of E217 and R266 in *E. coli* GDH

A schematic view of 5 Å region around the PQQ binding domain in *E. coli* GDH shows the hydrogen bonds (indicated in dotted lines) with several amino acid residues. The amino acid residues Glu-217, Arg-266 and Leu-712 were chosen for site directed mutagenesis for the present study (Source: Cozier and Anthony 1995).

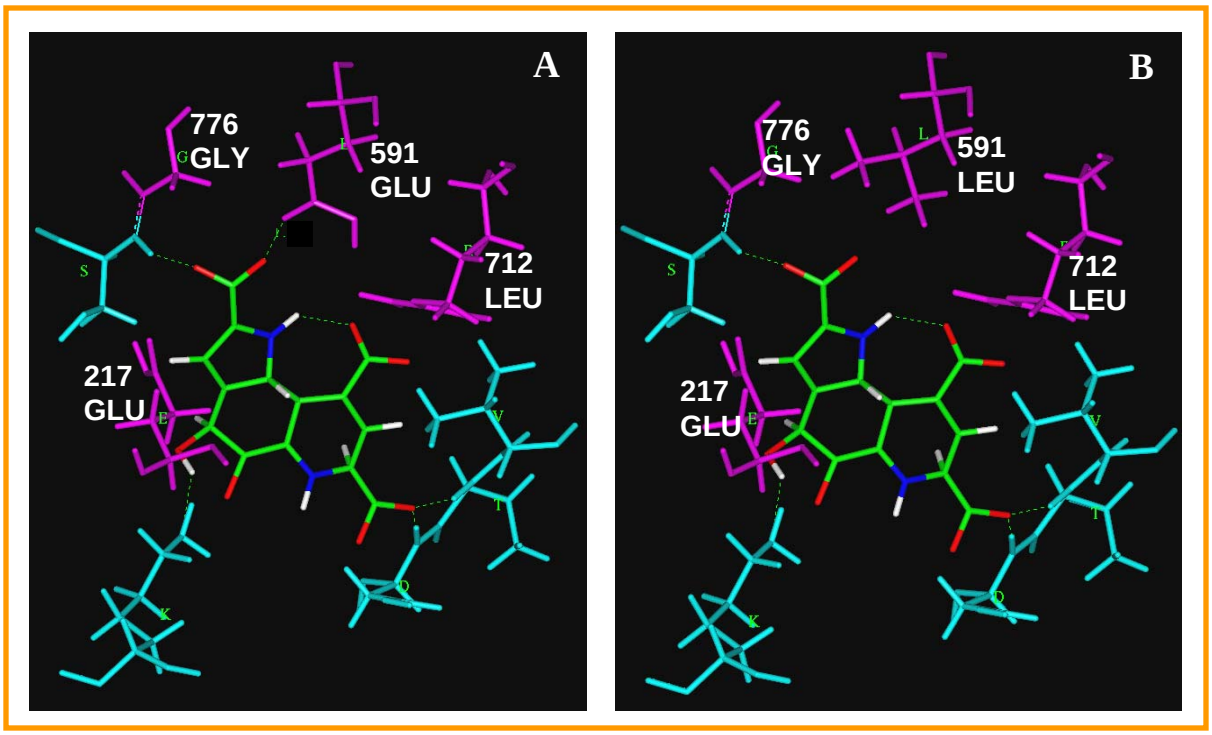

Figure 42: Site directed mutagenesis of E591 in *E. coli* GDH

A schematic view of 5 Å region around the PQQ binding domain in *E. coli* GDH shows the hydrogen bonding (green doted lines). The side chain of Glu-591 position forms hydrogen bonding with PQQ (**A**). Upon *in silico* mutation E591L, hydrogen bonding interaction is lost (**B**).

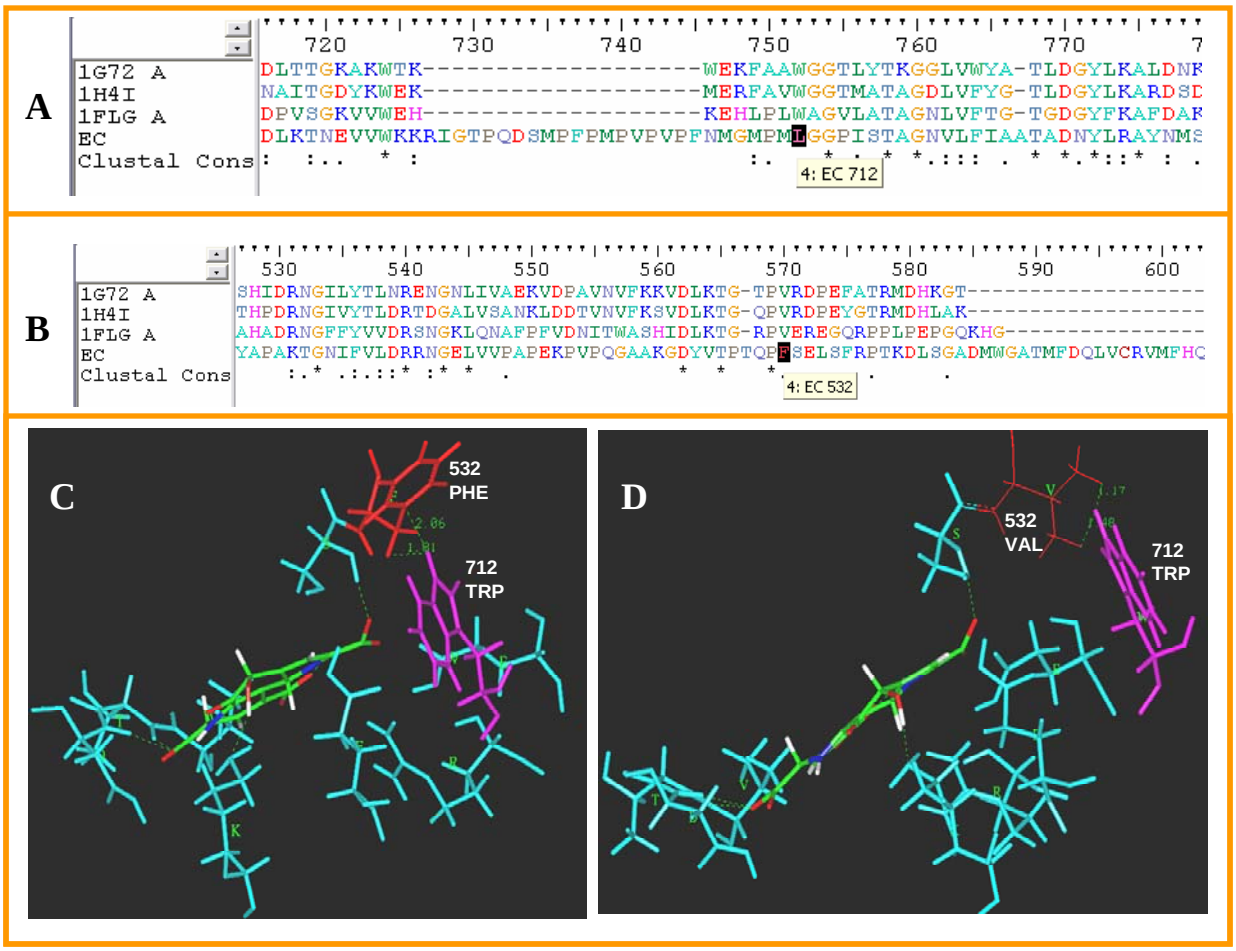

Figure 43: Site directed mutagenesis of L712 in *E. coli* GDH

Multiple sequence alignment of *E. coli* GDH with the PDB_ID's: 1G72, 1H4I and 1FLG indicates that the conserved tryptophan at 712 amino acid residue position in MDH and ADH is replaced by leucine in *E. coli* GDH. (**A**). From this alignment, it is also seen that the conserved valine at 532 amino acid residue position in MDH and ADH is replaced by phenylalanine in *E. coli* GDH (**B**). A schematic view of the *in silico* mutation of L712W indicates bulky group hindrance due to Phe-532 (**C**). A schematic view of the subsequent *in silico* mutation of F532V relieves the steric crowding (**D)**.

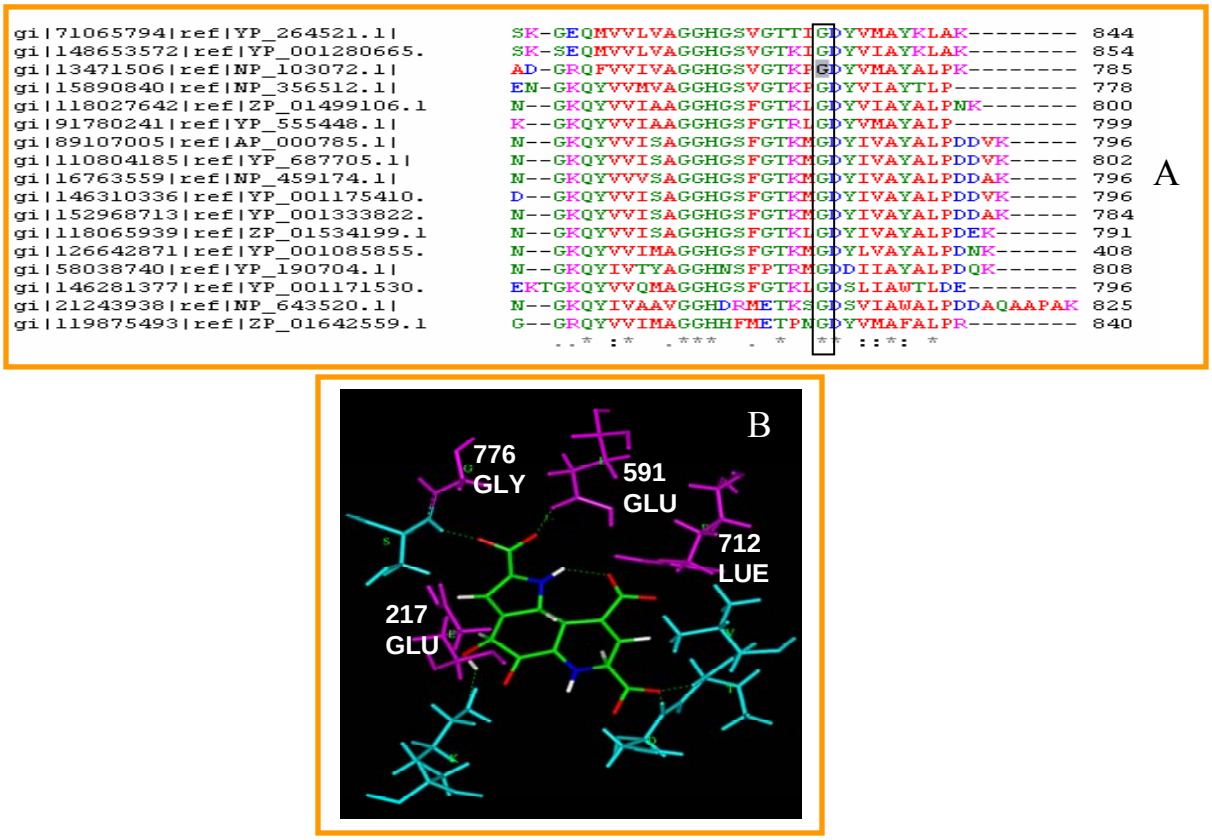

Figure 44: Site directed mutagenesis of Gly-776 in *E. coli* GDH

Multiple sequence alignment of mGDHs from seventeen different Gram-negative bacteria shows the highly conserved glycine amino acid residue at 776 position (**A**). Glu-217, Glu-591, Leu-712 and Gly-776 are indicated in purple. The PQQ cofactor is indicated in ball and stick (colouring according to atom type).

The sonicated samples were loaded on 10 % SDS-PAGE. SDS-PAGE analysis of the sonicated samples clearly showed a protein corresponding to ~90 kDa and comparable to *E. coli* GDH (Figure 45) confirmed the expression of GDH in the mutants. The expressed and sonicated samples of all the mutants were resolved on a 10 % SDS-poly acrylamide gel, transferred onto nitrocellulose membrane and probed with anti-His antibodies using BCIP-NBT as substrate. A signal corresponding to 90 kDa was detected for all the mutants along with the *E. coli* GDH (positive control) (Figure 46). The protein content of the pATEE mutants G776L, G776Q and G776K showed low levels in the immunoblot when compared to *E. coli* GDH and other pATEE mutants (Figure 46).

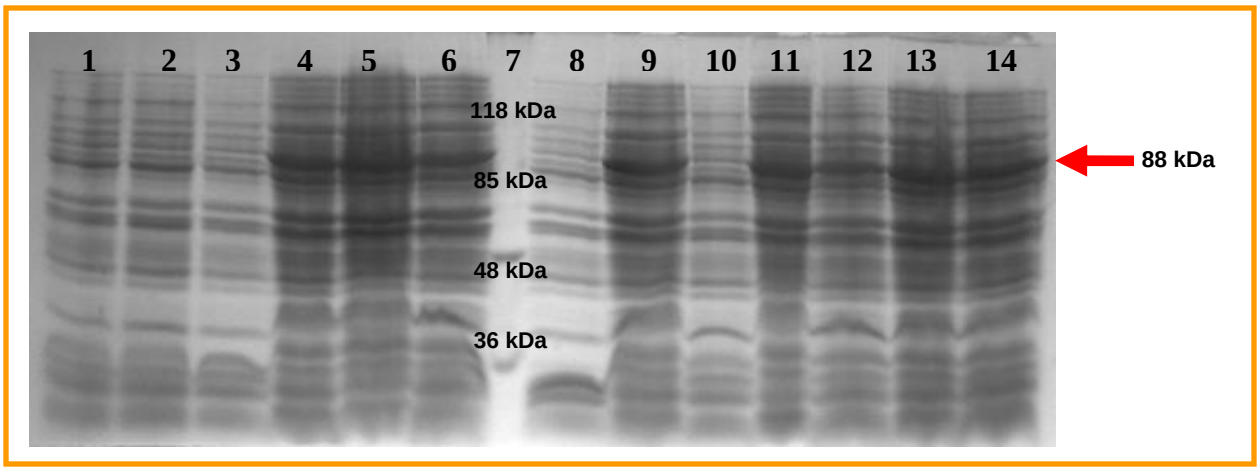

Figure 45: SDS-PAGE of the IPTG induced expression of *E. coli* GDH and its mutants in *E. coli* AT15

The *E. coli* AT15 harboring pATEE and the mutants were induced with IPTG and the cells harvested after 3 h was boiled for 5 min and the protein pattern was analyzed on a 10 % SDS-poly acrylamide gel.

Lane 1: 0 h ATEE **Lane 2:** 0 h E217L, **Lane 3:** 0 h E266Q, **Lane 4:** 3 h ATEE **Lane 5:** 3 h E217L, **Lane 6:** 3 h E266Q**, Lane 7:** Protein molecular weight marker, **Lane 8:** 0 h E591L, **Lane 9:** 3 h E591L, **Lane 10:** 0 h L712W, **Lane 11:** 0 h L712W, **Lane 12:** 3 h G776A, **Lane 13:** 3 h R201A and **Lane 14:** 3 h D204A.

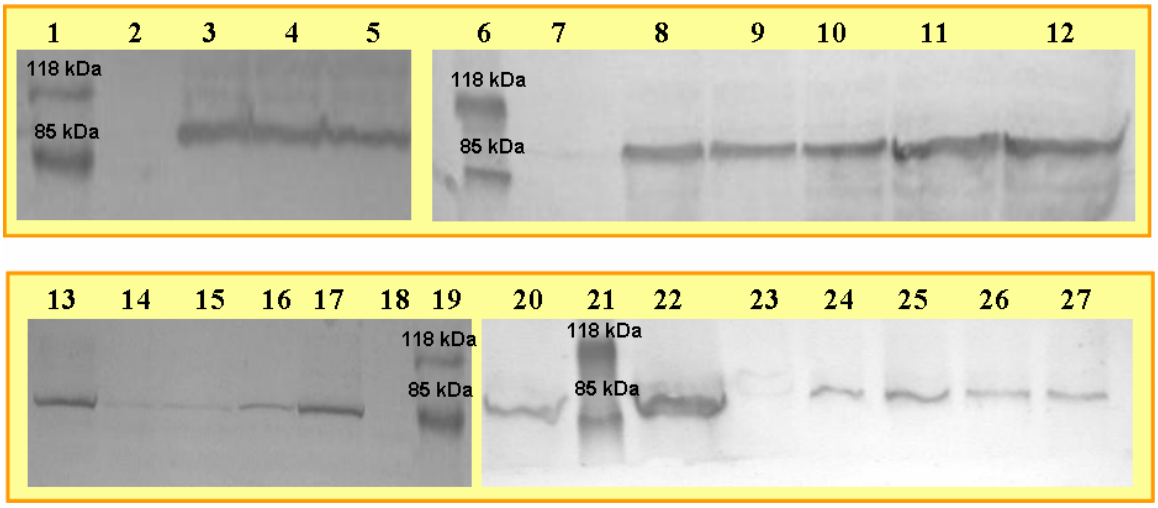

Figure 46: Western blot of *E. coli* GDH and its mutants

The sonicated fraction of *E. coli* GDH and the mutants were subjected to a 10 % SDS-PAGE, transferred onto nitrocellulose membrane and probed with anti-His antibodies. The mutant GDH bands corresponding with the ES chimeric GDH (~ 90 kDa) were identified using BCIP-NBT as substrate.

Lane 1, 6, 19 and 21: Prestained protein molecular weight marker, **Lane 2, 7, 18 and 23:** Negative controls (pQE30), **Lane 3-5:** ATEE, R201A and D204A**, Lane 8-12:** E217L, E217Q, E217A, E266Q and E266L, **Lane 13-17:** ATEE, G776L**,** G776Q**,** G776K and G776A **Lane 20:** E591L, **Lane 22** ATEE, and **Lane 24-27:** E591Q, E591K, L712W and L712R.

Discussion

4. 1 Gram-negative bacteria are efficient in mineral phosphate solubilization

Phosphorous is one of the most essential macro-nutrients for plant growth and metabolism, and also has the tendency to form a major limiting factor in the soil in terms of availability in free form for the ready absorption by the plants. The indiscriminate use of fertilizers and the re-precipitation of the phosphate back into the soil as insoluble salts due to presence of metal ions such as Ca^{2+}, Al^{3+} and Fe^{3+} etc., lead to the accumulation of large reserves of insoluble phosphate. Microorganisms play a significant role in phosphate metabolism by releasing the fixed forms of inorganic phosphate and bringing them into solution. Most soils are endowed with a plethora of naturally occurring bacteria, but their performance may be severely affected by the environmental factors especially under stress conditions (Yahya and Al-Azawi, 1989; Pal, 1998) during the summer seasons resulting in poor growth and survival, hence the use of phosphate solubilizing microorganisms (PSMs) as bioinoculants is often desirable.

Several isolates from our collection were screened for their MPS ability *in vitro* on semi-solid medium having both TCP and HAP (which is harder than TCP in terms of solubility) individually, to isolate efficient PSB. The larger and clearer zones of phosphate solubilization by the bacterial cultures on modified NBRIP medium, rather on PVK medium could be attributed to the inhibitory effect of the yeast extract on the cultures ability to solubilize mineral phosphate (Nautiyal, 1999). Since the plate method is only a preliminary qualitative technique for screening of MPS bacteria, the cultures were further tested in NBRIP liquid medium for quantitative estimation of the phosphate released for the selection of an efficient phosphate solubilizer.

The MPS trait is often linked to the secretion of organic acids. The solubilization of insoluble forms of inorganic phosphates was linked to the production and release of low molecular weight organic acids (Goldstein, 1986; Leyval and Berthelin, 1989; Salih *et al*., 1989). Phosphate regulation of MPS trait was known in *E. coli*, *Erwinia herbicola* and *E. asburiae* (Liu *et al*., 1992; Gyaneshwar *et al*., 1999). Krishnaraj and Goldstein (2001) reported a dramatic decrease in the levels of gluconic acid production in the medium of *S. marcescens* ER2, with a corresponding reduction in the TCP solubilization, indicating the possibility of the regulation of the MPS trait. The decrease in the soluble

phosphate towards the end of the incubation may be because of the utilization of the available phosphate by the culture for their own metabolism. Most of the Gram-negative bacteria were better solubilizers of mineral phosphate than Gram-positive bacteria (Tripura, 2006). The direct oxidation pathway forms the metabolic basis for the strong mineral phosphate solubilizing phenotype in Gram-negative bacteria involving the enzymatic conversion of glucose to gluconic acid ($pK_a \sim 3.4$) by the quinoprotein GDH requiring PQQ as the cofactor (Duine *et al*., 1979; Anthony, 1988; Duine, 1991).

All the *Serratia marcescens* strains, especially *S. marcescens* GPS 5, followed by *E. asburiae* and *E. coli* DH5α were identified as the best solubilizers among the various isolates screened (Tripura, 2006). Solubilization of phosphate complexes by *Pseudomonas cepacia*, *Erwinia herbicola* and *S. marcescens* was reported to be due to GDH-mediated production of gluconic acid (Goldstein *et al*., 1993; Liu *et al*., 1992; Krishnaraj and Goldstein, 2001). The GDH-mediated acidification was the main mechanism of phosphate solubilization by *E. asburiae* PS13, and the aldonic acids generated by the action of GDH on various sugars can bring about the phosphate solubilization (Sharma *et al*., 2005). *E. coli* DH5α, *S. marcescens* GPS 5 and *E. asburiae* were therefore selected for the isolation of *gcd* for further studies. *E. coli* produces PQQ-dependent GDH apoenzyme, but is unable to synthesize PQQ, and depends on external supply of PQQ for GDH activity (Hommes *et al*., 1984). The location of the GDH apoenzyme on the periplasmic side facilitates the binding of externally supplied PQQ to form the holoenzyme.

4. 2 EMS mutagenesis of *S. marcescens* GPS 5

EMS causes a spectrum of optimal mutations in bacteria without being lethal (Coulondre and Miller, 1977). Here we report isolation of mutants with either an increase or decrease in the MPS by EMS mutagenesis, and thereby the amenability of MPS for easy genetic manipulation. There was no correlation in the phosphate solubilization by the cultures in both solid and liquid medium either for the test strains or for the EMS mutants. Mutants with decreased MPS, and lack of pigmentation typical of *S. marcescens* strains (EMS III *Sm* 20) indicates the possibility of multiple mutations affecting both

MPS and the pigmentation traits. *S. marcescens* GPS 5 was identified as a good phosphate solubilizer (section 4.1) compared to the known Gram-negative PSB. Further isolation of MPS enhanced mutants of *S. marcescens* GPS 5 indicates the scope of improvement of the MPS through mutagenesis. As a biocontrol strain, controlling late leaf spot of groundnut (Kishore *et al*., 2005), *S. marcescens* GPS 5 holds great promise as a microbial inoculant for groundnut cultivation both in terms of disease control and also as an effective phosphate mobilizing PGPR.

4. 3 Cloning of *Azotobacter*-specific *gln*A and *pts* promoters

To express the MPS phenotype in transgenic *Azotobacter*, *Azotobacter*-specific glutamine synthetase (*gln*A) and phosphonate transport system (*pts*) promoters were selected. The MPS phenotype expression under regulation of *gln*A promoter may regulate negatively through the presence of fixed nitrogen in the soil. While the MPS phenotype expression under regulation of *pts* promoters may regulate positively in phosphate limited conditions in the medium. Promoter-specific primers were designed upstream to the genes of *A. vinelandii* AvOP with two forward primers starting at different positions and a common reverse primer. The 228 bp *gln*A-p1 and 134 bp *gln*A-p2 of glutamine synthetase gene promoter and the 182 bp *pts*-p1 and 128 bp *pts*-p2 of phosphonate transport system gene promoter were PCR-amplified form the genomic DNA of *A. vinelandii* AvOP using promoter-specific primers. Restriction analysis and PCR confirmed the constructs pUCGS1 (*Azotobacter*-specific *gln*A-*p*1 in pUC18), pUCGS2 (*Azotobacter*-specific *gln*A-*p*2 in pUC18), pUCPS1 (*Azotobacter*-specific *pts*-*p*1 in pUC18), pUCPS2 (*Azotobacter*-specific *pts*-*p*2 in pUC18). All the amplifications were carried out with *Pfu* DNA polymerase to minimize proof reading error during the amplification.

4. 4 PCR-based amplification of *E. coli, E. asburiae* and ES chimeric *gcd*

The 2.4 kb *gcd* sequence of *E. coli* was already reported and hence using gene specific primers *gcd* was PCR amplified from the genomic DNA of *E. coli*. Restriction

analysis and PCR confirmed the construct pUCGDE (*E. coli gcd* in pUC18). *gcd* sequence of *E. asburiae* was first reported and characterized form our laboratory (Tripura *et al*., 2007) and shares more than 95 % homology with the *E. coli gcd* sequence hence using gene specific primers the 2.4 kb gene was PCR amplified from the genomic DNA of *E. asburiae.* Since the 1.7 kb *S. marcescens* GPS5 *gcd* was not expressed when cloned under regulation of T5 based promoter in pQE30 (Tripura, 2006) because of the lack of membrane span domains, she had then fused N-terminal membrane span domain of *E. coli* and C-terminal *S. marcescens* partial *gcd* and the clone was designated as pATESE (*ES* chimeric *gcd* in pQE30). The ES chimeric GDH was expressed and characterized (Tripura and Podile, 2007). The 2.4 kb ES chimeric *gcd* was PCR-amplified using pATESE as templates and Fp EGD & Rp SMGD.

4. 5 Cloning of *E. coli, E. asburiae,* ES chimeric *gcd* under regulation of *Azotobacter*-specific *gln*A and *pts* promoters

To express *E. coli*, *E. asburiae*, ES chimeric *gcd* under regulation of *Azotobacter*-specific *gln*A and *pts* promoters. The 2.4 kb *E. coli gcd* was released form pUCGDE and cloned in pUCPS1 & pUCGS1. Restriction analysis and PCR confirmed the constructs pGDEPS1 (*E. coli gcd* under *pts*-*p*1 in pUC18) and pGDEGS1 (*E. coli gcd* under *gln*A-*p*1 in pUC18). Similarly the 2.4 kb *E. asburiae* and ES chimeric *gcd* was individually cloned in pUCPS1 & pUCGS1. Restriction analysis and PCR confirmed the constructs pGDNTPS1 (*E. asburiae gcd* under *pts*-*p*1 in pUC18), pGDNTGS1 (*E. asburiae gcd* under *gln*A-*p*1 in pUC18), pGDESPS1 (*ES* chimeric *gcd* under *pts*-*p*1 in pUC18) and pGDESGS1 (*ES* chimeric *gcd* under *gln*A-*p*1 in pUC18).

4. 6 GDH complementation studies

The phosphotransferase system (PTS) is the principal pathway for glucose metabolism in *E. coli* where the sugars are directly phosphorylated by enzyme I of the PTS and metabolized *via* the Embden-Meyerhof-Parnas (EMP) pathway, the pentose phosphate pathway (HMP shunt) or by the less common Entner-Doudoroff (ED)

pathway. In *E. coli* PTS$^-$ mutants where the utilization of several carbohydrates, including glucose, is impaired by the deterioration of the PTS system [concomitant phosphorylation and penetration of the carbohydrate substrate through the cytoplasmic membrane (Postma *et al*., 1989; Erni, 1989)], glucose is directly oxidized to gluconic acid, which is in turn presumably catabolized *via* the ED pathway, thus providing an alternative route to glucose utilization (Gottschalk, 1986). Since glucose can be utilized either by the PTS pathway or by the GDH pathway it would be ideal to study the *in vivo* activity of GDH in a PTS and GDH deficient mutant.

gcd complementation studies were, therefore, carried out in *E. coli* PP2418 (PTS$^-$ GDH$^-$), which cannot utilize glucose either by the PTS or the GDH pathway. Glucose can be utilized only when *gcd* cloned in the plasmid is expressed. Since *E. coli* is deficient in PQQ synthesis, it was supplied externally in the medium. The location of the active site of the enzyme towards the periplasm facilitated the binding of the cofactor to form the holoenzyme. Colonies of *E. coli* PP2418 transformed with pUC18, pUCGDE, pGDEPS1, pGDEGS1, pGDNTPS1, pGDNTGS1, pGDESPS1 and pGDEGPS1 were spotted on MacConkey glucose agar plates both with and without PQQ, supplemented with ampicillin. After 24 h incubation at 37 ^oC (for ES chimeric *gcd* clones 28 ^oC), colonies of *E. coli* PP2418 harboring pGDEPS1, pGDEGS1, pGDNTPS1, pGDNTGS1, pGDESPS1 and pGDEGPS1 were pink with a purple halo due to the expression of cloned *gcd* under regulation of *Azotobacter*-specific *gln*A and *pts* promoters. GDH oxidizes glucose in the medium to gluconic acid and brings about a change in the pH of the medium thereby imparting a pink colour to the colony, and because of diffusion of the acid a purple zone around the colony was also seen. The *E. coli* PP2418 harboring pUC18 and pUCGDE clones were spotted on MacConkey agar with the addition of PQQ, were all white. The purple halo formed by the expression of *gcd* under regulation of *pts* promoter was smaller than the *gcd* expression under *gln*A promoter (Figure 20). The clones were spotted on MacConkey agar, without supplementation of PQQ, were all white. Though the protein was expressed in *E. coli* PP2418 harboring pGDEPS1, pGDEGS1, pGDNTPS1, pGDNTGS1, pGDESPS1 and pGDEGPS1, the holoenzyme could not be reconstituted since PQQ was not included in the medium, and hence there was no complementation (Figure 20).

4. 7 Mineral phosphate solubilization by various clones

Once the expression was confirmed, all the clones were verified for their MPS ability on NBRIP agar with PQQ. Clear zones of solubilization on NBRIP agar (with PQQ), spotted with *E. coli* PP2418 harboring pGDEPS1, pGDEGS1, pGDNTPS1, pGDNTGS1, pGDESPS1 and pGDEGPS1 indicated the expression of *gcd* and the oxidation of glucose to gluconic acid, because of which there were clear zones of solubilization. *E. coli* PP2418 harboring pUC18 and pUCGDE, negative control did not show zone of solubilization since there was no complementation/expression of *gcd*.

Quantitative estimation of the soluble phosphate in NBRIP liquid medium was done with *E. coli* PP2418 harboring pGDEPS1, pGDEGS1, pGDNTPS1, pGDNTGS1, pGDESPS1 and pGDEGPS1. *E. coli* PP2418 harboring pUC18 and pUCGDE released a negligible amount of soluble phosphate in the medium. *gcd* of *E. coli*, *E. asburiae* and ES chimera clones expressed under control of *gln*A promoter released more amount of phosphate in the medium than the *gcd* of *E. coli*, *E. asburiae* and ES chimera cloned under control of *pts* promoter indicating that the promoter activity of *gln*A promoter is more than that of *pts* promoter. The *in silico* promoter prediction analysis (http://www.fruitfly.org/seq_tools/promoter.html) also revealed that promoter prediction for *gln*A promoter showed high score compared to promoter prediction for *pts* promoter.

4. 8 Cloning of *E. coli gcd* with promoters in broad-host-range vector pMMB206 and mobilization in to *Azotobacter*

The codon preferences between these organisms were checked in order to express the MPS phenotype in *Azotobacter*. *S. marcescens* and *Azotobacter* showed least mean difference in codon preference compared to *E. coli* and/or *E. asburiae* with *Azotobacter* (Figure 22). However, the ES chimera did not express at 37 ^{o}C and expressed at 28 ^{o}C (Tripura, 2006). We therefore preferred to express the *E. coli gcd* in *Azotobacter* under regulation of *Azotobacter*-specific *gln*A and *pts* promoters. When pUC18, pUCGDE, pGDEPS1 and pGDEGS1 were mobilized to *A. vinelandii* AvOP, and the plasmids were

not recoverable form the transformants, the pUC18-based vectors appeared to be unstable in *A. vinelandii* AvOP. Hence, wide-host-range low-copy-number vector pMMB206 (Morales *et al*., 1997) was selected to clone the promoters with *E. coli gcd* and mobilize into *Azotobacter*. The promoter and *E. coli gcd* was released form the pGDEPS1 & pGDEGS1 and cloned in pMMB206. Restriction analysis and PCR confirmed the constructs pMMBEPS1 (*E. coli gcd* under *pts-p*1 in pMMB206) and pMMBEGS1 (*E. coli gcd* under *gln*A-*p*1 in pMMB206).

The plasmids pMMB206, pMMBEPS1 and pMMBEGS1 were mobilized into *Azotobacter* by the standard protocol (Glick *et al*., 1985). Plasmids were isolated by alkaline lysis method form the transformed *Azotobacter* confirmed the stable maintenance of the pMMB206-based vectors in *Azotobacter*. The transformation of high molecular weight plasmid DNA to *Azospirillum brasilence* Cd affected the morphology and growth rate of the bacterium (Holguin and Glick, 2003). Similar changes were observed when the broad-host-range plasmids pMMB206, pMMBEGS1 and pMMBEPS1 were introduced in *A. vinelandii* AvOP (Figure 26). The transformed cells showed changes in size and morphology from the parent *Azotobacter* cells (Glick *et al*., 1985; Kennedy and Toukdarian, 1987). Transformed cells were smaller, produced more capsular exopolysaccharide, less ability to fix nitrogen or synthesize siderophores (Kennedy and Toukdarian, 1987) and with the production of the characteristic yellow-green *Azotobacter* sp. pigment (Glick *et al*., 1985). In contrast there was no change in the morphology and nitrogen fixation ability of *Azospirillum* when broad-host-range vector pMCG898 was transformed (Vikram *et al*., 2007). The exopolysaccharide being highly hygroscopic matrix should increase the water availability to the bacteria and showed better survival in the adverse environmental conditions (Holguin and Glick, 2003**).** The nitrogen fixation ability by the transgenic *Azotobacter* was analyzed using acetylene reductase assay (ARS). *A. vinelandii* AvOP harboring pMMB206, pMMBEPS1 and pMMBEGS1 were grown in Burk's nitrogen-free medium and checked for the reduction of acetylene to ethylene. Nitrogen fixing ability of the transgenic *Azotobacter* marginally was affected probably not because of introduction of MPS phenotype into it but because of high molecular weight broad-host-range vector pMMB206.

4. 9 Expression of *E. coli gcd* in transgenic azotobacters

Colonies of *A. vinelandii* AvOP transformed with pMMB206, pMMBEGD, pMMBPS1 and pMMBEGS1 were spotted on MacConkey glucose agar plates without PQQ, supplemented with chloramphenicol. *A. vinelandii* AvOP harboring pMMB206 and pMMBEGD were used as a negative control. After 48 h incubation at 30 ^{o}C, colonies of *A. vinelandii* AvOP harboring pMMBPS1 and pMMBEGS1 were pink without any purple halo around the colony as in *E. coli* PP2418 harboring pGDEPS1 and pGDEGS1 (Figure 29) suggesting that the *Azotobacter* was able to synthesize the cofactor PQQ. The genome sequencing data for *A. vinelandii* also predicted the presence of genes responsible for the PQQ biosynthesis (http://genome.ornl.gov/microbial/avin/ or http://azotobacter.org/). The pink colour, without purple halo around the colony could be due to low level of expression of the cloned *gcd* under regulation of *Azotobacter*-specific *gln*A and *pts* promoters in transgenic *Azotobacter* or may be because of low-copy-number vector pMMB206.

4. 10 Mineral phosphate solubilization by transgenic azotobacters

Once the expression was confirmed, all the clones were checked for their MPS ability on NBRIP agar without PQQ. There was no zone of clearance on buffered NBRIP agar was spotted with pMMBPS1 and pMMBEGS1 where as a small zone of clearance of solubilization on non-buffered NBRIP agar was observed when spotted with pMMBPS1 and pMMBEGS1 indicated the low level of expression of *E. coli gcd* in transgenic *Azotobacter* under regulation of *Azotobacter*-specific *gln*A and *pts* promoters. *A. vinelandii* AvOP harboring pMMB206, negative control did not show zone of solubilization since there was no expression of *gcd*.

Quantitative estimation of the soluble phosphate in NBRIP liquid medium was done with pMMBPS1 and pMMBEGS1. *A. vinelandii* AvOP harboring pMMB206 released very less amount of soluble phosphate in the medium. *A. vinelandii* AvOP harboring pMMBPS1 and pMMBEGS1 expressed *E. coli gcd* under regulation of *pts*-p1 promoter released more amount of phosphate in the medium than under regulation of

*gln*A-p1 promoter. The *in silico* promoter prediction showed a high score for *gln*A promoter compared to *pts* promoter (http://www.fruitfly.org/seq_tools/promoter.html), this could be probably due to the presence of ammonium sulphate in the NBRIP medium, which may negatively regulate glutamine synthetase expression/activity. Replacement of ammonium sulphate, with salt III of *Azotobacter* in Burk's nitrogen-free medium enhanced the phosphate release, supported the possible negative influence of excess of reduced forms of nitrogen on glutamine synthetase gene promoter activity.

4. 11 Green house evaluations of transgenic azotobacters

To check the biofetrilizer potential in terms of MPS and nitrogen fixing ability of transgenic *Azotobacter* expressing the *E. coli gcd* was evaluated in green house. Sorghum seeds were bacterized with transgenic *Azotobacter* with carboxy methyl cellulose (CMC) according to Kishore *et al*., (2005). Different combinations of super phosphate with *Azotobacter* (positive control), TCP with *Azotobacter* (comparative controls), TCP with transgenic *Azotobacter* (experimental), TCP with vermiculate and only vermiculate (negative controls) were evaluated in green house. The growth of sorghum seedlings bacterized with transgenic *Azotobacter* steadily increased over a period of 4 weeks, although there was no significant increase in the first two weeks. The significant enhancement in growth of sorghum in the third and fourth weeks indicated that these transgenic azotobacters imparted long term benefits to the plants like other biofertilizers.

We conclude that the biofertilizer potential of transgenic *Azotobacter vinelandii* AvOP was enhanced. The heterologous expression of *E. coli gcd* under the control of *Azotobacter*-specific *gln*A and *pts* promoters in transgenic *A. vinelandii* AvOP significantly improved the MPS ability and the plant growth promoting activity of the transgenic strains with least compromise in the nitrogen fixing ability.

4. 12 Homology modeling and identification of amino acid targets for site directed mutagenesis

In order to identify the amino acid residues in the active site and amino acid residues responsible for binding of PQQ, ubiquinone and concomitant transfer of electrons we made an attempt to build homology model 3D structure of *E. coli* GDH. The protein data base (PDB) blast search and FUGUE (Shi *et al*., 2001; http://tardis.nibio.go. jp/fugue/align.php) method for fold recognition, identified crystal structures of heavy chain A subunit of PQQ-dependent two methanol dehydrogenase (MDH) of *Methylobacterium extorquens,* and *Methylophilus methylotrophus* W3A1 and a PQQ-dependent ethanol dehydrogenase (ADH) of *Pseudomonas aeruginosa* (Figure 34) with nearly 25 % identity and 40 % similarity of sequences. Therefore, three structures (PDB_ID's: 1H4J, 1G72 and 1FLG) were used as templates to build the model structure of *E. coli* GDH. The multiple sequence alignment of GDH with two MDH and an ADH as obtained from FUGUE server indicated small regions of irregularities (insertions and deletions) and these sequences were deleted from *E. coli* GDH prior to model building.

E. coli GDH 3D model structure was built earlier by Cozier and Anthony (1995), and reported that PQQ forms stacking interactions between His-262 & Trp-404 and His-262 and this may maintain the position of PQQ in the active site. The function of His-262 to maintain the position of PQQ was demonstrated by chemical modification at this residue in the GDH of *P. fluorescens* (Imanaga, 1989). The site directed mutation of H262Y in *E. coli* GDH greatly diminished its catalytic efficiency for all other hexoses, except glucose, this suggested that His-262 is mainly involved in substrate affinity (Cozier *et al*., 1999). The interactions between the metal ion (Ca^{2+}) and the amino acid residues Asp-354, Asn-355 and Thr-424 in the active site of the *E. coli* GDH was demonstrated by 3D model structure and by generating SDMs of these residues (James and Anthony, 2003).

Goldstein *et al*., (2003) through protein engineering and homology modeling of *E. coli* GDH identified highly conserved region (HCR) of quinoprotein dehydrogenase and indicated that this region may play an important role in regulating the size of the funnel that controls access to the catalytic site at the base of the eight-bladed super barrel

structure of GDH. Through SDM in the HCR, a strategy was developed that might open the funnel, there by increase the rate of catalysis (V_{max}) with a concomitant increase in gluconic acid production and CaP solubilization. Series of mutations at Pro-757 in GDH provided the range of activities form 77 % (P757A) to knock out mutants (P757F and P757Y). It was concluded that Pro-757 in GDH is identical to Pro-520 of PQQMDH α subunit of *M. extorquens* in maintaining the funnel diameter. Based on the model structure of *E. coli* GDH, Elias *et al*., (2000) identified several amino acid residues in the active site and studied their functional role through SDM. Of these, H262A mutant showed reduced affinities for both, glucose and PQQ without affecting glucose oxidase activity, and W404A mutant showed decreased affinity for PQQ. Mutants D466N, D466E and K493A showed very low glucose oxidase activity without influence in the affinity for PQQ and concluded that Asp-466 initiates glucose oxidation reaction by abstraction of proton for the glucose and Lys-493 is involved in electron transfer from $PQQH_2$. The topological model structure for membrane bound quinoprotein GDH was described by Yamada *et al*., (2003) (Figure 3).

In our work, we built the model structure of *E. coli* GDH using MODELER InsightII suite of programs provided by Accelrys. The N-terminal 150 amino acid residues corresponding to five membrane spanning domains and irregularities in the sequence were removed manually. The model structure was similar to structures that were reported previously and have super barrel made up of eight topologically identical four stranded anti parallel β-sheets arranged with radial symmetry like blades of the propeller. The PQQ was buried in the interior of the super barrel in the active site. The Ca^{2+} ion maintains the PQQ in correct configuration by interacting directly with PQQ and other amino acid residues present in the vicinity (Figure 35 A). The Ramachandran plot analyzed for the structure model of *E. coli* GDH showed more than 95.8 % amino acid residues were present in the allowed region indicating the correctness of the geometry of the 3D structure model. Only 2.2 % amino acid residues were present in the disallowed regions (Figure 36). Mapping of these residues on the 3D structure indicated that these residues are located at the region close to deletion loops in the multiple alignments. These residues are far away form the PQQ binding site and hence may not hinder the structure-function correlation studies. Five amino acid residues that are either directly or indirectly

involved in PQQ binding in the active site were selected for SDM. Two amino acid residues on the surface of the model structure that were predicted to have probable UQ binding and concomitantly transfer of electrons to UQ in the electron transfer chain were also selected for SDM. Mutations in these seven amino acid residues were not reported experimentally in any of the previous studies.

4. 13 Generation of SDMs on pATEE and structure-function correlation studies

4. 13. 1 Generation of *E. coli* GDH mutants: Several mutations were reported in the *E. coli* GDH, to improve the enzymatic properties and also to study the structure-function relationship (Table 1). Based on the previous reports on *E. coli* GDH (Cozier *et al*., 1999; James and Anthony 2003; Goldstein *et al*., 2003), the amino acid residues targeted for mutations in *E. coli* GDH were His 262 Tyr, Asp 354 Asn, Asn 355 Asp and Pro-757 X. It was proposed that the highly conserved region (HCR) of GDH (amino acid residues region 748-780) maintains the structural integrity of the channel that controls access of the substrate to the active site and hence is conserved across the range of bacterial quinoprotein dehydrogenases (Goldstein *et al*., 2003). Hence the five amino acid targets (Glu-217, Arg-266, Glu-591, Leu-712 and Gly-776) were selected form the model structure of GDH in the 5 Å region of the active site where PQQ and metal ion domain were concentrated (Figure 37 B). Two amino acids targets (Arg-201 and Asp-204) were selected on the surface of the model structure GDH (Figure 37 A). Site specific mutants were generated with the $VENT_R$ DNA polymerase using the plasmid pATEE as the template and the respective mutagenic primers. The parental methylated pATEE was digested after 22 cycles of PCR reaction using *Dpn* I enzyme. Sequencing of the plasmid confirmed the change in the codon and the subsequent mutation in the amino acid. The mutants were designated as pATEE R201A, D204A, E217L, E217Q, E217A, R266Q, R266E, E591L, E591Q, E591K, L712W, L712R, G776A, G776K, G776D and G776L.

4. 13. 2 *E. coli* GDH mutants complementation and expression studies: The mutants were studied for the GDH complementation in *E. coli* YU423 on MacConkey glucose agar. Since *E. coli gcd* was expressing at 37 ^{o}C, all the expression studies with the

mutants were carried out at 37 ^{o}C. The mutants R201A, D204A, E217L, E217A, R266Q, R266E, E591L, E591Q, E591K, L712W, L712R, G776K, G776D and G776L were white without purple halo suggested that these mutations negatively affected the function of the GDH. The mutants E217A and G776A were pink with a purple halo similar to *E. coli* YU423 harboring pATEE indicated innocuous nature of these mutation on the function of GDH.

Once the expression of mutants GDH was confirmed, pATEE and mutants were tested for expression in expression host. The expression host for pQE30 is *E. coli* M15 (pREP4) and *gcd* expression direct by IPTG induction under the control of T5 promoter. *E. coli* M15 (pREP4) where *lac* repressor is plasmid encoded (kanamycin selection) and since *gcd* was already present in the host genome, a mutant lacking a functional *gcd* was generated using phage P1 mediated transduction *gcd*::*cm* from *E. coli* PP2419 was transferred to *E. coli* M15 resulting in *E. coli* AT15 (Tripura, 2006). The transformed colonies were selected on LB chloramphenicol and kanamycin medium. Because of the transfer of chloramphenicol acetyl transferase (*cm*) gene to *E. coli* M15, and because of the presence of pREP4 carrying *npt*2, the transduced colonies grow on LB chloramphenicol and kanamycin double selection medium.

4. 13. 3 Alteration in the properties *E. coli* GDH mutants: The mutants R201A and D204A have lost the GDH activity, mainly because of the loss of its interaction with ubiquinone and concomitant transfer of electron in the respiratory chain hence there was no complementation seen on MacConkey medium. Previous reports identified the amino acid residues that are involved in electron transfer and ubiquinone binding site through SDM and structural studies (Friedrich *et al*., 1990; Elias *et al*., 2001; Cozier *et al*., 1999). By analysis of protein fusions with reporter proteins, alkaline phosphatase or β-galactosidase, the N-terminal hydrophobic domain (residues 1–150) consists of five segments lacking charged amino acid residues and presumably enough to span the inner membrane, which thus ensures a strong anchorage of the protein to the membrane (Yamada *et al*., 1993).

The N-terminal domain of mGDH was previously speculated to be involved in secretion of the C-terminal domain, ubiquinone binding, and functional interaction with

the C-terminal domain in addition to anchoring the membrane (Yamada *et al*., 2001). From the structural comparison with one protein of the mitochondrial NADH dehydrogenase complex, Arg-91 and Asp-93, in the N-terminal transmembrane domain of *A. calcoaceticus* mGDH had been proposed to interact with ubiquinone (Friedrich *et al*., 1990), but the corresponding two residues (Arg-93 and Asp-95) in *E. coli* mGDH were substituted with other amino acids and showed that these two amino acids were not responsible for the UQ binding (Yamada et al., 2003)**.** However, the possibility that the N-terminal domain to be involved in ubiquinone binding has not been ruled out.

We have modeled the superbarrel structure of the large C-terminal domain of *E. coli* mGDH (cGDH) based on MDH α-subunit (Coizer *et a*l., 1995), that lacks some loops or segments in the domain because there were no corresponding sequences in the MDH α-subunit. Furthermore, cGDH lacking membrane spaning domain reconstructed in the membrane fractions could exhibit glucose oxidase activity (Elias *et al*., 2001). Therefore, it is likely that cGDH bears the ubiquinone-binding site. These facts and the evidence that cGDH was recovered in membrane fractions and required detergents for its solubilization suggest that there is a membrane-binding site in the cGDH domain. It was observed that the stability of cGDH was remarkably low compared to that of the wild-type mGDH. The N-terminal hydrophobic domain thus seems to be required for the stability of cGDH and therefore a possible interaction between the N- and C-terminal domains is assumed. Yamada *et al*., (2003) introduced a four-amino acid sequence as a cleavage site for signal peptidase into the region just after the N-terminal hydrophobic domain in mGDH, the C-terminal domain was stably expressed with the N-terminal domain. The successful cleavage of the C-terminal domain was detected after treatment with mercaptoethanol, suggesting possible Cys–Cys bridge(s) between the N- and C-terminal domains. Therefore, the N-terminal domain seems to somehow stabilize the C-terminal domain *via* domain–domain interactions, and to have a potential as a signal sequence for the C-terminal domain. From the multiple sequence alignment among 17 different GDHs, it is observed that the basic nature of amino acid at position 201 is conserved and Asp-204 is highly conserved (Figure 42 A) in the corresponding positions. The 5 Å region around these amino acid residues in the 3D model of *E. coli* GDH suggests that this domain region is in the neighbourhood of hydrophobic amino acids and

that Arg-201 and Asp-204 are embedded in the hydrophobic core (Figure 42 B). These observations suggested that this domain might possibly interact directly with membrane and as well as UQ, hence the loss of the activity was observed when these positions were substituted with alanine.

The mutants E217L, E217A, R266Q, R266E, E591L, E591Q and E591K have lost the activity of the GDH mainly because of the loss of the hydrogen bonding interactions with the PQQ cofactor. These amino acids are directly involved in interaction with PQQ through hydrogen bonding, which is embedded in the active site of the GDH in the native protein. Previous reports on the mutations where the structure of the enzyme is known indicated that the subtle structural changes caused by the mutations, both distant (far from the active site) and close (< 10 Å from the active site) can significantly change the reaction rate as well as activity (Morley and Kazlauskas, 2005). Since these mutations were targeted in the PQQ binding active-site which are directly involved in hydrogen bonding with PQQ, we believe that these mutants have lost the hydrogen bonding capability due to the substitutions with other amino acids, thus leading to the loss of the activity. However, the mutant E217Q retained the activity similar to that of the wild-type GDH and this may be because of the hydrogen bonding capability of N atom in the glutamine similar to that of the O atom of glutamate. The mutants R266Q and R266E also lost the activity of GDH. We initially thought that the glutamine and glutamate will have the ability to form the hydrogen bonding with PQQ but the length of the side chain for arganine is longer, and this may be a reason for glutamine and glutamate substitution to lose the activity of GDH. For similar reasons, the mutants E591L, E591Q and E591K have also lost the GDH activity (Figure 44).

The mutants L712W and L712R have lost the activity of GDH. Based on the multiple sequence alignment among MDH, ADH and GDH, Leu-712 position in *E. coli* GDH is occupied by tryptophan in MDH and ADH, we initially thought that the substitution Leu-712 in GDH with tryptophan might increase the GDH activity but to our surprise L712W had no activity. On examination of *E. coli* GDH structure on the graphics, we observed that a phenylalanine at 532 position is spatially close to Trp-712 and undesirable close contacts are present between the bulky side chains of these two amino acids (distance ≤ 2.0 Å). These close contacts may disturb the confirmation of the

protein at active site and thus leads to loss of the activity. Examination of the multiple sequence alignment indicates that the 532 position is occupied by phenylalanine in *E. coli* GDH, whereas it is Leucine in MDH and ADH. This observation suggests that these dehydrogenases are beautifully optimized in nature such that the positions of aliphatic nonpolar amino acid (L) and aromatic nonpolar amino acid (F) in *E.coli* GDH are swapped by aromatic nonpolar amino acid (W) and aliphatic nonpolar amino acid (V) in MDH and ADH sequences. These swapping of amino acids retains the nature and size of binding site. Similarly the long side chain charged amino acid substitution at L712R leads to the confirmation change in the active site and lost GDH activity.

The mutants G776K, G776D and G776L have also lost the activity of GDH. This residue is in the HCR of the *E. coli* GDH which maintains the structural integrity of the channel that controls access of the substrate to the active site (Goldstein *et al*., 2003). Substitutions of amino acids in the HCR region also showed the knockout to 78 % target to the membrane (Goldstein *et al*., 2003). Several different amino acid substitutions in the HCR of this protein were reported (Sode and Kojima 1997; Yamada *et al*., 1998; Goldstein *et al*., 2003). H775N and H775D mutants showed increased substrate specificity, H775R and H775A showed a pronounced reduction of affinity for a prosthetic group, PQQ, suggesting that His-775 may directly interact with PQQ. From our model structure, we observe that Ser-777 interacts directly with PQQ through hydrogen bonding interactions and it has been shown that S777A mutation decreased affinity with PQQ (Goldstein *et al*., 2003). Also we observe that Gly-776 is close to the PQQ binding site. The multiple sequence alignment of 17 different GDHs showed highly conserved nature of Gly-776 (Figure 46A). From graphical examination, we observe that there is no room for a large side chain at this position and in our mutants, G776K, G776D and G776L, in order to accommodate large side chain, the main chain C-α of the protein may get deviated. This implies that substitution of any charged or hydrophobic amino acid at Gly-776 may alter the size of active site and in turn lose the activity. Also, G776K, G776D and G776L showed weak signal in the western blot suggesting that mutation might have changed the protein confirmation that lead to internal degradation of the expressed protein. Whereas substitution of G776A retained the activity suggests that only small side chain amino acids are allowed in the pocket.

A great deal of the work has been done on the *gcd* of *E. coli* and the application of the enzyme for MPS was also reported. The present study reports *S. marcescens* GPS 5 (a potent biocontrol agent against LLS of groundnut) as best phosphate solubilizer among the different isolates we have screened. Through random mutagenesis the MPS ability was enhanced for potential application for MPS by *S. marcescens* GPS5. The biofertilizer potential of the *Azotobacter* was enhanced by expressing the *E. coli gcd* under regulation of *Azotobacter*-specific *gln*A and *pts* promoters with out compromise on the nitrogen fixation ability of the *Azotobacter*. Through homology modeling and site directed mutagenesis the critical amino acid residues that are involved in ubiquinone binding and concomitant transfer of electrons to ubiquinone in the respiratory chain have been demonstrated. Through 3D structural analysis of GDH and site directed mutagenesis we reported the critical amino acid residues around the PQQ binding site and as well as the active-site. The generation of the mutants and studying the structure-function relationship of the GDH indicates the possibility and future scope for the further improvement of the enzyme to suit its varied application in industry and MPS.

Summary

5. 1 Background and objective

Phosphorus is one of the most important macronutrients required for plant growth and production. The total content of phosphorus nutrient in natural environment is normal, but this invariably forms large number of insoluble chemical complexes with many ions present in the soil which makes this nutrient a paradox. Numerous soil microflora were reported to solubilize insoluble phosphorous complexes into solution and make it possible for its use by the plants. This mineral phosphate solubilization (MPS) ability was attributed to the secretion of low molecular weight organic acids. Among different low molecular weight organic acids, gluconic and 2-keto gluconic acids are strongest in MPS. The direct oxidation (DO) pathway, which is the principal pathway for glucose metabolism in Gram-negative bacteria, forms the metabolic basis for a strong MPS.

Glucose dehydrogenase (GDH), the first and principal enzymes of the DO pathway is a member of the largest group of quinoproteins, requiring pyrrolo quinoline quinone (PQQ) as the cofactor for its activity. The enzyme catalyzes the oxidation of glucose to gluconic acid in the periplasmic space of Gram-negative bacteria. Hence, the products of oxidation are directly released into the extra cellular space leading to the acidification of the surrounding medium and there by releasing the insoluble phosphate. Among 24 different bacterial isolates screened for their ability in MPS, *S. marcescens* GPS 5, a good biocontrol agent against late leaf spot (LLS) disease of groundnut isolated form groundnut phyllosphere was found to have maximum phosphate solubilization ability. *E. coli* and *E. asburiae* were also competent enough in MPS. The present study aimed at the following aspects of MPS: 1. Isolation of the MPS-related mutants of *S. marcescens* GPS 5 through EMS mutagenesis. 2. Cloning of glucose dehydrogenase genes form selected Gram-negative bacteria. 3. Generate transgenic *Azotobacter* capable of multiple agronomic benefits in terms of MPS by introducing glucose dehydrogenase gene with out affecting nitrogen fixation and 4. Homology modeling and site directed mutagenesis to identify critical amino acid residues at different positions and their structure-function correlation.

5. 2 Isolation of MPS-related mutants of *S. marcescens* GPS 5

S. marcesecens GPS 5 culture was grown to mid log phase and washed twice with buffer A, pH 7.3 and EMS at 1.4 % was added. Every 15 min 1 ml of the culture was with drawn over 1 h. The survival of the *S. marcescens* GPS 5 was decreased drastically over exposure for 1 h. Among 1700 different *S. marcescens* GPS 5 cells were screened for their ability to solubilize mineral phosphate supplemented as HAP as a sole source of phosphate in NBRIP medium, 13 different MPS-related mutants were isolated based on the difference in the zone of clearance around the colony on semisolid NBRIP agar and as well as amount of the phosphate released in liquid NBRIP medium when compared to the wild-type. Among 13 different MPS-related mutants, 7 showed increased MPS (increased-MPS mutants) and 6 showed decreased MPS (decreased-MPS mutants). All seven increased-MPS mutants were efficient at solubilizing phosphate in both solid and liquid NBRIP medium. Among the increased-MPS mutants, EMS XVIII Sm 39 showed the maximum (40 %) increase in the amount of phosphate released in liquid medium compared with wild-type *S. marcescens* GPS 5. EMS III Sm 3 showed the lowest solubilization of phosphate among the 6 decreased-MPS mutants.

5. 3 Isolation of *Azotobacter*-specific *gln*A and *pts* gene promoters and glucose dehydrogenase gene from *E. coli*, *E. asburiae*, and ES chimera

Promoter-specific primers were designed upstream to the glutamine synthetase (*gln*A) and phosphonate transport system (*pts*) genes, with two forward primers starting at different position and with a common reverse primer. *Azotobacter*-specific *gln*A-p1 (228 bp), *gln*A-p2 (134 bp), *pts*-p1 (182 bp) and *pts*-p2 (128 bp) gene promoters were PCR amplified and cloned in pUC18, resulting in pUCGS1, pUCGS2, pUCPS1 and pUCPS2, respectively. *gcd* form *E. coli* DH5α (2.4 kb), ES chimera (2.4 kb), and *E. asburiae* (2.4 kb), were PCR amplified. *gcd* of *E. coli* was cloned in pUC18, resulting in pUCGDE. *S. marcescens* GPS 5 *gcd* was not expressed because of lack of the membrane spanning domain (Tripura, 2006). *gcd* of *E. coli*, ES chimera and *E. asburiae*, were cloned individually in pUCPS1 and pUCGS1, resulting in pGDEPS1 (*E. coli gcd*

under *pts*-p1), pGDEGS1 (*E. coli gcd* under *gln*A-p1) pGDESPS1 (chimeric ES *gcd* under *pts*-p1), pGDESGS1 (chimeric ES *gcd* under *gln*A-p1), pGDNTPS1 (*E. asburiae gcd* under *pts*-p1) and pGDESGS1 (*E. asburiae gcd* under *gln*A-p1), respectively.

5. 4 Expression of glucose dehydrogenase under regulation of *Azotobacter*-specific promoters

Expression of the cloned *gcd* from the various sources was studied in *E. coli* PP2418 by the GDH complementation in MacConkey glucose agar medium supplemented with the cofactor PQQ. The development of pink colonies with a purple halo around the colony confirmed the expression of *gcd*. The pink colour was due to the oxidation of glucose to gluconic acid by the recombinant GDH and the corresponding change in the pH of the medium. The MPS ability of *E. coli*, *E. asburiae* and ES chimeric GDH on NBRIP agar medium was indicated by the clear zone of solubilization and the phosphate released in the liquid medium, (due to the secretion of gluconic acid by the clones) was also quantified.

5. 5 Cloning, mobilization and expression of *E. coli gcd* under regulation of *Azotobacter*-specific promoters in azotobacters

The pUC18-based vectors were not stably maintained in *Azotobacter*. The codon preference of the *Azotobacter*, was more compatible with *S. marcescens* but the GDH expression was limited to 28 ^{o}C. We therefore preferred to clone the *E. coli gcd* in *Azotobacter*. *E. coli gcd* along with *pts*-p1 and *E. coli gcd* with *gln*A-p1 were released from pGDEPS1 (*E. coli gcd* under *pts*-p1) and pGDEGS1 (*E. coli gcd* under *gln*A-p1) and cloned in pMMB206 (broad host range vector), resulting in pMMBEPS1 and pMMBEGS1, respectively. The recombinant clones pMMBEPS1 and pMMBEGS1 were mobilized into *Azotobacter* according to the Glick *et al*., (1985). The transformed colonies showed large and mucoid distinct colony morphology. Expression of the cloned *E. coli gcd* under regulation of *pts*-p1 and *gln*A-p1 was studied in *Azotobacter* in MacConkey glucose agar medium not supplemented with the cofactor PQQ. The

development of pink colonies without purple halo around the colony confirms the expression of *gcd*. The pink colour was due to the oxidation of glucose to gluconic acid by the recombinant GDH and the corresponding change in the pH of the medium. The MPS ability of *E. coli* GDH on NBRIP agar medium was indicated by the small clear zone of solubilization and the phosphate released in the liquid medium, (due to the secretion of gluconic acid by the clones) was also quantified. Semi-quantitative estimation of the *gcd* expression was done using RT-PCR analysis.

Nitrogenase activity of transgenic *Azotobacter* expressing *E. coli gcd* was not affected significantly in terms of acetylene reduction assay, except that the transgenic strains had slow growth rate when compared to the wild type. The slow growth rate could be due to the broad-host-range vector maintained in *Azotobacter* and not may be because of the expression of *E. coli gcd* in transgenic *Azotobacter*.

5. 6 Green house evaluation of transgenic azotobacters

Sorghum seeds were surface sterilized and suspended in 0.5 % carboxy methyl cellulose (CMC) containing transgenic *Azotobacter*. Bacterized sorghum seeds were raised in green house experimental pots containing sterilized vermiculite, TCP and different combinations of super phosphate, only vermiculate *Azotobacter*. Both transgenic and wild-type showed better growth in terms of plant height and plant fresh weight. The fresh weight of sorghum seedlings was significantly higher in inoculated plants with transgenic *Azotobacter* as compared to that of non-transgenic *Azotobacter* inoculated plants.

5. 7 Homology modeling and site directed mutagenesis of *E. coli* GDH to understand the structure-function relationship

Molecular modeling of *E. coli* GDH was done using the crystal structure of the heavy chain α subunit of PQQ-dependent methanol dehydrogenase (MDH) of *Methylobacterium extorquens,* and *Methylophilus methylotrophus* W3A1 and a PQQ-dependent ethanol dehydrogenase (ADH) of *Pseudomonas aeruginosa* as templates and

using Insight II suite of programs. For molecular modeling of GDH the N-terminal 150 amino acids corresponding to five membrane spanning domains and irregularities in the alignments were removed manually. The model structure of GDH showed to be a super barrel made up of eight topologically identical four stranded anti parallel β-sheets arranged with radical symmetry like blades of the propeller. The PQQ is buried in the interior of the super barrel in the active site. The Ca^{2+} ion maintains the PQQ in correct configuration by interacting directly with PQQ and amino acids present at that position. The molecular model structure was verified using Ramachandran plot.

Five amino acids in the PQQ binding site and two amino acids on the surface of model structure were selected for site directed mutations. Mutation of the target codon CGT to GCT confirmed change in the amino acid Arg 201 Ala and the mutated plasmid designated as pATEE R201A. Similarly D204A (Asp 204 Ala), E217L (Glu 217 Leu), E217A (Glu 217 Ala), E217Q (Glu 217 Gln), R266Q (Arg 266 Gln), R266E (Arg 266 Glu), E591L (Glu 591 Leu), E591Q (Glu 591 Gln) E591K (Glu 591 Lys), L712W (Leu 712 Trp), L712R (Leu 712 Arg), G776A (Gly 776 Ala), G776K (Gly 776 Lys), G776D (Gly 776Asp) and G776L (Gly 776 Leu). pATEE (*E. coli gcd* in pQE30) was used as the template for the mutations using the $VENT_R$ DNA polymerase. The methylated parental DNA was cleaved by DpnI digestion and the amplified mutated plasmid was used to transform competent cells of *E. coli* XL1-Blue MRF'.

The GDH complementation studies were carried out on MacConkey glucose medium with PQQ. *E. coli* YU423 harboring pATEE and pATEE mutants E217Q and G776A were pink, with a purple halo around the colony, and other mutants showed no colouration and was similar to the negative control after 24 h incubation at 37 ^{o}C. The mutant proteins were expressed in *E. coli* AT15 harboring the plasmids. A band ~ 90 kDa matching with the expected size of *E. coli* GDH was observed with all the GDH mutants and transferred onto nitrocellulose membrane and probed with anti-His antibodies using BCIP-NBT as substrate a signal corresponding to 90 kDa was detected for all the mutants along with the *E. coli* GDH band (positive control).

5. 8 MAJOR FINDINGS

- ✓ Through EMS mutagenesis 7 MPS enhanced mutants and 6 MPS decreased mutants were isolated.
- ✓ Isolated *Azotobacter*-specific glutamine synthetase (*gln*A) and phosphonate transport system (*pts*) gene promoters using PCR-based approach.
- ✓ Cloned and expressed *E. coli*, *E. asburiae* and ES chimeric *gcd* under regulation of *Azotobacter*-specific *gln*A and *pts* gene promoters in *E. coli* PP2418 & *Azotobacter* and involvement of *gcd* in MPS was demonstrated.
- ✓ Demonstrated the possible negative effect of fixed nitrogen on expression of MPS phenotype in transgenic *Azotobacter* expressing *E. coli gcd* under regulation of *Azotobacter*-specific *gln*A.
- ✓ Developed transgenic *Azotobacter* strain capable of both mineral phosphate solubilization and nitrogen fixation and that enhanced the growth of the sorghum.
- ✓ Homology model structure for *E. coli* GDH was developed and identified five amino acids in the PQQ binding domain and two amino acids on the surface of the model for site directed mutagenesis.
- ✓ Involvement of Arg-201 and Asp-204 in electron transport was demonstrated through SDM. Glu-217, Arg-266 and Glu-591 are involved in direct interaction with PQQ and alteration at Leu-712 and Gly-776 leads to change in the PQQ binding pocket.

References

REFERENCES

Afolabi, P. R., Mohammed, F., Amaratunga, K., Majekodunmi, O., Dales, S. L., Gill, R., Thompson, D., Cooper, J. B., Wood, S.P., Goodwin, P.M., Anthony, C. (2001). Site-directed mutagenesis and X-ray crystallography of the PQQ-containing quinoprotein methanol dehydrogenase and its electron acceptor, cytochrome c. *Biochemistry* **40:** 9799-9809.

Ames, B. N. (1964). Assay of inorganic phosphate, total phosphate, and phosphatases. *Methods Enzymol*. **8**: 115-118.

Ameyama, M., Shinagawa, E., Matsushita, K. and Adachi, O. (1981). D-Glucose dehydrogenase of *Gluconobacter suboxydans*: Solubilization, purification and characterization. *Agri. Biol. Chem*. **45:** 851-861.

Anderson, S., Marks, C. B., Lazarus, R., Miller, J., Stafford, K., Seymour, J., Light, D., Rastetter, W. and Estell, D. (1985). Production of 2-keto-L-gluconate, an intermediate in L-ascorbate synthesis, by a genetically modified *Erwinia herbicola*. *Science* **230:** 144-149.

Anthony, C. (1988). Quinoproteins and energy transduction. In: *Bacterial EnergyTransduction* (C. Anthony, eds.), pp.293-315. Academic Press; New York.

Babu-Khan, S., Yeo, T. C., Martin, W. L., Duron, M. R., Rogers, R. D. and Goldstein, A. H. (1995). Cloning of a mineral phosphate-solubilizing gene from *Pseudomonas cepacia. Appl. Environ. Microbiol*. **61:** 972-978.

Beever, R. E. and Burns, D. J. W. (1980). Phosphate uptake, storage and utilization by fungi. *Adv. Bot. Res.* **8**: 128-219.

Bolan, N. S., Naidu, R., Mahimairaja, S. and Baskaran, S. (1994). Influence of low-molecular weight organic acids on the solubilization of phosphates. *Biol. Fertil. Soil*. **18:** 311-319.

Burnette, W. N. (1981). "Western Blotting": Electrophoretic transfer of proteins from sodium dodecyl sulfate-polyacrylamide gels to unmodified nitrocellulose and radiographic detection with antibody and radioiodinated protein A. *Analytical Biochemistry*, **112**: 195-203

Cleton-Jansen, A-M., Dekker, S., van de Putte, P. and Goosen, N. (1991). A Single amino acid substitution changes the substrate specificity of quinoprotein glucose dehydrogenase in *Gluconobacter oxydans. Mol. Gen. Genet.* **229:** 206-212.

Cleton-Jansen, A-M., Goosen, N., Fayet, O., and van de Putte. P. (1990). Cloning mapping and sequencing of the gene encoding *Escherichia coli* quinoprotein glucose dehydrogenase. *J. Bacteriol.* **172:** 6308-6315.

Cleton-Jansen, A-M., Goosen, N., Vink, K. and van de Putte, P. (1989). Cloning, characterization and DNA sequencing of the gene encoding the M_r 50 000 quinoprotein glucose dehydrogenase from *Acinetobacter calcoaceticus. Mol. Gen. Genet.* **217:** 430-436.

Cleton-Jansen, A-M., Goosen, N., Wenzel, T. J. and van de Putte, P. (1988). Cloning of the gene encoding quinoprotein glucose dehydrogenase from *Acinetobacter calcoaceticus*: evidence for the presence of a second enzyme. *J. Bacteriol*. **170:** 2121-2125.

Coulondre, C. and Miller, J. H. (1977). Genetic studies of the *lac* repressor III: Additional correlation of mutational sites with specific amino acid residues. *J. Mol. Biol.* **117**: 525-567.

Cozier, G. E. and Anthony, C. (1995). Structure of the quinoprotein glucose dehydrogenase of *Escherichia coli* modelled on that of methanol dehydrogenase form *Methylobacterium extorquens*. *Biochem. J.* **312**: 679-685.

Cozier, G. E., Salleh, R. A. and Anthony, C. (1999). Characterization of the membrane quinoprotein glucose dehydrogenase from *Escherichia coli* and chracterization of a site directed mutant in which histidine^{262} has been changed to tyrosine. *Biochem. J.* **340:** 639-47.

Dawes, E. A. (1981). Carbon metabolism. In: *Continuous culture of cells*. (Boca Raton. Fla. eds.), Vol.2, pp. 1-38. CRC Press, Inc., P.H. Calcott.

Duff, R. B., Webley, D . M . & Scott, R. O. (1963). Solubilization of minerals and related materials by 2-ketogluconic acid producing bacteria. *Soil Science,* **95:** 105-114.

Duine, J. A. (1991). Quinoproteins: enzymes containing the quinonoid cofactor pyrroloquinoline quinone, topaquinone or tryptophan-tryptophan quinone. *Eur. J. Biochem*. **200:** 271-284.

Duine, J. A., Frank, J. and van Zeeland, J. K. (1979). Glucose dehydrogenase from *Acinetobacter calcoaceticus*: a 'quinoprotein'. *FEBS letters* **108:** 443-446.

Elias, M. D., Tanaka, M. Izu, H., Matsushita, K., Adachi, O. and Yamada, M. (2000). Functions of amino acid residues in the active site of *Escherichia coli* pyrroloquinoline quinine-containing quinoprotein glucose dehydrogenase. *J. Biol. Chem.* **275**: 7321-7326.

Elias, M. D., Tanaka, M., Sakai, M., Toyama, H., Matsushita, K., Adachi, O. and Yamada, M. (2001). C-terminal periplasmic domain of *Escherichia coli* quinoprotein

glucose dehydrogenase transfers electrons to ubiquinone. *J. Biol. Chem*. **276:** 48356-48361.

Epstein, E. (1972). Mineral nutrition of plants. p- 44. J. Wiley and sons Inc., New York.

Erni, B. (1989). Glucose transport in *E. coli*. *FEMS Microbiol. Rev.* **63**: 13-24

Felder, M., Gupta, A., Verma, V., Kumar, A., Qazi, G. N. and Cullum, J. (2000). The pyrrolo quinoline quinone synthesis genes of *Gluconobacter oxydans. FEMS Microbiol. Lett.* **193:** 231-236.

Fliege, R., Tong, S., Shibata, A., Nickerson, K. W. and Conway, T. (1992). The Entner-Doudoroff pathway in *Escherichia coli* is induced for oxidative glucose metabolism *via* pyrroloquinoline quinone-dependent glucose dehydrogenase. *App. Environ. Microbiol*. **58:** 3826-3829.

Friedrich, T., Strohdeicher, H., Hofhaus, G., Preis, D., Sahm, H. and Weiss, H. (1990). The same domain motif for ubiquinone reduction in mitochondrial or chloroplast NADH dehydrogenase and bacterial glucose dehydrogenase. *FEBS Lett.* **265:** 37-40.

Gaur, A. C. (2002). In: National symposium on mineral phosphate solubilizing bacteria, Nov.14-16, UAS, Dharwad.

Gaur, A. C. and Ostwal, K. P. (1972). Influence of phosphate solubilizing Bacilli on yield and phosphate uptake of wheat. *Indian J. Exp. Biol*. **10:** 393–394.

Glick, B. R., Brooks, H. E. and Pasternak, J. J. (1985). Transformation of *Azotobacter vinelandii* with plasmid DNA. *J. Bacteriol.* **162:** 276-279.

Goldstein, A. H. (1986). Bacterial mineral phosphate solubilization: historical perspectives and future prospects. *Am. J. Alt. Agri*. **1:** 57-65.

Goldstein, A. H. (1994). Solubilization of exogenous phosphates by Gram-negative bacteria. In: *Cellular and Molecular Biology of Phosphate and Phosphorylated Compounds in Microorganisms*. (Silver S, *et al*., eds.), pp. 197-203. ASM Washington, D. C.

Goldstein, A. H. (1995). Recent progress in understanding the molecular genetics and biochemistry of calcium phosphate solubilization by Gram-negative bacteria. *Biol. Agri. Hort*. **12:** 185-193.

Goldstein, A. H. (2001). Bioprocessing of rock phosphate ore: essential technical considerations for the development of a successful commercial technology. IFA technical conference, New Orleans, USA.

Goldstein, A. H., Braverman, K. and Osorio, N. (1999). Evidence for mutualism between a plant growing in a phosphate–limited desert environment and a mineral phosphate solubilizing (MPS) rhizobacterium. *FEMS Microbiol. Ecology* **30:** 295-300.

Goldstein, A. H., Lester, T. and Brown, J. (2003). Research on the metabolic engineering of the direct oxidation pathway for extraction of phosphate from ore has generated preliminary evidence for PQQ biosynthesis in *Escherichia coli* as well as a possible role for the highly conserved region of quinoprotein dehydrogenases. *Biochem. Biophys. Acta.* **1647:** 266-271.

Goldstein, A. H. and Liu, S-T. (1987). Molecular cloning and regulation a mineral phosphate-solubilizing gene from *Erwinia herbicola. Biotechnol.* **5:** 72-74.

Goldstein, A. H., Rogers, R. D. and Mead, G. (1993). Mining by Microbes. *Biotechnol.* **11:** 1250-1254.

Goosen, N., Horsman, H. P. A., Huinen, R. G. and van de Putte, P. (1989). *Acinetobacter calcoaceticus* genes involved in biosynthesis of the coenzyme pyrrolo-quinolone-quinone: nucleotide sequence and expression in *Escherichia coli* K-12. *J. Bacteriol.* **171:** 447-455.

Goosen, N., Huinen, R. G. M. and van de Putte, P. (1992). A 24-amino-acid polypeptide is essential for the biosynthesis of the coenzyme pyrrolo-quinoline-quinone. *J. Bacteriol.* **174:** 1426-1427.

Goosen, N., Vermaas, D. A. M. and van de Putte, P. (1987). Cloning of the genes involved in synthesis of coenzyme pyrrolo-quinoline quinone from *Acinetobacer calcoaceticus. J. Bacteriol*. **169:** 303-307.

Gottschalk, G. (1986). *Bacterial Metabolism*, 2nd eds. Springer- Verlag: Berlin.

Gyaneshwar, P., Naresh Kumar, G., Parekh, L. J. (1998). Effect of buffering on the phosphate-solubilizing ability of microorganisms. *World J. Microbiol. Biotechnol.* **14**: 669-673.

Gyaneshwar, P., Parekh, L. J, Archana, G., Poole, P. S, Collins, M. D, Hutson, R. A. and Kumar, N. G. (1999). Involvement of a phosphate starvation inducible glucose dehydrogenase in soil phosphate solubilization by *Enterobacter asburiae*. *FEMS Microbiol. Lett.* **171:** 223-229.

Hanahan, D., Jessee, J. and Bloom, F. R. (1991). Plasmid transformation of *Escherichia coli* and other bacteria. *Methods Enzymol.* **204:** 63-113.

Hauge, J. G. (1966). Glucose dehydrogenase: *Pseudomonas* and *Bacterium anitratum*. *Methods Enzymol*. **9:** 92-98.

Heilmann, H. J., Magert, H. J. and Gassen, H. G. (1988). Identification and isolation of glucose dehydrogenase genes of *Bacillus megaterium* M1286 and their expression in *Escherichia coli*. *Eur. J. Biochem.* **174**: 485–490.

Holguin, G. and Glick, B. R. (2003). Transformation of *Azospirillum brasilence* Cd with an ACC deaminase gene from *Enterobacter cloacae* UW4 fused to the tet^r gene promoter improves its fitness and plant growth promoting ability. *Microbiol*. *Ecol.* **46**: 122-133.

Hommes, R. W. J., Postma, P. W., Neijssel, O. M., Tempest, D. W., Dokter, P. and Duine, J. A. (1984). Evidence of a quinoprotein glucose dehydrogenase apoenzyme in several strains of *Escherichia coli. FEMS Microbiol. Lett*. **24:** 329-333.

Illmer, P., and Schinner, F. (1995). Solubilization of inorganic calcium phosphates-Solubilization mechanisms. *Soil. Biol. Biochem.* **27:** 265-270.

Imanaga, Y. (1989). In: PQQ and Quinoproteins. (Jongejan, J. A. and Duine, J. A., eds.), pp. 87-96. Kluwer Academic Publishers, Dordrecht, The Netherlands.

James, P. L. and Anthony, C. (2003). The metal ion in the active site of the membrane glucose dehydrogenase of *Escherichia coli*. *Biochem. Biophys. Acta.* **1647:** 200-205.

Katznelson, H., Peterson, E. A. and Rouatt, J. W. (1962). Phosphate dissolving microorganisms on seed and in the root zone of plants. *Can. J. Bot.* **40:** 1181-1186.

Keitel, T., Diehl, A., Knaute, T., Stezowski, J. J., Hohne, W. and Gorisch, H. (2000). X-ray structure of the quinoprotein ethanol dehydrogenase from *Pseudomonas aeruginosa*: basis of substrate specificity. *J. Mol. Biol*. **297**: 961-974.

Kennedy, C. and Toukdarian, A. (1987). Genetics of Azotobacters: Application to nitrogen fixation and related aspects of metabolism. *Ann. Rev. Microbiol.* **41:** 227-258.

Kepert, D. G, Robson, A. D. and Posner, A. M. (1979). The effect of organic root product on the availability of phosphorous to plants. In: "*The soil root interface*. J. L. Harley and R. Scott-Russell eds. Academic Press, London. pp.115-124.

Kim, K. Y, Jordan, D. and Krishnan, H. B. (1997a). *Rahnella aquatilis*, a bacterium isolated from soybean rhizosphere, can solubilize hydroxyapatite. *FEMS Microbiol. Lett*. **153:** 273-277.

Kim, K. Y, Jordan, D. and Krishnan, H. B. (1998). Expression of genes from *Rahnella aquatilis* that are necessary for mineral phosphate solubilization in *Escherichia coli. FEMS Microbiol. Lett*. **159:** 121-127.

Kim, K. Y, McDonald, G. A. and Jordan, D. (1997b). Solubilization of hydroxyapatite by *Enterobacter agglomerans* and cloned *Escherichia coli* in culture medium. *Biol. Fertil. Soils*. **24:** 347-352.

Kishore, G. K., Pande, S. and Podile, A. R. (2005). Phylloplane bacteria increased seedlings emergence, growth and yield of field-grown groundnut (*Arachis hypogaea* L.). *Lett. in Appl. Microbiol.* **40**: 260-268.

Krishnaraj, P. U. and Goldstein, A. H. (2001). Cloning of a *Serratia marcescens* DNA fragment that induces quinoprotein glucose dehydrogenase-mediated gluconic acid production in *Escherichia coli* in the presence of a stationary phase *Serratia marcescens. FEMS Microbiol. Lett.* **205:** 215-220.

Kucey, R. M. N., Janzen, H. H. and Legget, M. E. (1989). Microbially mediated increases in plant available phosphorous. *Adv. Agron*. **42:**198-228.

Laemmli, U. K. (1970). Cleavage of structural proteins during the assembly of the head of bacteriophage T4. *Nature* **227:** 680-685.

Lessie, T. G. and Phibbs, P. B. (1984). Alternative pathways of carbohydrate utilization in *Pseudomonas*. *Ann. Rev. Microbiol.* **38:** 359-387.

Leyval, C. and Berthelin, J. (1989). Interactions between *Laccaria laccata*, *Agrobacterium radiobacter* and beech roots: influence on P, K, Mg and Fe mobilization from minerals and plant growth. *Plant and Soil* **117:** 103-110.

Lindsay W. L., Frazier, A. W. and Stephenson, H. F. (1962). Identification of reaction products from phosphate fertilizers in soils. *Soil. Sci. Soc. Am. Proc.* **26:** 446-452.

Liu, S-T., Lee, L-Y., Tai, C-Y., Hung, C-H., Chang, Y-S., Wolfram, J. H., Rogers, R. and Goldstein, A. H. (1992). Cloning of an *Erwinia herbicola* gene necessary for the gluconic acid production and enhanced mineral phosphate solubilization in *Escherichia coli* HB101: nucleotide sequence and probable involvement in biosynthesis of the coenzyme pyrrolo quinoline quinone. *J. Bacteriol.* **174:** 5814-5819.

Matsushita, K., Ohno, Y., Shinagawa, E., Adachi, O. and Ameyama, M. (1980). Membrane bound D-glucose dehydrogenase from *Pseudomonas* sp: solubilization, purification, and characterization. *Agri. Biol. Chem*. **44:** 1505-1512.

Matsushita, K., Shinagawa, E., Inoue, T., Adachi, O. and Ameyama, M. (1986). Immunological evidence for two types of PQQ dependent D-glucose dehydrogenase in bacterial membranes and the location of the enzyme in *Escherichia coli*. *FEMS Microbiol. Lett.* **37:** 141-144.

Matsushita, K., Arents, J. C., Bader, R., Yamada, M., Adachi, O. and Postma, P. W. (1997). *Escherichia coli* is unable to produce pyrroloquinoline quinone (PQQ). *Microbiology* **143**: 3149-3156.

Meulenberg, J. J. M., Sellink, E., Riegman, N. H. and Postma, P. W. (1992). Nucleotide sequence and structure of the *Klebsiella pneumoniae pqq* operon. *Mol. Gen. Genet*. **232:** 284-292.

Midgley, M. and Dawes, E. A. (1973). The regulation of glucose and methyl glucose uptake in *Pseudomonas aeruginosa*. *Biochem. J*. **132:** 141-154.

Moghimi, A., Tate, M. E., and Oades, J. M. (1978). Characterization of rhizosphere products especially 2-ketogluconic acid. *Soil. Biol. Biochem.* **10:** 283-287.

Morales, V. M., Backman, A. and Bagdasarin, M. (1991). A series of wide-host-range low-copy-number vectors that allow direct screening for recombinants. *Gene* **97**: 39-47

Morley, K. L. and Kazlauskas, R. J. (2005). Improving enzyme properties: when are closer mutations better? *Trend. Biotechnol.* **23:** 231-237.

Nautiyal, C. S. (1999). An efficient microbiological growth medium for screening phosphate solubilizing microorganisms. *FEMS Microbiol. Lett* 170: 265-270.

Neijssel, O. M., Tempest, D. W., Postma, P. W., Duine, J. A. and Frank, J. (1983). Glucose metabolism by K-limited *Klebsiella aerogenes*, evidence for the involvement of a quinoprotein glucose dehydrogenase. *FEMS Microbiol. Lett*, **20:** 35-39.

Newton, J. W., Wilson, P. W. and Burris, R. H. (1953). Direct demonstration of ammonia as an intermediate in nitrogen fixation by *Azotobacter*. *J. Biol. Chem.* **204**: 445-451.

Ogawa, T., Shinohara, A. and Ogawa, H. (1992). Functional structures of the RecA protein found by chimera analysis. *J. Mol. Biol*. **226:** 651-660.

Pal, S. S. (1998). Interactions of an acid tolerant strain of phosphate solubilizing bacteria with a few acid tolerant crops. *Plant and Soil*. **198:** 169-171.

Postma, P. W., Broekhuizen, C. P. and Geerse, R. H. (1989). The role of PEP: Carbohydrate phosphotransferase system in the regulation of bacterial metabolism. *FEMS Microbiol. Rev.* **63:** 69-80.

Raghothama, K. G. (2000). Phosphorous acquisition; plant in the driver's seat! *Trend. Plant. Sci*. **5:** 412-413.

Ramachandran, G. N., Ramakrishan, C. and Sasisekhran, V. (1963). Stereochemistry of polypeptide chain configuration. *J. Mol. Biol.* **7**: 95-99

Rodriguez, H., Gonzalez, T. and Selman, G. (2000). Expression of a mineral phosphate-solubilizing gene from *Erwinia herbicola* in two rhizobacterial strains. *J. Biotechnol*. **84:** 155-161.

Salih, H. M., Yahya, A. I., Abdul-Rahem, A. M. and Munam, B. H. (1989). Availability of phosphorous in a calcareous soil treated with rock phosphate or superphosphate as affected by phosphate dissolving fungi. *Plant and Soil.* **120:** 181-185.

Sambrook, J., Fritsch, E. F. and Maniatis, T. (1989). Molecular Cloning: A Laboratory Manual, Cold Spring Harbor Laboratory, New York. Cold Spring Harbor laboratory Press.

Sample, E. C., Soper, R. J. and Racz, G. C. (1980). Reactions of phosphate fertilizers in soils. In: *The role of phosphorous in agriculture*, Khasawneh F.E., Sample E. C., and Kamprath E. J. (eds), American Society of Agronomy, Madison, WI. pp, 263-304

SasiKala, K., Ramana, Ch. V., Raghuveera Rao, P. and Subrahmanyam, M. (1990). Photoproduction of hydrogen, nitrogenase and hydrogenase activities of free and immobilized whole cells of *Rhodobacter sphaerodies* OU 001. *FEMS Microbiol. Lett.* **72**: 23-28.

Sharma, V., Kumar V., Archana, G. and Kumar, N. G. (2005). Substrate specificity of glucose dehydrogenase (GDH) of *Enterobacter asburiae* PS13 and rock phosphate solubilization with GDH substrates as C sources. *Can. J. Microbiol.* **51:** 477-482.

Shi, J., Blundell, T. L.and Mizuguchi, K. (2001). FUGUE: Sequence-structure homology recognition using environment-specific substitution tables and structure-dependent gap penalties. *J. Mol. Biol.* **310:** 243-257.

Shinagawa, E., Matsushita, K., Adachi, O. and Ameyama, M. (1984). D-gluconate dehydrogenase, 2-keto-D-gluconate yielding, from *Gluconobacter dioxyacetonicus*: Purification and characterization. *Agri. Biol. Chem.* **48:** 1517-1522.

Sode, K. and Kojima, K. (1997). Improved substrate specificity and dynamic range for glucose measurement of *Escherichia coli* PQQ glucose dehydrogenase by site directed mutagenesis. *Biotechnol. Lett*. **19:** 1073-1077.

Sode, K. and Sano, H. (1994). Glu 742 substitution to Lys enhances the EDTA tolerance of *Escherichia coli* PQQ glucose dehydrogenase. *Biotechnol. Lett.* **16:** 455-460.

Sode, K., Ito, H., Witarto, A. B., Watanabe, K., Yoshida, H. and Postma, P. (1996). Increased production of recombinant pyrroloquinoline quinone (PQQ) glucose dehydrogenase by metabolically engineered *Escherichia coli* capable of PQQ biosynthesis. *J. Biotechnol*. **49:** 239-243.

Sode, K., Watanabe, K., Ito, S., Matsumura, K. and Kikuchi, T. (1995b). Thermostable chimeric PQQ glucose dehydrogenase. *FEBS Letters*. **364:** 325-327.

Sode, K., Witarto, A. B., Watanabe, K., Noda, K., Ito, S. and Tsugawa, W. (1994). Over expression of PQQ glucose dehydrogenase in *Escherichia coli* under holoenzyme forming condition. *Biotechnol. Lett.* **16:** 1265-1268.

Sode, K., Yoshida, H., Matsumura, K., Kikuchi, T., Watanabe, M., Yasutake, N., Ito, S. and Sano, H. (1995a). Elucidation of the region responsible for EDTA tolerance in PQQ glucose dehydrogenase by constructing *Escherichia coli* and *Acinetobacter calcoaceticus* chimeric enzymes. *Biochem. Biophys. Res. Commun*. **211:** 268-273.

Tisdale, S. L. and Nelson, W. L. (1975). In: Soil fertility and fertilizers. MacMillan Publishing Co., New York, pp. 225.

Tripura, C. B. (2005). Molecular approach to alter the properties of membrane bound quinoprotein glucose dehydrogenase of Gram-negative bacteria involved in mineral phosphate solubilization. Ph. D. Thesis, University of Hyderabad, India.

Tripura, C. B., Sashidhar, B. and Podile, A. R. (2005). Transgenic mineral phosphate solubilizing bacteria for improved agricultural productivity In: *Microbial Diversity Current Perspectives and Potential Applications*. eds. T. Satyanarayana and B. N. Johri. I. K. International Pvt. Ltd. pp. 375-392.

Tripura, C. B. Sashidhar, B. and Podile, A. R. (2007). Ethyl methanesulfonate mutagenesis enhanced mineral phosphate solubilization by groundnut-associated *Serratia marcescens* GPS 5. *Current Microbiology* **54**: 79-84.

Tripura, C. B., Sudhakar Reddy, P., Reddy, M. K., Sashidhar, B. and A. R. Podile (2007). Glucose dehydrogenase of a rhizobacterial strain of Enterobacter asburiae involved in mineral phosphate solubilization shares properties and sequence homology with other members of enterobacteriaceae. *Indian J. Microbiol.* **47**: 126-131.

Tripura, C. B. and Podile, A. R. (2007). Properties of chimeric glucose dehydrogenase improved by site directed mutagenesis. *J. Biotechnol.* **131**: 197-204.

van Schie, B. J, Hellingwerf, K. J, van Dijken, J. P, Elferink, M. G. L, van Dijl, J. M., Kuenen, J. G. and Konings, W. N. (1985). Energy transduction by electron transfer via pyrrolo-quinoline quinone-dependent glucose dehydrogenase in *Escherichia coli, Pseudomonas aeuriginosa, and Acinetobacter calcoaceticus* (var.*lwoffi*). *J. Bacteriol*. **163:** 493-499.

van Schie, B. J, van Dijken, J. P. and Kuenen, J. G. (1984). Non-coordinated synthesis of glucose dehydrogenase and its prosthetic group PQQ in *Acinetobacter* and *Pseudomonas* species. *FEMS Microbiol. Lett*. **24:** 133-138.

Vikram, A., Alagawadi, A. R., Krishnaraj, P. U. and Mahesh Kumar, K. S. (2007). Transconjugation studies in *Azospirillum* sp. negative to mineral phosphate solubilization. *World J. Microbiol. Biotechnol.* **23**: 1333-1337.

Yahya, A. I. and Al-Azawi, S. K. (1989). Occurrence of phosphate-solubilizing bacteria in some Iraqi soils. *Plant and Soil* **117:** 135-141.

Yamada, M., Elias, M. D., Matsushita, K., Migita C. T. and Adachi, O. (2003). *Escherichia coli* PQQ-containing quinoprotein glucose dehydrogenase: its structure comparison with other quinoprioteins. *Biochem. Biophys. Acta* **1647:** 185-192.

Yamada, M., Inbe, H., Tanaka, M., Sumi, K., Matsushita, K. and Adachi, O. (1998). Mutant isolation of the *Escherichia coli* quinoprotein glucose dehydrogenase and anlaysis of crucial residues Asp-730 and His-775 for its Function. *J. Biol. Chem.* **273:** 22021-22027.

Yamada, M., Sumi, K., Matsushita, K., Adachi, O. and Yamada, Y. (1993). Topological analysis of quinoprotein glucose dehydrogenase in *Escherichia coli* and its ubiquinone binding site. *J. Biol. Chem.* **268:** 12812-12817.

Yoshida, H., Kojima, K., Witarto, A. B. and Sode, K. (1999). Engineering a chimeric pyrroloquinoline quinone glucose dehydrogenase: improvement of EDTA tolerance, thermal stability and substrate specificity. *Protein Engineering* **12:** 63-70.

Yum, D-Y., Lee, Y-P., and Pan, J. G. (1997). Cloning and expression of a gene cluster encoding three subunits of membrane-bound gluconate dehydrogenase from *Erwinia cypripedii* ATCC 29267 in *Escherichia coli*. *J. Bacteriol*. **179:** 6566-6572.

Zheng, Y. J., Xia, Z. X., Chen, Z. W., Mathews, F. S., Bruice, T. C. (2001). Catalytic mechanism of quinoprotein methanol dehydrogenase: A theoretical and x-ray crystallographic investigation. *Proc. Natl. Acad. Sci. USA* **98:** 432-434.